Investigating Gas Entrapment Within Biocemented Composites

Erick Martinez Mendoza

A thesis

submitted in partial fulfillment of the

requirements for the degree of

Master of Science in Civil Engineering

University of Washington

2024

Committee:

Michael G. Gomez

Brett W. Maurer

Program Authorized to Offer Degree:

Civil and Environmental Engineering

University of Washington

Abstract

Investigating Gas Entrapment Within Biocemented Composites

Erick Martinez Mendoza

Chair of the Supervisory Committee:
Michael G. Gomez
Civil and Environmental Engineering

Microbially-induced calcite precipitation (MICP), or biocementation, is a bio-mediated ground improvement method that can improve the engineering behavior of granular soils through the precipitation of calcium carbonate materials. While resulting bonds and particle coatings can provide large increases in soil initial shear stiffness, peak shear strength, and liquefaction resistance, alternative strategies such as microbial desaturation have shown the significant potential of increases in pore fluid compressibility to reduce excess pore pressure generation in contractive soils during undrained loading. In this study, a suite of experiments were performed to investigate the potential of novel biocementation treatment processes to enable entrapment of gasses within biocemented composites. Entrapped gas bubbles within biocemented materials may afford the ability to increase pore fluid compressibility and reduce excess pore pressure generation during undrained shearing following material damage and cemented bond fracture through the

release of trapped gases. Batch experiments were employed to identify effective methods to both generate and entrap gasses within an organic polymer layer applied intermittently between biocementation treatments. During all experiments, aqueous chemical measurements were used to monitor cementation formation and gas entrapment processes with scanning electron imaging, material cross-sectioning, and energy dispersive spectroscopy employed to characterize achieved gas inclusions, material elemental composition, and resulting impacts on cementation morphology and fabric. Results suggest that gas voids can be successfully entrapped within biocementation through the application of organic polymers and microbial mixed acid fermentation (MAF) treatments, which can enable carbon dioxide production from both dissolution of existing biocementation and as a fermentation byproduct. Magnesium chloride treatment additions were also found to enable more effective coating of gas-containing polymer films during subsequent biocementation treatments when compared to control treatments not amended with magnesium. The novel biocemented composites developed through this research may enable significant improvements in engineering performances afforded by biocementation soil improvement and the environmental and financial efficacy of the technology.

ACKNOWLEDGEMENTS

As my time concludes at the University of Washington, I recognize that this personal goal of mine was possible thanks to one person who was willing to take me into his group, nurture, and guide me as a researcher. My advisor, Dr. Michael Gomez, has been an integral part of my time here. Working in Professor Gomez's research group has been a blessing; I don't know many people that have as much care and passion for their work as he does. His ability to lead with compassion and empathy has made working with him a joy. I can honestly say stumbling onto his research website back in November of 2021 is one of the best things that could have happened to me. I am very proud to say I had the chance to work with him.

In that research group were brilliant students that I had the honor to work with. I would like to thank Bruna Gabrielly Oliveira Ribeiro and Trent A. Shepherd who showed me everything I needed to know in the laboratory. None of my work could have been possible without their help. Outside of the lab, I'd like to thank them for their friendship; they made my time at UW so much easier. Next, I would like to thank Kelly Hillard and Chungen Tai who I was able to work with for my second year here. Their support in the lab was beyond what anyone could ask for and I am grateful for the time I got to spend working with them.

When I first joined the geotechnical group in the Civil and Environmental Engineering department at the University of Washington, I had no idea the journey I was in for. In my two years here, I had the chance to work alongside some of the smartest people I have ever met. Thankfully, many of those people became great friendships that I deeply cherish and will miss seeing as often as I did.

In the geotechnical group, there are also amazing faculty who all deserve major praise. Dr. Brett Maurer is one of the best instructors I have ever had. I attribute my interest in performance-

based design and earthquake engineering to him. I would like to deeply thank him for all the support he provided me in my time here, as well as for forming part of my thesis committee. There are not enough words to describe Dr. Pedro Arduino, who goes above and beyond in everything he does for us. Although he is always extremely busy, he still finds a way to provide immense support to his students. My time working with Dr. Joseph Wartman as his lab teaching assistant was a huge pleasure. His passion for his work is inspiring.

I'd like to thank my family for their constant and unwavering support throughout my entire education. Thank you for celebrating my achievements with me but also for being there for me at my lowest points. I am eternally grateful for the amazing family I have. I'd also like to thank my partner, Nick Alvarez, for constantly pushing me to be a better version of myself. His constant support has been integral in my success at UW.

Finally, I'd like to thank the University of Washington and the National Science Foundation for providing me with the funding to complete this research. Funding for this research is provided by the University of Washington and the National Science Foundation (NSF) grant no. ECI-2045058. Presented SEM and EDS images were made possible by the Molecular Analysis Facility, a National Nanotechnology Coordinated Infrastructure site at the University of Washington that is supported in part by the National Science Foundation Grants NNCI-1542101 and NNCI-2025489, the University of Washington, the Molecular Engineering & Science Institute, and the Clean Energy Institute. Any opinions, findings, conclusions, or recommendations expressed in this document are those of the author and do not necessarily reflect the views of the National Science Foundation or other funding sources.

Table of Contents

List of Figures

Chapter 1: Introduction

1.1 Background & Motivation

Ground improvement is an ever-evolving area in geotechnical engineering. Some of the most common methods of ground improvement include forms of grouting, deep soil mixing, and dynamic compaction among many other methods (Raju 2010). While these methods have been shown to effectively improve soil engineering properties, environmental concerns related to greenhouse gas emissions and aqueous toxicity, among other concerns, have sparked interest in more environmentally conscious soil improvement technologies. Microbially induced calcite precipitation (MICP), or biocementation, is one such method that has been extensively researched as an environmentally beneficial technology, relying on microbial urea hydrolysis activity to cement soils with calcium carbonate minerals (Stocks-Fischer et al. 1999). The process eliminates the use of portland cement, however, there are other important considerations related to ammonium byproduct generation and resulting brittle engineering behaviors.

Past research has shown that soils treated with biocementation can achieve large increases in shear stiffness and shear strength (DeJong et al. 2006; Montoya & DeJong 2015; Gomez & DeJong 2017), reductions in hydraulic conductivity (Baek et al. 2024), and improvements in liquefaction resistances (Montoya et al. 2012; Lee et al. 2022; Lee & Gomez 2023). While biocementation can greatly improve the behavior of granular soils at smaller strain levels, at large-strains, cemented bond failure results in materials behaving more similar to a denser uncemented sand with significant strain softening and brittle behaviors observed under confining stresses typical of most ground improvement applications (i.e., < 200 kPa) (Montoya & DeJong, 2015; Mortensen & DeJong 2011; Lee & Gomez 2023). Although these large-strain behaviors can be improved with

higher levels of cementation which increasingly densify the soil with added mineral solids, such strategies may not be the most economical and environmentally beneficial approach. If larger-strain behaviors can be improved at low levels of cementation, it is expected that transformative environmental and financial benefits may be achieved.

The mechanical performance of soil treated with biocementation have been shown to depend on the morphology of precipitates as well as the distribution of cementation on particle surfaces and contacts. For example, there can be large differences in the crystalline polymorphs of calcium carbonate that are precipitated during biocementation depending on treatment approaches used and environmental factors present (Burdalski et al. 2022). Despite this, almost all past studies on biocementation have examined improvements afforded by calcium carbonate as a single cementitious material phase. In contrast, biogenic calcium carbonate materials found in marine organisms including mollusks and marine arthropods are composed of nearly identical minerals, but incorporate small amounts of organics to yield mechanically superior composites with increased fracture resistance, tensile strength, ductility, and other multifunctionalities. Thus, an opportunity exists to draw inspiration from the structure and mechanisms associated with biogenic composites to modify conventional bio-cementation and achieve new bio-cemented composites that can further enhance soil engineering behaviors.

In this study, a suite of batch experiments were performed to specifically investigate the potential of novel biocementation treatment processes to enable entrapment of gasses within biocementation. Entrapped gas bubbles within biocemented materials may afford the ability to increase pore fluid compressibility and reduce excess pore pressure generation during undrained

shearing following material damage and cemented bond fracture through the release of trapped gases. A brief review of existing knowledge on soil desaturation and biogenic composites is first described followed by an overview of the experimental program with specific batch experiments presented in subsequent chapters.

1.2 Potential of Soil Desaturation

Although this study specifically focuses on entrapping gas voids within biocemented composites, the effect of gas bubbles on soil behaviors alone has been extensively investigated. For example, Takemura et al. (2009) and O'Donnell et al. (2017) found that low levels of desaturation (< ≈99% saturation) can increase pore fluid compressibility, dampen excess pore pressure generation during undrained shearing, and increase soil liquefaction resistances. Such results indicating the high material efficiency of the desaturation process has sparked interest in methods to desaturate soils, specifically for the purpose of earthquake-induced liquefaction mitigation (He et al. 2016; Takemura et al. 2009). This includes the use of microbial denitrification to produce biogas bubbles as well as other abiotic air injection methods (Stallings Young et al. 2021; Hall et al. 2018; Eseller-Bayat, 2009; Byle et al., 2017).

As described previously, biocementation can achieve large improvements in liquefaction triggering resistance owing to the stiff cemented bonds that restrict soil contraction and excess pore pressure generation (Lee et al. 2022; Lee & Gomez 2023). However, following bond breakage at large-strains, the post-triggering resistance of biocemented soils can be comparable to uncemented soils for the same dry density, indicative of the more minimal improvements afforded by cementation following damage. An opportunity exists to incorporate gas bubbles within

biocementation to enable gas release during cemented bond damage and further improvements in liquefaction behaviors at larger strains following triggering. Such methods may be transformative of the technology, enabling improvements across a wide spectrum of strain-levels while minimizing environmental and financial impacts.

1.3 Developing Biocemented Composites with Entrapped Gasses

Through millions of years of evolution, organisms have optimized the behavior of mineral-based materials by combining ductile organics with brittle inorganic phases to produce composites. These composites are pervasive in nature and consist almost exclusively of calcium, silica, and phosphate-based minerals that are incorporated with biopolymers. Natural bio-composites have unique attributes including mechanical properties that can be far superior to the constituents from which they are assembled. For example, mollusk nacre consists of approximately 95% aragonite, a $CaCO_3$ mineral, with only 5% biopolymers yet exhibits near 3 orders of magnitude greater resistance to cracking from impact loading than pure calcite (Sun & Bushan 2012). This insight provides a unique opportunity to develop bioinspired biocemented composites with improved engineering behaviors relative to conventional biocementation. The incorporation of biopolymers within biocementation can be used to develop films and inclusions that can prevent stress-concentrations thereby achieving enhanced fracture toughness and ductility. Such polymer layers may also permit development of new functionalities such as entrapped gasses which themselves may permit improved engineering behaviors under undrained conditions, although through an entirely different mechanism.

Our experiments investigate for the first time, the use of polymer layers to be incorporated within a biocemented composite for the purpose of gas release and pore fluid desaturation following cemented material damage. More specifically, a treatment process was investigate wherein (i) soils were first cemented via MICP, (ii) a polymer solution was injected into cemented soils with fermentable substrates to enable mixed acid fermentation, dissolution of cementation and carbon dioxide generation (referred to as "PolyMAF"), and (iii) subsequent cementation treatments were applied to re-precipitate calcium carbonate minerals over the gas containing polymer layer, thereby creating gas inclusions within a biocemented composite material.

Preliminary proof-of-concept testing considered a variety of different candidate polymers including xanthan gum, guar gum, and sodium alginate for the PolyMAF injection. Following this testing, sodium alginate was found to be an optimal candidate due to the polymer's ability to cross-link with released calcium during dissolution and form a stiffer calcium alginate gel to entrap bubbles. The method was applied to proof-of-concept soil column tests and results indicated that crystal surfaces could be modified using such techniques. However, clear trapped gas bubbles were not easily observed in samples obtained from these column tests suggesting that further development of the treatment process would be required. An extensive series of batch experiments were then performed to optimize the treatment process and establish methods to entrap gasses more effectively, which are described in detail in this thesis.

1.4 Scope of Research

The scope of the research presented in this thesis will focus on three select batch experiments completed after preliminary soil column and batch experiments, which allowed for identification

of treatment protocols used throughout the testing program. In Chapter 2, results from batch experiments examining the effect of applied polymer concentrations are presented. These experiments identified the abilities of higher polymer concentrations to entrap gas bubbles generated during calcium carbonate degradation and through the mixed acid fermentation process. In Chapter 3, results from batch experiments examining the effect of chemical additives and rinsing techniques are presented. These experiments identified unexpected morphological effects when adding magnesium chloride as well as the improvements in gas entrapment when performing a calcium rinse. Finally, in Chapter 4, the magnesium amended treatment process is investigated in greater detail, thereby demonstrating a treatment process through which gas inclusions may be achieved. In each chapter, a brief description of the motivation for each experiment set is provided, followed by a description of the employed methods, materials used, experimental set-up, sampling program, and treatment scheme. Results related to each experiment set are then presented along with primary conclusions and remaining knowledge gaps.

Chapter 2: Effect of Chemical Additives on 2nd Cementation Treatment and Air-Entrapment

2.1 Introduction

MICP, or biocementation, is a ground improvement method that can improve the engineering behavior of granular soils through the precipitation of calcium carbonate minerals which can form interparticle bonds and particle surface coatings (refs). Although the behavior of biocemented sands can be significantly improved at small-strains, at large-strains more minimal improvement is observed following the degradation of cemented bonds with improvements primarily related to the addition of mineral solids and soil matrix densification. Although higher magnitudes of cementation may improve material behaviors at larger strains through increased dilatancy, increases in material and energy consumption will reduce the environmental and financial efficacy of the process.

As described earlier, it may be possible to incorporate polymers within biocemented composites to achieve improved engineering properties as well as new functionalities such as the release of gasses during loading. Although not reported in this thesis, preliminary experiments were conducted to identify the treatment protocols needed to employ such processes including the type of biopolymer to be introduced, the augmentation methods needed to enable biocementation and mixed acid fermentation, and the protocols needed to enable multiple treatment phases including intermediate treatment rinses. In this chapter, eight different batch experiments were conducted which specifically investigated the (i) behavior of a standard MICP control experiment, (ii) the use of mixed acid fermentation as a method of cementation degradation and carbon dioxide generation, (iii) the ability of augmented soils to enable multiple cementation treatments, and (iv) the effects of different polymer concentrations on gas entrapment.

2.2 Material and Methods

2.2.1 Experiment Overview

Eight individual batch experiments were performed to evaluate gas entrapment testing protocols. Five experiments, with a polymer concentration of 0.0005%, were performed to establish baseline methods for future comparisons and three experiments were performed to investigate the effect of differences in organic polymer concentrations during the PolyMAF treatment. All experiments contained an Ottawa F-65 Sand and Concrete Sand mixture in a glass petri dish with approx. 44 mL of solution. Although each experiment differed slightly in treatment approach, the primary treatment phases were as followed (with small differences described later): (i) a single cementation treatment intended to first biocement soils, (ii) a PolyMAF treatment including sodium alginate biopolymer with substrates required to enable mixed acid fermentation (i.e., MAF inoculant, glucose, yeast extract), and (iii) a second cementation treatment intended to coat the polymer film containing entrapped gases. Table 2.1 (in Appendix) describes all eight experiments including test number, test name, and specific solution chemical compositions of the (i) first augmentation, cementation, and post-treatment rinse solutions, (ii) PolyMAF/Poly injections and post-treatment rinse solutions, and the (iii) second augmentation, cementation, and post-treatment rinse solutions.

Experiment 1 was a control experiment that followed a similar treatment protocol as the preliminary soil column experiments containing sodium alginate. Experiment 2 was a second control experiment that was augmented and received only a single cementation treatment similar to Burdalski et al. 2022. Experiment 3 was a third control experiment that was augmented, received a single cementation treatment, and then received a PolyMAF treatment. Experiment 4 was a fourth control experiment that was identical to Experiment 1, intended to evaluate the repeatability

of experiments. Experiment 5 was a fifth control experiment that was augmented, received a single cementation treatment, and then received a polymer treatment alone (referred to as "Poly") without MAF substrates to evaluate the effect of mixed acid fermentation activity.

Experiments 6 through 8 were used to evaluate the effect of polymer concentration on gas entrapment. Earlier soil column experiments identified that concentrations of 0.10% and 0.30% could not be applied to soil columns due to interactions between sodium alginate and free calcium present within biocemented columns which resulted in large solution viscosity increases and clogging during injections. Following additional testing, it was found that much lower concentrations below 0.01% could be applied to a biocemented column with success. Experiments 6, 7, and 8 received treatments identical to Experiment 1 but received lower sodium alginate concentrations of 0.001%, 0.005%, and 0.01%, respectively.

2.2.2 Batch Experiment Set-up

All batch experiments contained a mixture of 95% Ottawa F-65 sand and 5% Concrete Sand (by mass). This was intended to provide native soil microorganisms needed to complete mixed acid fermentation. Each batch experiment contained 5.3 grams of soil, 44 mL of solution, and were conducted in 100x15 mm Corning bottom glass petri dishes that were covered with aluminum foil to minimize temperature changes and mitigate evaporation effects and potential contamination.

2.2.3 Biogeochemical Sampling, Monitoring, and Imaging

Aqueous samples were collected daily during cementation treatments with sterile pipettes. Additional samples were collected at 2 hours, 4 hours, and 8 hours after each cementation treatment was initiated. The volume collected for each sample was 120 μL and no more than 10% of the total sample volume was collected to minimize sample effects. All collected aqueous samples were acid stabilized with 300 μL of 1M hydrochloric acid (HCl) to ensure that urea hydrolysis and calcium carbonate precipitation activity after sampling was minimized. Collected samples were used to determine urea concentrations in time for each experiment during the first and second cementation treatments following protocols outlined in Knorst (1997). Assays were performed in a 96-well plate in which 25 μL of sample, 185 μL of hydrochloric acid, and 40 μL of urea assay reagent were combined within each well, with the spectrophotometer providing an optical density value within the plate. This OD value was then correlated to a cellular density based on standards specific to the laboratory spectrophotometer.

After all treatments, samples were rinsed with 70% ethanol and oven dried. After oven drying, soils were prepared for SEM imaging. Soil subsamples were mounted onto a pedestal with carbon tape and then sputter coated using a Leica EM ACE600 sputter coater with ~4 nm of platinum to increase the conductivity of the samples to improve image quality. All samples were imaged using 2 kV and 13 pA using T1, ETD, and Mixed (T1 & ETD combined) detectors to examine different aspects of specimen morphology.

2.2.4 Treatment Scheme and Overview

All soil specimens were initially augmented with *S. pasteurii* (ATCC 11859) (Yoon et al. 2001) a well-studied ureolytic bacteria used in many previous MICP studies (Gomez et al. 2015, San Pablo

et al. 2020, van Paassen 2009, Gomez et al. 2016, van Der Star 2009). *S. pasteurii* was grown in 500 mL volumes of standard ATCC 11859 growth media (15.74 g/L Tris Base, 20 g/L yeast extract, 10 g/L ammonium sulfate, pH adjusted to 9.0) using a process similar to that outlined in Burdalski (2020). After mixing, growth media was autoclaved using a liquid cycle for 24 minutes at 121^{o}C to sterilize prior to inoculation. After autoclaving, media volumes were inoculated with a -80^{o}C *S. pasteurii* glycerol stock culture, covered with sterile foil, and placed on an orbital shaker for approximately 36 hours at 180 rpm. OD_{600} values were monitored in time and reached a value near 3.00E+09 cells/mL after ~36 hours, after which cells were harvested for experiments.

During harvesting, 50 mL of growth media was transferred to a sterile 50 mL conical tube and centrifuged at 4200 rpm for 10 minutes. Following centrifugation, supernatant solutions were removed, and cells at the bottom of the conical tube were retained. Sterile isotonic saline solution (9 g/L sodium chloride in DI water) was then added to the conical tube, shaken to free cells from the bottom of the tube, and centrifuged at 4200 rpm for 10 minutes to rinse. After rinsing, the supernatant was again decanted, and an additional 10 mL of saline solution was added to the tube. The conical tube was then shaken to achieve homogenization of the cell pellet throughout the solution. Cell pellets were refrigerated until use (between one and two days after pelleting to ensure high cellular activity). Specified volumes of cell pellets were mixed with 5 mL of sterile saline solution and the 5.3 grams of the soil mixture in a 50 mL conical tube and placed in the refrigerator to reside overnight. Added volumes were determined from the growth media cell density in order to achieve a cell density of 7 x 10^{7} cells/mL within experiments once fully mixed with cementation solutions. The augmented soil and cell pellet mixture was poured into glass dishes prior to the start of experiments.

In order to start the first cementation treatment, cementation solutions were added to glass dishes containing the augmented soil. Cementation solutions were formulated to obtain concentrations of 250 mM calcium and urea once mixed with the augmenting solution volumes. All experiments had a total volume after adding the cementation solution of 44 mL. All cementation solutions were prepared using urea (Fisher Chemical, U15-50), calcium chloride dihydrate (Fisher Chemical, C79-3), and contained 0.2 g/L of yeast extract (Fisher BioReagents, BP1422-500). Cementation treatments were allowed to react within samples over 72 hours to ensure reaction completion. Following the cementation treatment period, solutions were decanted, and samples were rinsed with 35% ethanol to remove treatment byproducts. Although other samples received additional treatments, Experiment 5 was oven-dried immediately after this rinse.

In experiments receiving a subsequent polymer solution, the solution was first prepared and then applied to the cemented samples following rinsing. Polymer concentrations were calculated by dividing the mass of polymer by the total volume of solution (DI water) and converting into percentage. All PolyMAF treatments contained sodium alginate prepared from a 0.50% stock solution. This stock solution was diluted to the specific concentrations required for each experiment. PolyMAF solutions contained both sodium alginate polymer as well as 10 g/L glucose, 1 g/L yeast extract, and 1 mL per 300 mL of a mixed acid fermentation inoculation solution intended to enable mixed acid fermentation activity. The PolyMAF solution was expected to generate carbon dioxide gas within the polymer from both the dissolution of calcium carbonate and as a fermentation byproduct. The mixed acid fermentation inoculation solution was prepared similar to Ribeiro et al. 2024 by adding 50 g of Delta Sand to a solution of 10 g/L

glucose and 5 g/L yeast extract in a sealed flask. This solution was sealed with an air lock to provide anaerobic conditions and was allowed to sit until a pH below 5.0 was achieved indicative of substantial fermentation activity. After applying to batch experiments, PolyMAF treatments were allowed to reside within experiments for 72 hours without sampling disturbances to limit oxygen intrusion. After the residence period, solutions were carefully decanted. Poly treatments involved similar procedures but received polymer only solutions without added glucose, yeast extract, or mixed acid fermentation inoculation solutions.

In order to determine methods for the second cementation treatment, a set of batch experiments were performed. These experiments specifically considered how specimens would be augmented following the PolyMAF treatment in order to complete the second cementation. Three methods were considered including (i) mixing cells directly with cementation solutions and applying this mixture to samples after PolyMAF, (ii) adding cells to soils within the glass dishes and allowing them to sit overnight (~12 hours), with the addition of the cementation solution occurring afterwards, and (iii) scraping the treated soil after the PolyMAF treatment into a conical tube containing cells and isotonic saline solution and allowing this to sit overnight (~12 hours), with again the addition of the cementation solution occurring afterwards. Following these tests, the method of scraping the treated soil after the PolyMAF treatment into a conical tube containing cells and isotonic saline solution was selected as the optimal approach for re-augmentation, with the other two re-augmentation approaches appearing to increasingly nucleate small precipitate crystals within samples, possibly due to the increased abundance of cells in free solution.

For all experiments completed in this set, treated soils were scraped after the PolyMAF treatment into a 50 mL conical tube and re-augmented. The applied cell density for the second augmentation identical to the first augmentation of 7 x 10^7 cells/mL when diluted with the cementation solution. Following augmentation and the residence period, augmented soils were poured into glass dishes and the second cementation treatment was applied. The second cementation solution was identical in composition to the first cementation solution (250 mM urea and calcium chloride with 0.2 g/L yeast extract) and was allowed to reside within samples for 72 hours. Following the residence period, samples were rinsed with 35% ethanol and then oven-dried.

2.3 Results & Discussion

2.3.1 Biogeochemical Behavior

Urea concentrations were monitored in all experiments during the initial cementation treatment up to 72 hours. **Figure 2.1** presents measured urea concentrations versus elapsed time for all experiments during the first cementation injection. All experiments exhibited similar reaction rates, with near 200 mM urea being hydrolyzed within the first eight hours following treatments. After 24 hours, urea concentrations in all experiments were near zero suggesting that urea hydrolysis was largely complete. Urea concentrations were also monitored during the second cementation treatment for all experiments receiving a second cementation treatment. Similar to the initial cementation treatment, all experiments had similar urea degradation behaviors with perhaps somewhat greater variability in reaction rates likely due to the presence of various polymer concentrations. Both data sets confirmed that the biocementation process was completed both during the initial cementation treatment and following both PolyMAF and Poly treatments during the second cementation treatment.

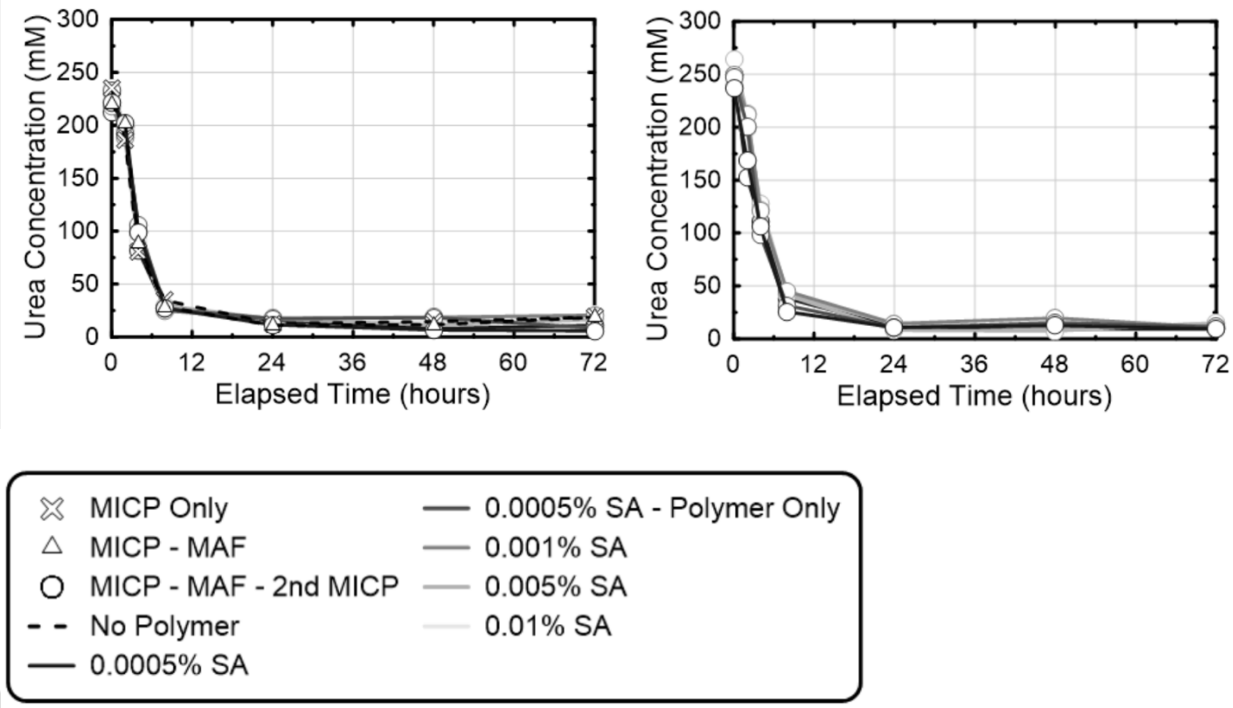

Fig. 2.1. Batch experiment urea concentrations versus time during the first cementation (left) and second cementation (right) treatments.

2.3.2 Morphological Effects

In order to assess differences in material morphology, SEM imaging of treatment and untreated soil samples was performed. **Figure 2.2** presents SEM images of untreated Ottawa F-65 soil prior to all treatments. As shown, clean mineral surfaces and subrounded grains are visible due to the absence of biocementation treatments.

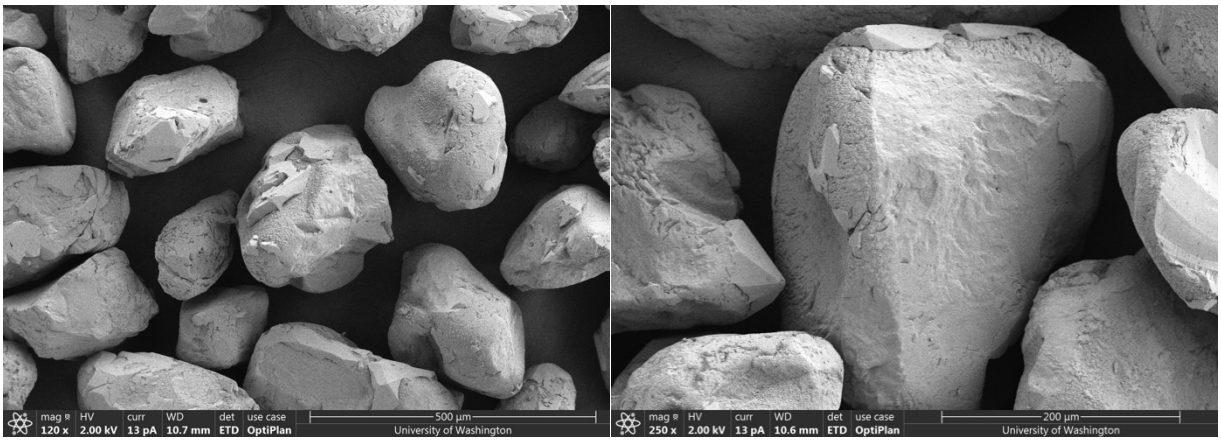

Fig. 2.2. SEM images of untreated Ottawa F-65 sand.

Following all treatments, soil samples from batch experiments were SEM imaged. **Figure 2.3** presents images of the treated soil from Experiment 1, which received a biocementation treatment followed by a 0.0005% sodium alginate PolyMAF treatment and a second biocementation treatment. As shown, the presence of the biopolymer can be observed and appears to coat larger biocementation crystals likely resulting from the first biocementation treatment. Smaller biocementation crystals can also be seen likely resulting from the second biocementation treatment, however the spatial distribution of these crystals appeared to be poorly organized with some small crystals filling free void space, growing on other larger crystals, or residing within voids likely resulting from fermentation-induced dissolution. These smaller crystals also appeared to have somewhat rounded edges, unlike the more cubic forms expected for calcite (Burdalski et al. 2020). When examining the morphologies of crystals in the Experiment 4 sample, which was treated identically to Experiment 1, similar morphologies were observed suggesting that the process could be reliably repeated.

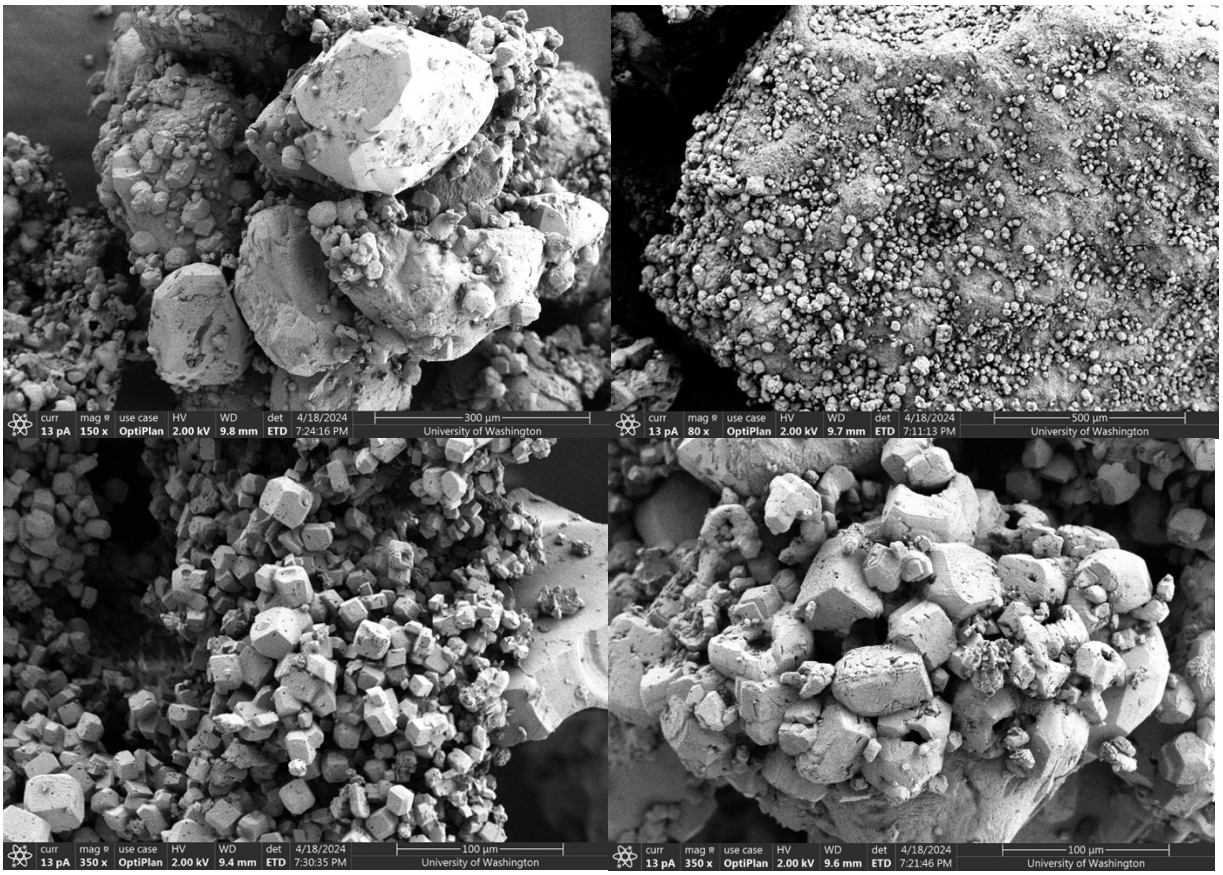

Fig. 2.3. SEM images of the Experiment 1 (MICP – PolyMAF (0.0005%) – 2nd MICP) treated soil specimen at various magnification levels.

Figure 2.4 presents images of the treated soil from Experiment 2, which received only a single biocementation treatment. As shown, crystal morphologies in this specimen appeared similar to other biocemented sands with calcium carbonate crystals precipitating on the surface of the sand particles and forming interparticle bonds. Unlike the experiments of Burdalski et al. (2020) the calcite crystals observed in this specimen had more rounded edges, likely due to the presence of yeast extract. Similar crystal morphologies have also been observed in biostimulation experiments when yeast extract was present (Gomez et al. 2017), suggesting the possibility of yeast extract altering crystal morphologies and/or unintended stimulation of native bacteria in these experiments

due to non-sterile conditions. On some of the crystal surfaces, bacterial voids on the order of several micrometers in size could also be observed, suggesting the close association of bacterial cells with biocementation crystals.

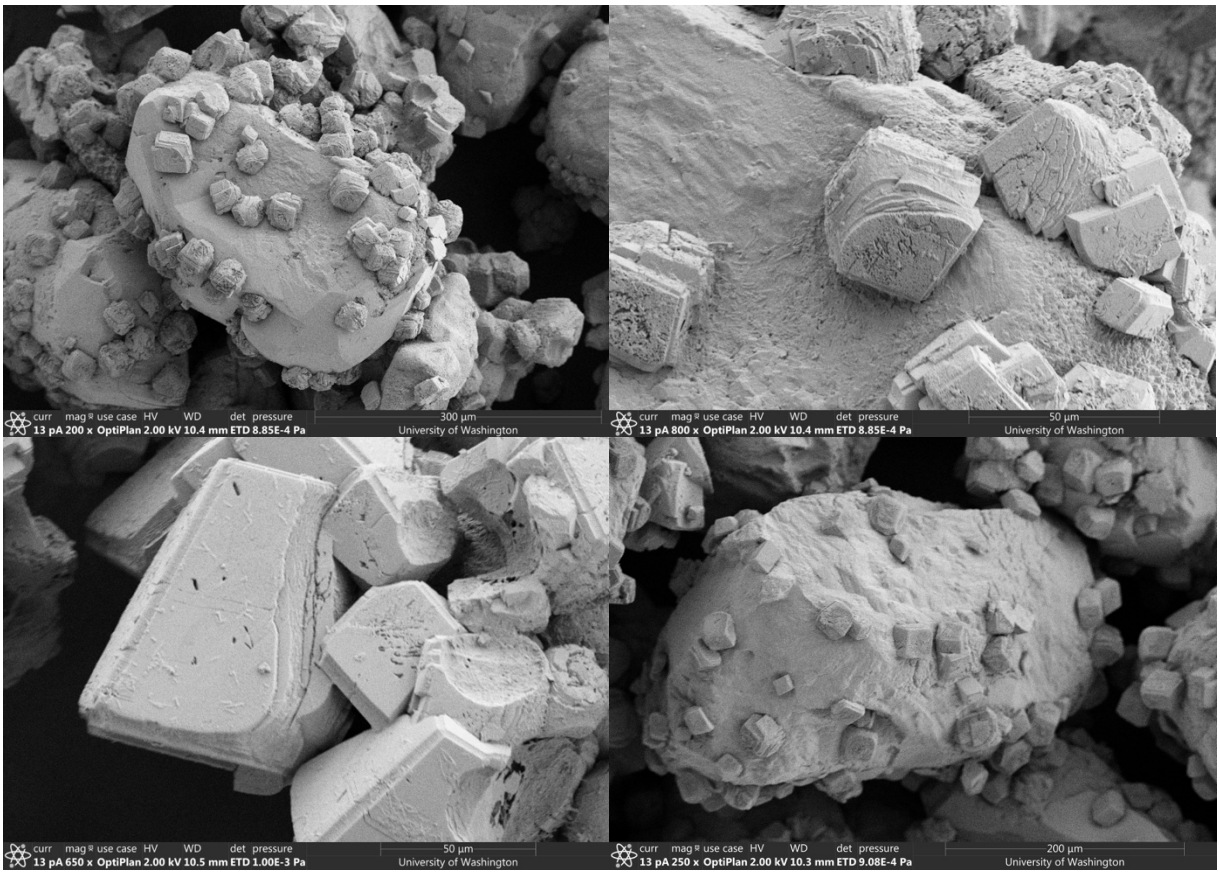

Fig. 2.4. SEM images of the Experiment 2 (MICP) treated soil specimen at various magnification levels.

Figure 2.5 presents images of the treated soil from Experiment 3, which received a single biocementation treatment followed by a single PolyMAF treatment, but no second cementation treatment. As shown, a polymer coating can be observed over some of the soil and existing calcite crystals. The surface degradation of calcite crystals could also be observed likely due to the effects

of mixed acid fermentation. Both increased deterioration of cemented bonds between crystals and the presence of larger voids on the surface of crystals were observed.

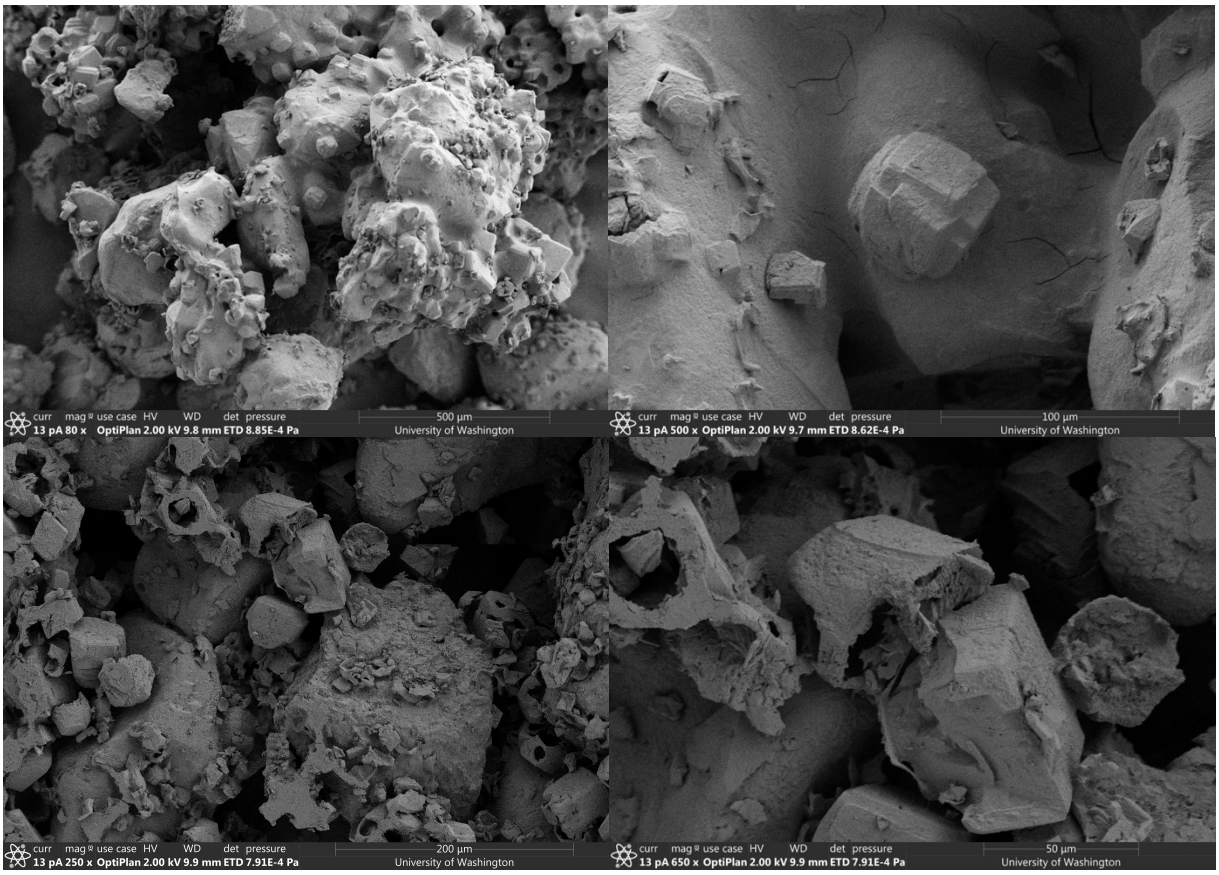

Fig. 2.5. SEM images of the Experiment 3 (MICP – PolyMAF 0.0005%) treated soil specimen at various magnification levels.

Figure 2.6 presents images of the treated soil from Experiment 5, which received a single biocementation treatment followed by a single polymer only Poly treatment (without mixed acid fermentation), and one second cementation treatment. Experiment 5 was conducted to assess the contribution of mixed acid fermentation towards altering crystal surfaces and generating carbon dioxide within the polymer. As shown, crystal surfaces appeared to be much more well defined

than those observed in Experiment 1 and 4 which had identical treatments with mixed acid fermentation. This suggested that the mixed acid fermentation process altered crystal surfaces through dissolution and that the application of sodium alginate alone could not recreate these effects. In addition, the second cementation appeared to nucleate much smaller crystals in a random pattern spatially across the samples, suggesting that the addition of the polymer between treatments may have altered nucleation of subsequent biocementation.

Fig. 2.6. SEM images of the Experiment 5 (MICP – Poly (0.0005%) – 2nd MICP) treated soil specimen at various magnification levels.

Figure 2.7 presents images of the treated soil from Experiment 6, which received a biocementation treatment followed by a higher concentration 0.001% sodium alginate PolyMAF treatment (2x standard concentration) and a second biocementation treatment. Although clear polymer coatings were not visible in the majority of the other experiments with lower sodium alginate concentrations, at this high concentration significant coating of cementation crystals with a polymer film was observed. In some instances, polymer strands connecting particles could also be observed which may have become more pronounced following oven drying. The presence of this film was expected to have resulted from interactions between released calcium during calcium carboante dissolution and the supplied sodium alginate polymer which can cross-link to form a stiffer water-insoluble calcium alginate gel (Ching et al. 2017). **Figure 2.8** presents images of the treated soil from Experiment 7, which received a biocementation treatment followed by a higher concentration 0.005% sodium alginate PolyMAF treatment (10x standard concentration) and a second biocementation treatment. Again, the polymer films and strands were more pronounced than earlier experiments receiving the standard polymer concentration (0.0005% sodium alginate). **Figure 2.9** presents images of the treated soil from Experiment 8, which received a biocementation treatment followed by a higher concentration 0.01% sodium alginate PolyMAF treatment (20x standard concentration) and a second biocementation treatment. This sample indicated the presence of spherical shapes which appeared to be coated by polymers and were thought to be indicative of possible gas inclusions. This result was promising and suggested that higher polymer concentrations may afford an improved ability to entrap gas voids within biocemented composites.

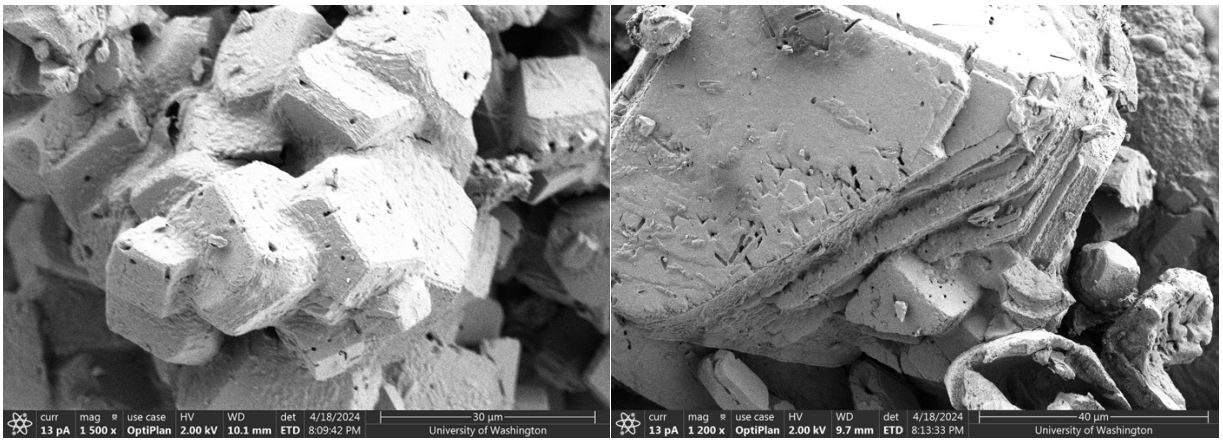

Fig. 2.7. SEM images of treated soil samples from Experiment 6 (upper left, MICP – Poly (0.001%) – 2nd MICP).

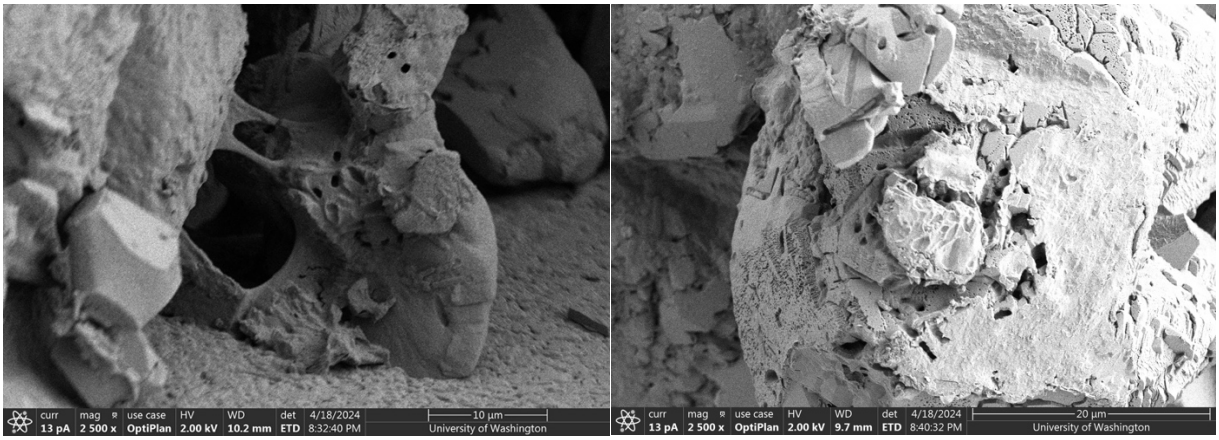

Fig. 2.8. SEM images of treated soil samples from Experiment 7 (upper right, MICP – Poly (0.005%) – 2nd MICP).

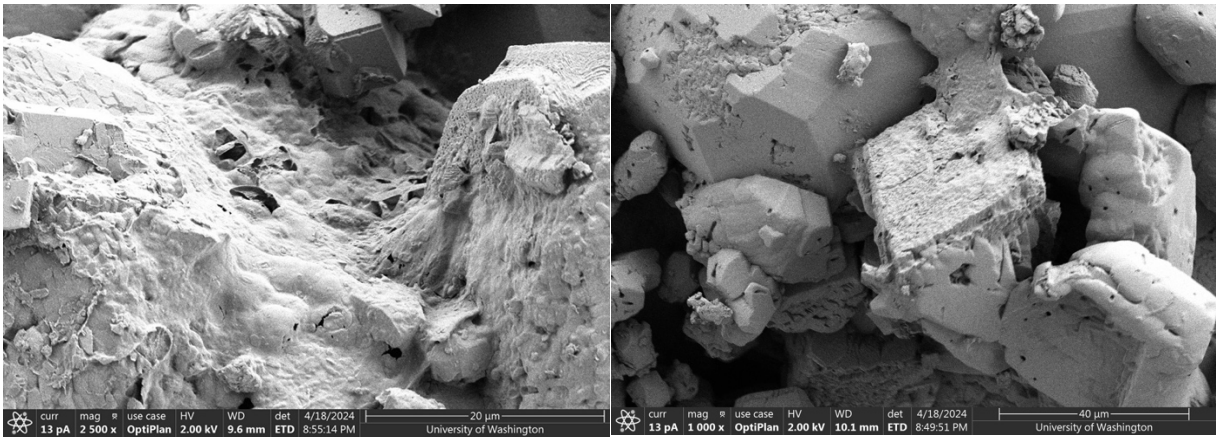

Fig. 2.9. SEM images from Experiment 8 (bottom center, MICP – Poly (0.01%) – 2nd MICP).

2.4 Conclusions & Remaining Knowledge Gaps

A series of eight batch experiments were performed to investigate the success of various gas entrapment processes including the impact of mixed acid fermentation, the effect of polymer additives, and the effect of applied polymer concentrations. The experiments demonstrated that applied polymer treatments with mixed acid fermentation could be used to dissolve crystal surfaces with possible entrapment of release carbon dioxide gases. Control experiments without polymer injections exhibited morphologies consistent with other biocementation experiments without polymers and with yeast extract. When the polymer was provided alone, this appeared to result in the nucleation of many small crystals during the second cementation event, however, minimal damage of existing crystals was observed due to the absence of mixed acid fermentation. As applied sodium alginate polymer concentrations were increased in the presence of mixed acid fermentation, polymer films and strands became more clearly visible in the samples with spherical shapes observed in the highest polymer concentration sample possibly indicative of entrapped gas bubbles. Although these results were promising, several important knowledge gaps still remained including: (i) while smaller crystals were observed in samples experiencing a second cementation treatment, it was unclear why crystals nucleated in this spatial pattern and if such crystals actually were precipitated during the second cementation treatment, (ii) although spherical forms were observed in the 0.01% polymer sample it was not clear if such forms were indeed trapped gas bubbles, and (iii) it was unclear if the second cementation treatment could be used to successfully coat the gas containing polymer layer within cemented materials or if the second cementation would only nucleate smaller crystals in a less ordered arrangement due to the presence of the polymer, which altered future precipitation events. Moving forward, higher polymer

concentrations near 0.01% sodium alginate appeared to be more optimal for future experimentation and examining strategies for distinguishing the various forms resulting from the different phases of treatment were prioritized.

Chapter 3: Investigating Effects of Chemical Tracers and Post-treatment Calcium Rinses on Biocemented Composite Morphology and Gas Entrapment

3.1 Introduction

As discussed in Chapter 2, protocols were identified to entrap gasses within biocemented composites including augmentation procedures, the usage of higher sodium alginate concentrations near 0.01% by mass to enable improved polymer film formation, and the use of mixed acid fermentation activity to degrade existing cementation crystals to release carbon dioxide gases. Although sufficient ureolytic activity was obtained to achieve a second cementation event, the employed treatment processes appeared to nucleate many small crystals when polymers were present. In an effort to track cementation progression and distinguish cementation formed during the first and second cementation events, it was hypothesized that chemical tracers could be added to experiments during various treatment phases in order to track materials formed during different stages of the process. It was expected that such tracers could facilitate detection using energy dispersive spectroscopy (EDS) which can identify chemical abundances and their spatial locations within materials. It was also recognized that the chemical tracers could result in additional challenges such as: (i) altering the precipitation morphology themselves and/or (ii) remaining passive and achieving minimal substitutions within the calcium carbonate and polymer layers thereby avoiding detection. In order to reduce possible effects on material morphology, reaction rates, and surrounding environmental conditions, chemical additives that were relatively inert and not detected in the parent soils and standard biocementation treatments were considered for the testing program. A batch experiment was therefore designed wherein small concentrations of magnesium chloride ($MgCl_2$), potassium bromide (KBr), and sodium bromide (NaBr) were added to specimens during the second cementation or PolyMAF phase with the potential to enable tracking of these phases.

Although these tracers were anticipated to have only small impacts on material morphology, such effects have been considered in previous studies. For example, Berner (1975) and Zhang & Dawes (2000) found that the presence of magnesium may slow the rate of calcium carbonate precipitation. Magnesium can also be substituted for calcium within calcite at select sites to form magnesian calcite with slightly different morphology (Morse et al., 2007). Park et al. (2008) found that increases in Mg^{2+} concentrations can also promote the precipitation of aragonite rather than more thermodynamically-stable calcite. Although there is more minimal understanding of how bromide concentrations may impact calcium carbonate precipitation, Okumura et al. (1986) found that bromide ions can be more easily co-precipitated with aragonite rather than calcite. Additionally, the sodium present within sodium bromide might also be incorporated within biocementation.

In addition to the eight batch experiments directed towards assessing the ability of chemical tracers to identify treatment phases, the effect of high calcium concentration rinses following PolyMAF treatments was also investigated in three separate batch experiments. It was anticipated that the application of high calcium rinses could promote the gelation of existing sodium alginate to better trap gas bubbles prior to the second cementation treatment. In all previous experiments, this rinse treatment was not applied and instead samples were immediately transitioned to the second cementation treatment after the PolyMAF treatment wherein the polymer layer may have been disturbed prior to crosslinking with calcium to form calcium alginate. It was expected that all eleven experiments would collectively provide new understandings regarding the materials formed during PolyMAF and the second cementation treatment as well as the preferred methods for transitioning samples from PolyMAF to the second cementation treatment.

3.2 Material and Methods

3.2.1 Experiment Overview

Chapter 3 batch experiments were treated using similar procedures as Chapter 2. Although each experiment differed slightly in treatment approach, the primary treatment phases were as follows (with small differences described later): (i) a single cementation treatment intended to first biocement soils, (ii) a PolyMAF or Poly treatment including sodium alginate biopolymer with or without substrates required to enable mixed acid fermentation (i.e., MAF inoculant, glucose, yeast extract), and (iii) a second cementation treatment intended to coat the polymer film containing entrapped gases. Experiments T1 through T8 investigated the use of chemical additives applied with treatments that were intended to serve as a tracer for either the PolyMAF/Poly or second cementation treatment. Experiments CR1 through CR3 investigated differences in applied rinse solutions following the PolyMAF/Poly treatment. **Table 3.1 (in Appendix)** describes all eleven experiments including test number, test name, and specific solution chemical compositions of the (i) first augmentation, cementation, and post-treatment rinse solutions, (ii) PolyMAF/Poly injections and post-treatment rinse solutions, and the (iii) second augmentation, cementation, and post-treatment rinse solutions. As shown, in select experiments chemical tracers were added to PolyMAF/Poly solutions to track polymer locations. In Experiment T2 the PolyMAF treatment was amended with 500 mM potassium bromide (KBr). In Experiment T3 the PolyMAF treatment was amended with 50 mM magnesium chloride ($MgCl_2$). In Experiments T4, T7, and CR2 the PolyMAF treatment was amended with 500 mM sodium bromide (NaBr). All other experiments did not have chemical additives applied in the PolyMAF treatment. In other select experiments chemical tracers were also added to the second cementation treatment. In Experiments T5 and T7, the second cementation treatment was amended with 50 mM magnesium chloride ($MgCl_2$). In Experiment T6, the second cementation treatment was amended with a higher 250 mM magnesium

chloride ($MgCl_2$). In Experiment T8, the second cementation treatment was amended with a higher 500 mM potassium bromide (KBr). Experiment T1 was a control and received no additives in either the PolyMAF treatment or second cementation treatment. In all of the calcium rinse experiments (Experiments CR1, CR2, and CR3), experiments also received a 250 mM $CaCl_2$ rinse treatment immediately after the PolyMAF treatment in an effort to better entrap gas bubbles through the formation of calcium alginate.

3.2.2 Batch Experiment Set-up

All batch experiments contained solely Ottawa F-65 sand. This change was made to avoid trace elements that may have been supplied from the Concrete Sand, which may have altered crystal morphology. The presence of Concrete Sand was also not expected to be critical for enabling mixed acid fermentation due to the addition of the mixed acid fermentation inoculant. Each batch experiment contained 5.3 grams of soil, 44 mL of solution, and were conducted in 100x15 mm Corning bottom glass petri dishes and were covered with aluminum foil to minimize temperature changes and mitigate evaporation effects and potential contamination.

3.2.3 Biogeochemical Sampling, Monitoring, and Imaging

Aqueous samples (120 μL) were collected 0, 2, 4, 8, 24, 48, and 72 hours after each cementation treatment was initiated. The volume collected for each sample was 120 μL and no more than 10% of the total sample volume was collected to minimize sample effects. All collected aqueous samples were acid stabilized with 300 μL of 1M hydrochloric acid (HCl) to ensure that urea hydrolysis and calcium carbonate precipitation activity after sampling was minimized. Collected samples were used to determine urea concentrations in time for each experiment during the first

and second cementation treatments following protocols outlined in Knorst (1997). Assays were performed in a 96-well plate in which 25 μL of sample, 185 μL of hydrochloric acid, and 40 μL of urea assay reagent were combined within each well, with the spectrophotometer providing an optical density value within the plate. This OD value was then correlated to a cellular density based on standards specific to the laboratory spectrophotometer.

After all treatments, samples were rinsed with 70% ethanol and oven dried. After oven drying, soils were prepared for SEM imaging. Soil subsamples were mounted onto a pedestal with carbon tape and then sputter coated using a Leica EM ACE600 sputter coater with ~4 nm of platinum to increase the conductivity of the samples to improve image quality. All samples were imaged using an acceleration voltage between 2 and 5 kV and current between 6.3 and 13 pA using T1, ETD, and Mixed (T1 & ETD combined) detectors to examine different aspects of specimen morphology. For experiments wherein chemical tracers were supplied, samples were prepared differently for energy dispersive spectroscopy (EDS). This included mounting specimens and coating with a 8 to 10 nm layer of carbon. All EDS samples were typically scanned using acceleration voltages between 5 and 20 kV (depending on the particular elements of interest) and a current high enough to generate a dead time (percentage of unprocessed x-rays generated from the sample) nearing 50%. For select samples, epoxy cross-section was also performed wherein samples were embedded within a hard epoxy and slow sawed using a diamond wafer microblade to reveal the internal structure of cemented crystals. During preparation, soil samples were placed in a mold, epoxy was added, and the epoxy was allowed to cure for 24 hours before samples were removed. A quick release spray was used in the molds to make sample removal easier. After curing, the epoxy pucks

were cut, polished, and mounted on 1-inch diameter pin mounts using carbon tape. Once mounted, samples were placed in a Leica coater and coated with 8-10 nm of carbon thread.

3.2.4 Treatment Scheme and Overview

All samples were treated using similar protocols as used in earlier Chapter 2 experiments with small differences described. At the start of experiments, all soil specimens were augmented with *S. pasteurii* (ATCC 11859). *S. pasteurii* was grown in 500 mL volumes of standard ATCC 11859 growth media (15.74 g/L Tris Base, 20 g/L yeast extract, 10 g/L ammonium sulfate, pH adjusted to 9.0) using a process similar to that outlined in Burdalski (2020). After mixing, growth media was autoclaved using a liquid cycle for 24 minutes at 121ºC to sterilize prior to inoculation. After autoclaving, media volumes were inoculated with a -80ºC *S. pasteurii* glycerol stock culture, covered with sterile foil, and placed on an orbital shaker for approximately 36 hours at 180 rpm. OD_{600} values were monitored in time and reached a value near 3.00E+09 cells/mL after ##### hours, after which cells were harvested for experiments.

During harvesting, 50 mL of growth media was transferred to a sterile 50 mL conical tube and centrifuged at 4200 rpm for 10 minutes. Following centrifugation, supernatant solutions were removed, and cells at the bottom of the conical tube were retained. Sterile isotonic saline solution (9 g/L sodium chloride in DI water) was then added to the conical tube, shaken to free cells from the bottom of the tube, and centrifuged at 4200 rpm for 10 minutes to rinse. After rinsing, the supernatant was again decanted, and an additional 10 mL of saline solution was added to the tube. The conical tube was then shaken to achieve homogenization of the cell pellet throughout the solution. Cell pellets were refrigerated until use (between one and two days after pelleting to ensure

high cellular activity). Specified volumes of cell pellets were mixed with 5 mL of sterile saline solution and the 5.3 grams of the soil mixture in a 50 mL conical tube and placed in the refrigerator to reside overnight. Added volumes were determined from the growth media cell density in order to achieve a cell density of 7×10^7 cells/mL within experiments once fully mixed with cementation solutions. The augmented soil and cell pellet mixture was poured into glass dishes prior to the start of experiments.

In order to start the first cementation treatment, a small change to the cementation procedure was made. In Chapter 2, cementation solutions were added directly to glass dishes containing the augmented soil. However, it was hypothesized that this method may have resulted in poor mixing of solutions with augmented soils and may have been responsible for the incomplete urea degradation observed in Chapter 2 experiments (approx. 50 mM remaining). To improve mixing, cementation solutions were added into the 50 mL conical tube containing the augmented soil after the residence period and vortexed. Once vortexed, the contents of the tube were poured into glass dishes to start the experiments. Cementation solutions were formulated to obtain concentrations of 250 mM calcium and urea once mixed with the augmenting solution volumes. All experiments had a total volume after adding the cementation solution of 44 mL. All cementation solutions were prepared using urea, calcium chloride dihydrate, and unlike earlier experiments did not contain yeast extract. The removal of yeast extract was intended to limit possible morphological effects (i.e., rounded precipitate edges) and possible contamination of experiments by other microorganisms. Cementation treatments were allowed to react within samples over 72 hours to ensure reaction completion. Following the cementation treatment period, solutions were decanted and samples were rinsed with 70% ethanol to remove treatment byproducts.

Following the first cementation, all experiments then received subsequent PolyMAF treatments containing 0.01% sodium alginate polymer, 10 g/L glucose, 1 g/L yeast extract, and 1 mL per 300 mL of a mixed acid fermentation inoculation solution intended to enable mixed acid fermentation activity. All PolyMAF treatments contained sodium alginate prepared from a 0.50% stock solution. This stock solution was diluted to the specific concentrations required for each experiment. The mixed acid fermentation inoculation solution was prepared similar to that described in Chapter 2. In select tests, various chemical additions were also applied during the PolyMAF treatment as a chemical tracer. After applying to batch experiments, PolyMAF treatments were allowed to reside within experiments for 72 hours without sampling disturbances to limit oxygen intrusion. After the residence period, solutions were carefully decanted. Experiments T1 through T8 were then immediately augmented in preparation for the second cementation treatment using the same scraping method described in Chapter 2. This involved scraping the treated soil after the PolyMAF treatment into a conical tube containing cells and isotonic saline solution and allowing this to sit overnight (~12 hours). The applied cell density for the second augmentation identical to the first augmentation of 7×10^7 cells/mL when diluted with the cementation solution. Calcium rinse experiments (CR1 to CR3), however, were scraped into conical tubes containing a 250 mM calcium chloride dihydrate rinse solution, vortexed, and then placed in the refrigerator for 24 hours to encourage calcium alginate formation. Experiment CR3 was immediately decanted and oven-dried after the calcium chloride rinse. For Experiments CR1 and CR2, however, the contents of the conical tube were poured into a glass dish after the calcium rinse, carefully decanted again, and prepared for re-augmentation using the same method used for the tracer experiments and other Chapter 2 experiments.

After re-augmentation, all specimens received a second cementation treatment (with the exception of Experiment CR3). The second cementation solution was identical in composition to the first cementation solution (250 mM urea and calcium chloride) and was allowed to reside within samples for 72 hours. For select samples, chemical additions were also supplied during the second cementation treatment. Following the 72 hour residence period, samples were rinsed with 35% ethanol and then oven-dried.

3.3 Results & Discussion

3.3.1 Biogeochemical Behavior

Urea concentrations were monitored in all experiments during the initial cementation treatment up to 72 hours. **Figure 3.1** presents measured urea concentrations versus elapsed time for all experiments during the first cementation injection. All experiments exhibited similar reaction rates, with near 225 mM urea being hydrolyzed within the first eight hours following treatments. After 24 hours, urea concentrations in all experiments were near zero suggesting that urea hydrolysis was largely complete. Urea concentrations were also monitored during the second cementation treatment for all experiments receiving a second cementation treatment. Similar to the initial cementation treatment, all experiments had similar urea degradation behaviors with again perhaps somewhat greater variability in reaction rates likely due to the presence of various polymer concentrations. Both data sets confirmed that the biocementation process was completed both during the initial cementation treatment and following PolyMAF treatments during the second cementation treatment. Interestingly, no significant differences in reaction rates were observed

during the second cementation treatment between experiments despite the presence of various chemical additions.

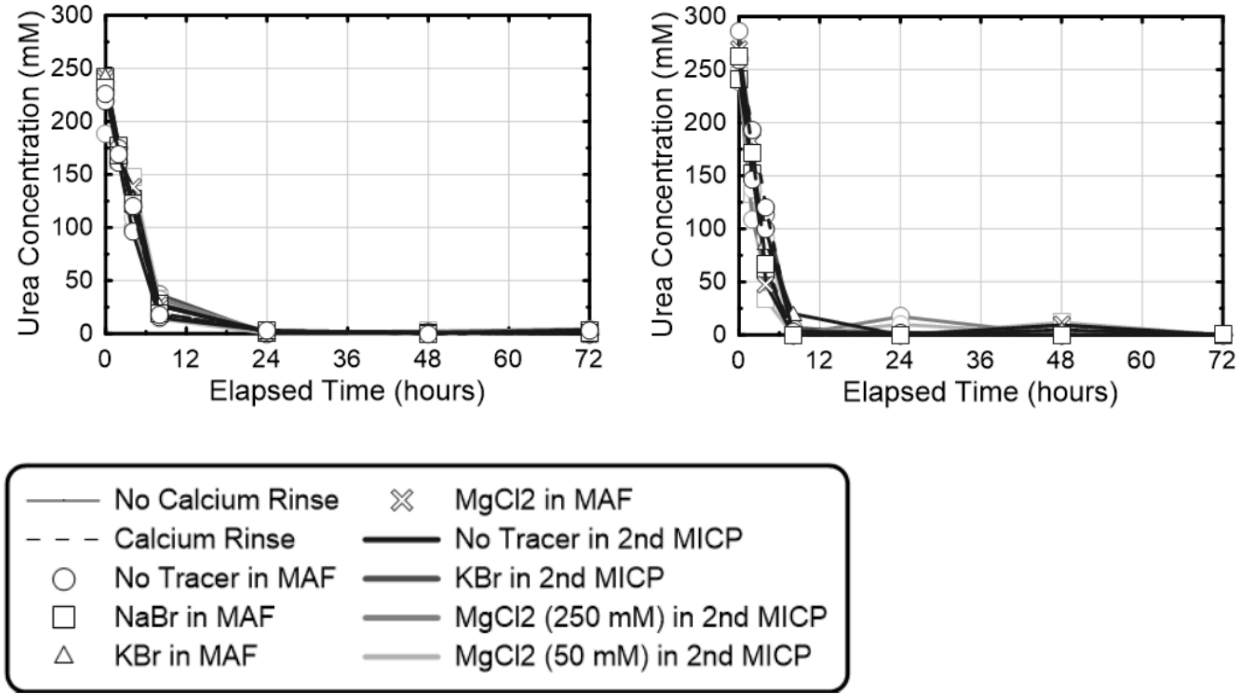

Fig. 3.1. Urea concentrations versus time during first (upper left) and second (upper right) cementation treatments.

3.3.2 Morphological Effects

Figure 3.2 presents images for Experiment T1 which received a biocementation treatment followed by a 0.01% sodium alginate PolyMAF treatment and a second biocementation treatment. As shown, in the non-cross-sectioned samples, large calcite crystals could be observed on the surface of sand grains that appeared to be chemically damage. This included the presence of spherical voids that resembled cavities possibly resulting from the presence of gas bubbles. The observed damage suggested that these larger crystals were likely present prior to the PolyMAF

treatment and thus were likely formed during the first cementation treatment. In addition, smaller crystals were also present on soil surfaces and on the top of the larger calcite crystals surfaces that exhibited more cubic forms and clean crystal surfaces. This suggested that such forms were likely not exposed to PolyMAF treatments and may have formed during the second cementation treatment. Cross-sectioned and polished samples were also imaged to examine material internal structures. As a consequence of cutting these samples, some damage to the material surfaces and structure can result including the propagation of fractures. In some cases, fragments of samples can also delaminate and be stripped off cross-sections. Despite these disturbances, the cross-sections provided an opportunity to examine the presence of the polymer layer and possible gas inclusions. As shown in the bottom left figure, a single crystal can be seen attached to the soil particle with an external coating existing around the crystal. At this coating discontinuity, several small voids could also be observed possibly indicating the presence of gas inclusions. Such clear coatings were not always observed, however. For example, in the bottom right figure an Ottawa sand particle can be seen with many calcite crystals existing around the particle surface. This included both larger crystals as well as some smaller crystals. Although some voids can be observed, a clear polymer discontinuity is not observed suggesting that precipitates formed during the second cementation did not always coat the polymer layer adjacent to larger crystals.

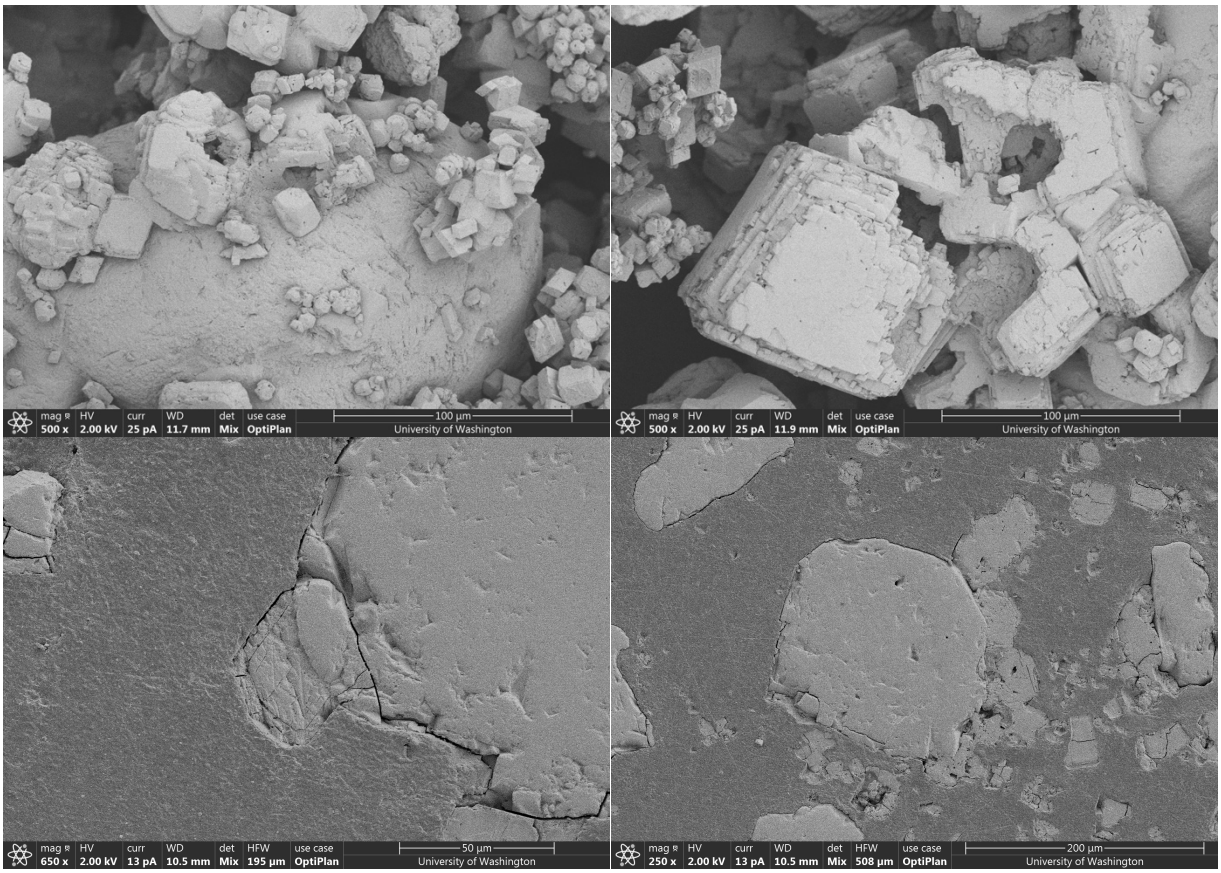

Fig. 3.2. SEM images of granular samples (top left and right) and polished cross-sections (bottom left and right) from Experiment T1 (MICP – PolyMAF – 2nd MICP).

Energy dispersive spectroscopy was also completed to determine the elemental compositions of these materials intended to distinguish the polymer layer from the parent soil and the calcium carbonate precipitates (**Fig. 3.3**). As shown, the soil particles could be clearly highlighted due to their higher silica concentrations with calcium carbonate precipitates showing high concentrations of calcium. During the PolyMAF treatment both sodium ions and alginate were introduced. This was expected to be most clearly identified through higher concentrations of sodium, as carbon present in the alginate was also present in the mounting tape and within calcium carbonate precipitates. As shown, higher concentrations of sodium could be observed near select precipitates

but was largely absent from silica surfaces likely suggesting the incorporation of the sodium alginate within select biocemented crystals. Interestingly, higher concentrations of aluminum and chloride were also found in these same locations.

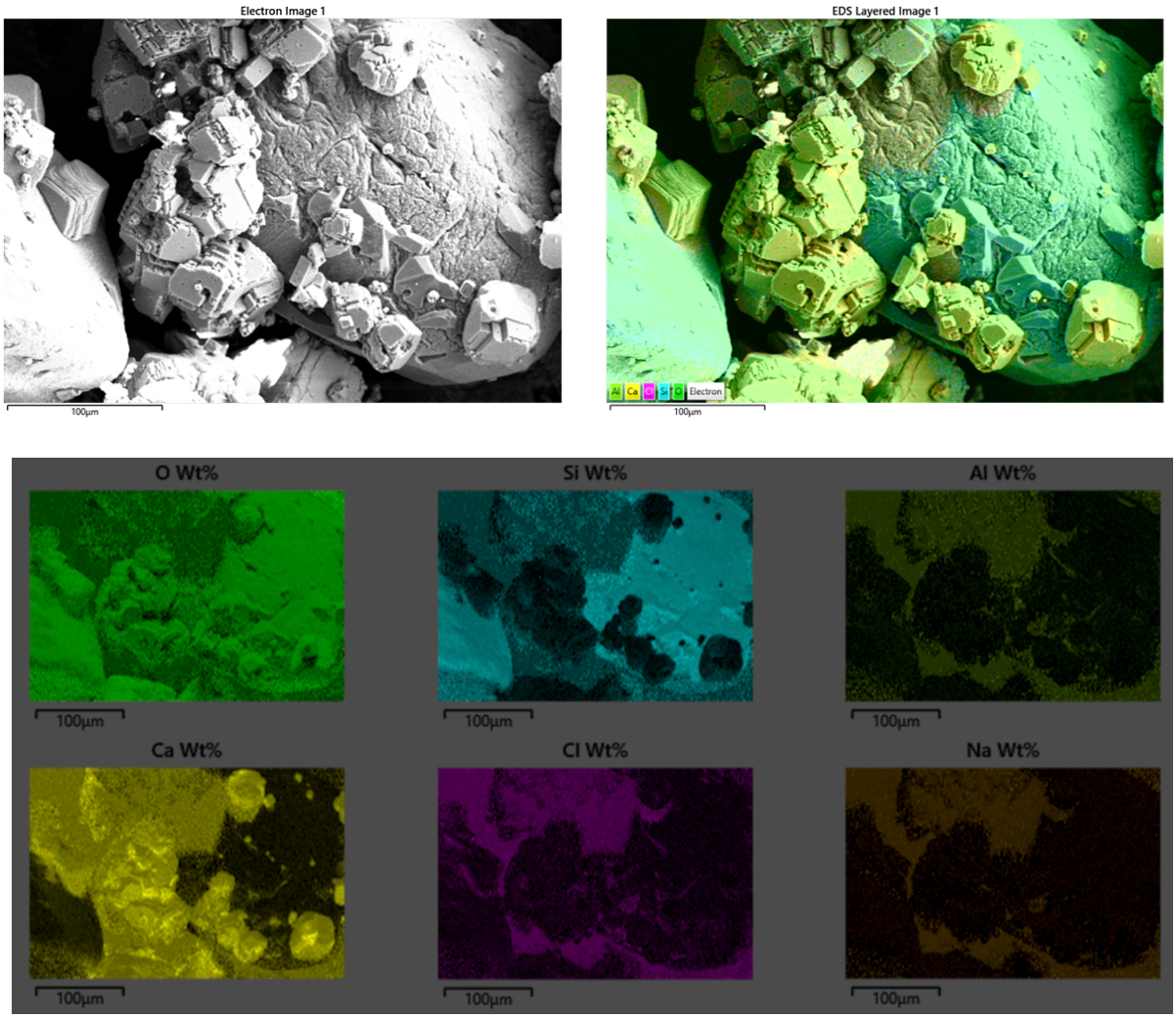

Fig. 3.3. SEM image (upper left) of a select region from Experiment T1 (MICP - PolyMAF (0.01%) - 2nd MICP) with an EDS layered image (upper right), and EDS elemental composition maps (bottom series of images).

In Experiments T2, T3, and T4, the inclusion of chemical tracers, KBr, $MgCl_2$, and NaBr during PolyMAF solely was explored. As shown in **Fig. 3.4, the** morphology of the precipitated materials

did not appear to be dramatically influenced when compared to the non-amended control Experiment T1. Again, large crystals could be observed on soil surfaces, with small crystals also precipitated throughout the sample likely from the second cementation treatment. When examining these materials using EDS (**Fig. 3.5, 3.6, and 3.7**), it appeared that the incorporation of certain tracers into PolyMAF solutions resulted in the presence of certain elements on soil and crystal surfaces alike but did not necessarily improve our ability to definitively differentiate different treatment phases. This may have resulted in part from the coating of all surfaces with some amount of the generated polymer film from the PolyMAF treatment.

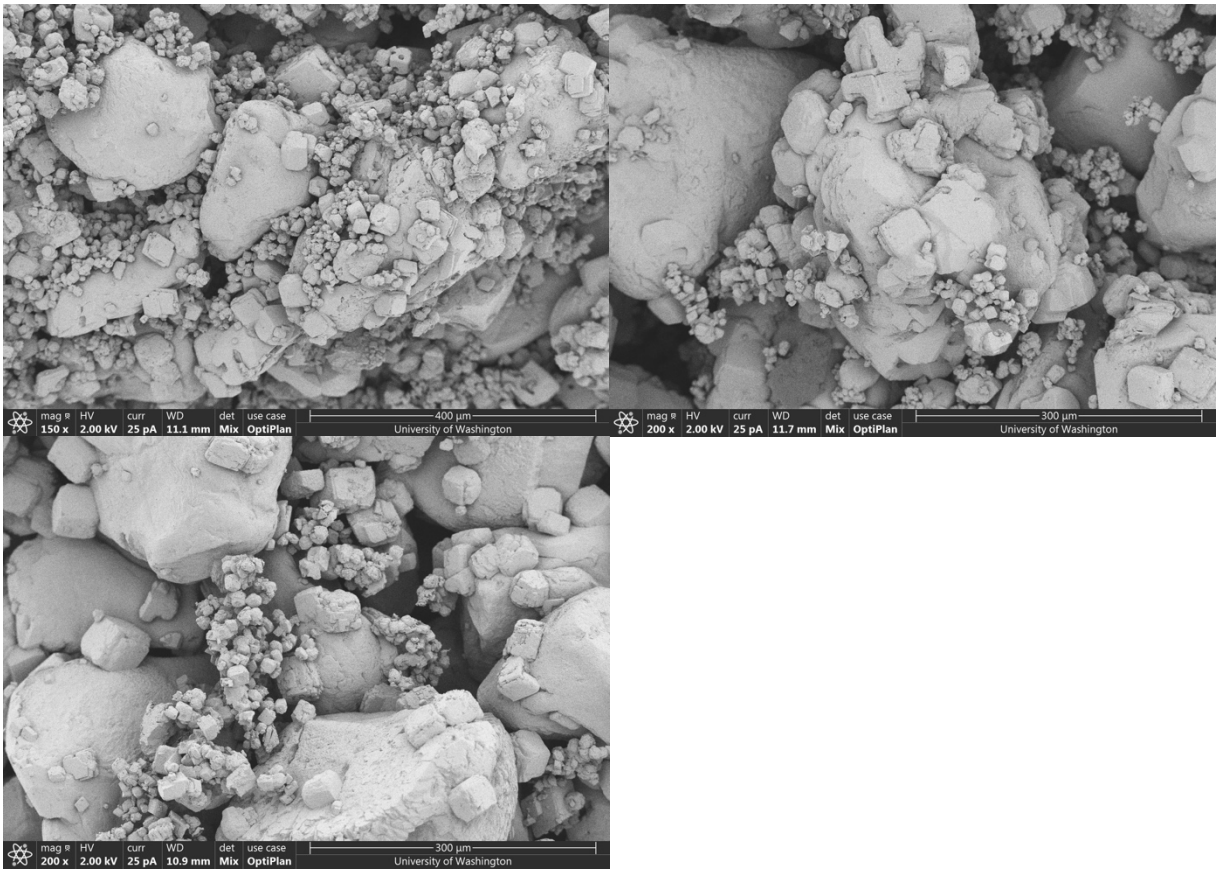

Fig. 3.4 SEM images of treated soil samples from Experiment T2 (upper left, MICP - PolyMAF (0.01%, 500 mM KBr) - 2nd MICP), T3 (upper right, MICP - PolyMAF (0.01%, 50 mM $MgCl_2$) - 2nd MICP), and T4 (bottom left, MICP - PolyMAF (0.01%, 500 mM NaBr) - 2nd MICP).

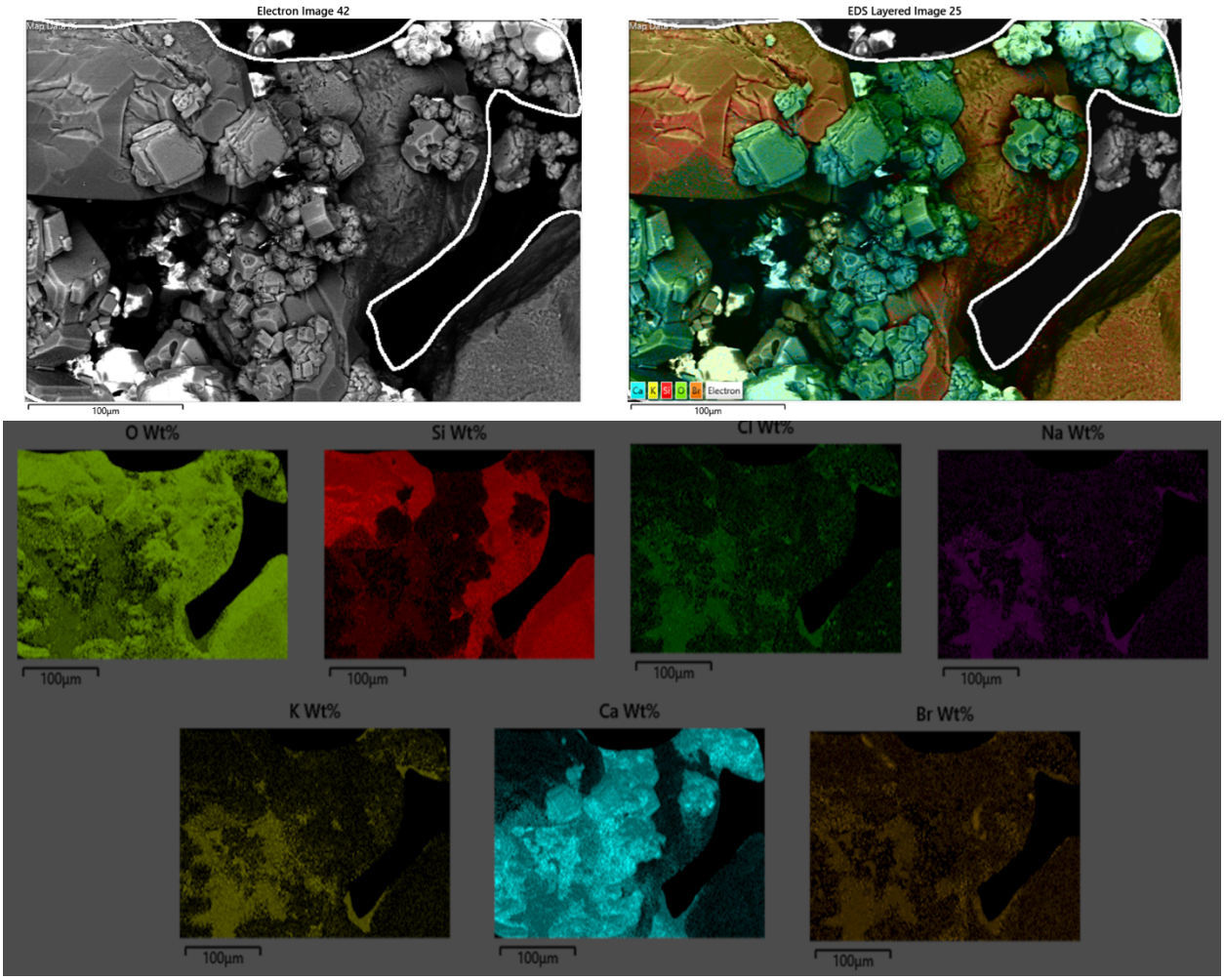

Fig. 3.5. SEM image (upper left) of a select region from Experiment T2 (MICP - PolyMAF (0.01%, 500 mM KBr) - 2nd MICP) with an EDS layered image (upper right), and EDS elemental composition maps (bottom series of images).

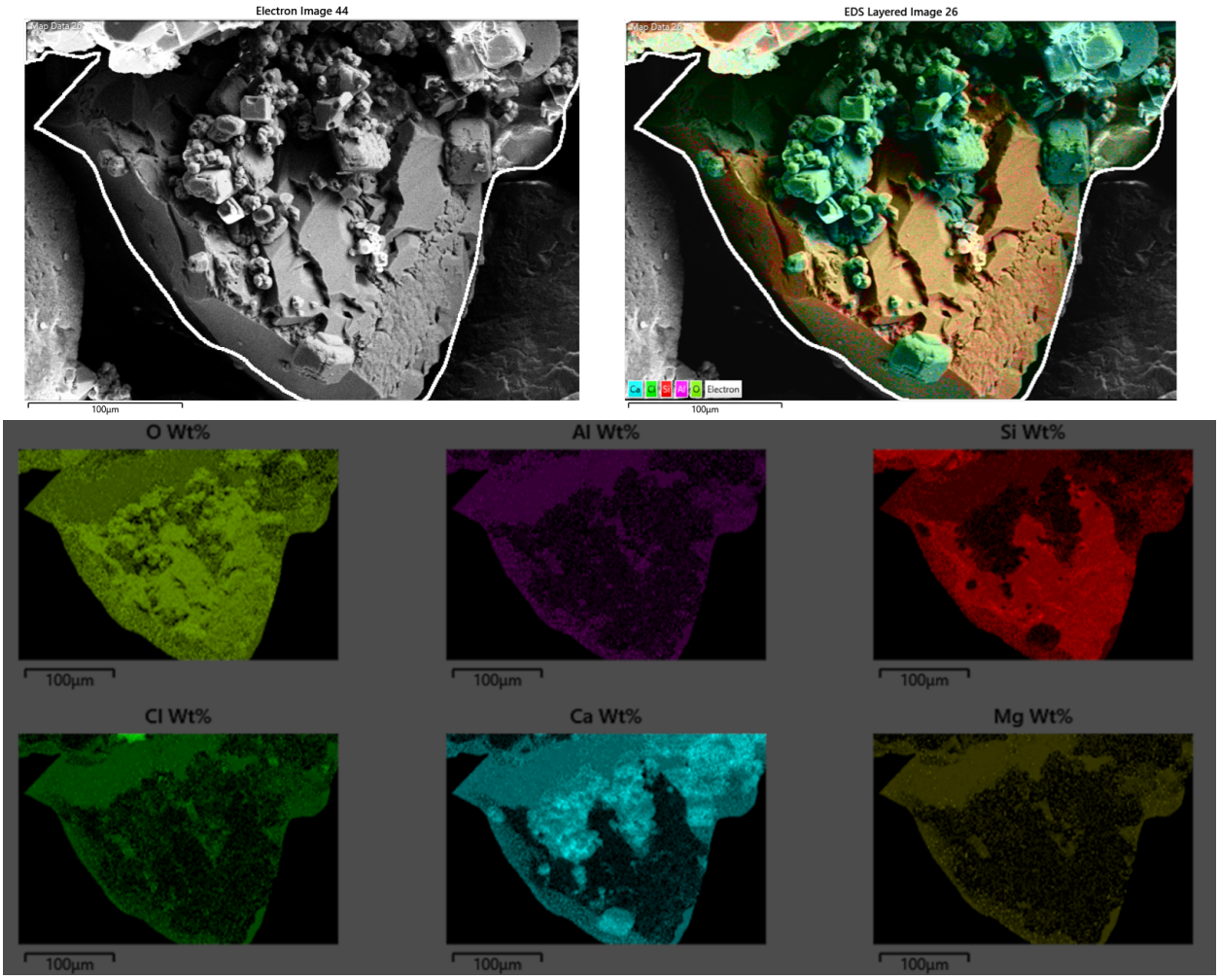

Fig. 3.6. SEM image (upper left) of a select region from Experiment T3 (MICP - PolyMAF (0.01%, 50 mM $MgCl_2$) with an EDS layered image (upper right), and EDS elemental composition maps (bottom series of images).

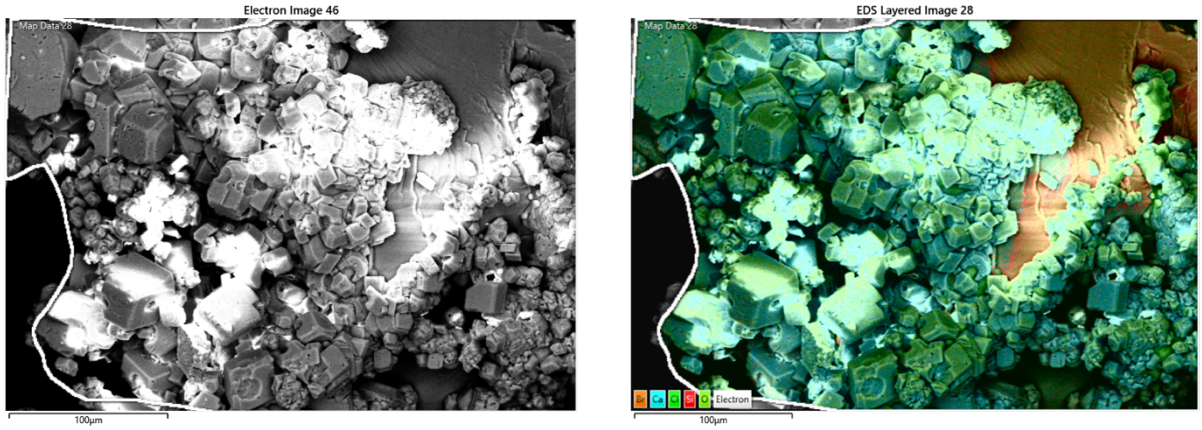

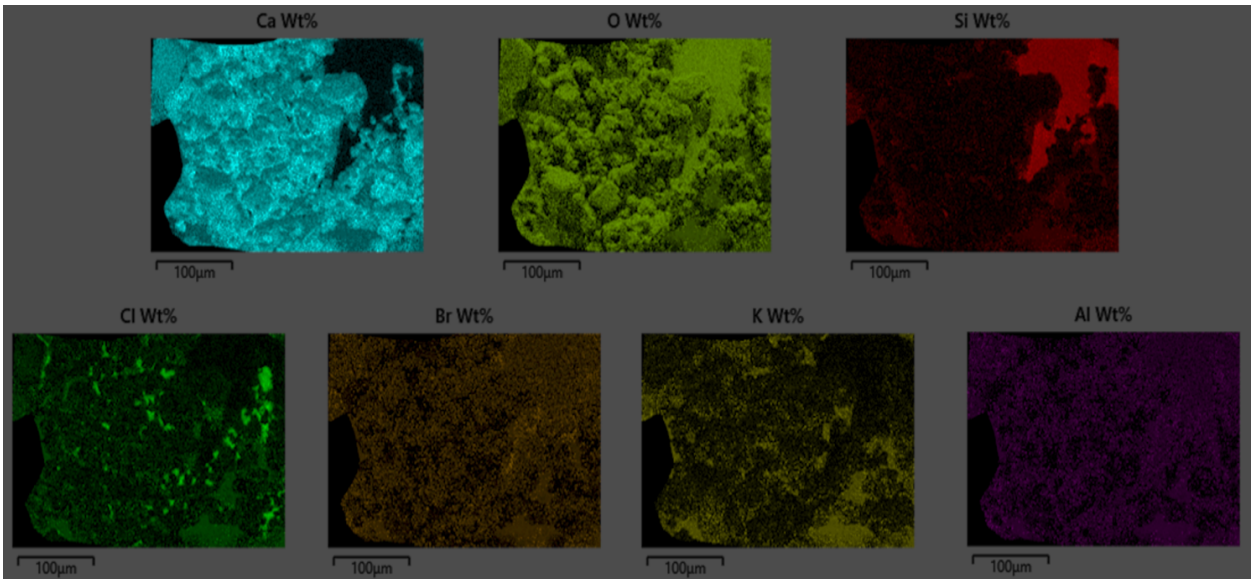

Fig. 3.7. SEM image (upper left) of a select region from Experiment T4 (MICP - PolyMAF (0.01%, 500 mM NaBr) - 2nd MICP) with an EDS layered image (upper right), and EDS elemental composition maps (bottom series of images).

Figure 3.8 presents images for Experiment T5 which received a biocementation treatment followed by a 0.01% sodium alginate PolyMAF treatment and a second biocementation treatment containing 50 mM magnesium chloride. As shown, large differences in cementation morphology were observed when compared to other experiments not receiving the magnesium chloride additions in the second cementation treatment. While larger crystals were still observed likely resulting from the first cementation event, the smaller crystals believed to result from the second cementation injection were oriented closely with larger crystals forming a near uniform coating of the existing larger crystals. This was unlike all other previous experiments, wherein the second cementation treatment appeared to generate smaller crystals sporadically throughout soil samples with minimal coating of existing precipitates. There also appeared to be small voids on the surface of these smaller crystal coatings in the Experiment T5 specimen possibly due to incomplete coating of precipitates and/or underlying gas bubbles within the polymer film presumed to exist beneath

this layer. Treated soil samples from Experiment T5 were also embedded within epoxy and cross-sectioned to examine material internal structure. As shown in **Figure 3.9.**, in numerous instances a clear material discontinuity within crystals could be observed likely at the location of the polymer film and between the larger crystals formed from the first cementation injection and the smaller crystal-based coating formed during the magnesium amended second cementation treatment. At this discontinuity where the polymer film was likely present, small voids were also observed which were to be entrapped gas bubbles that remained on the surface of these larger crystals within the polymer film and were coated later with the materials formed during the second cementation event.

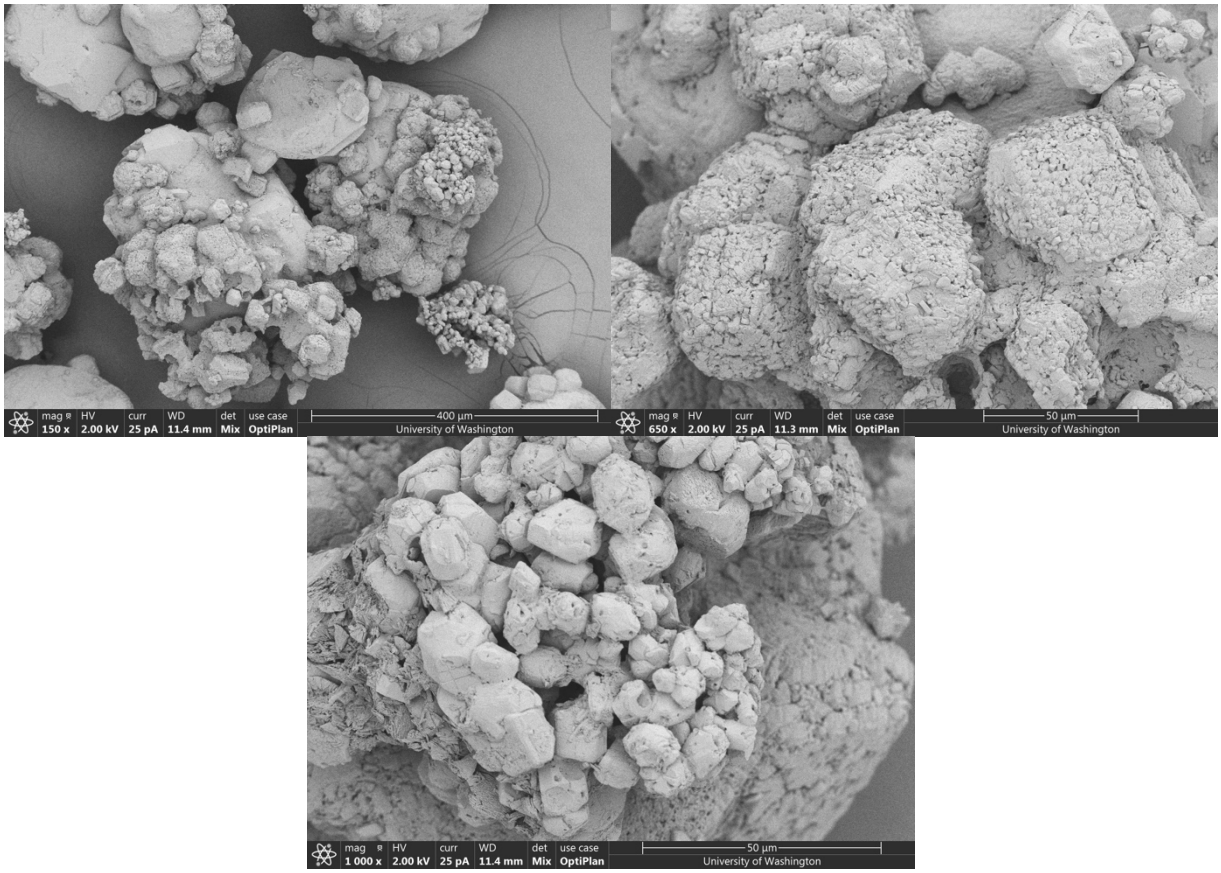

Fig. 3.8. SEM images of treated soil samples from Experiment T5 (MICP - PolyMAF (0.01%) - 2nd MICP (50 mM $MgCl_2$)) at various magnifications.

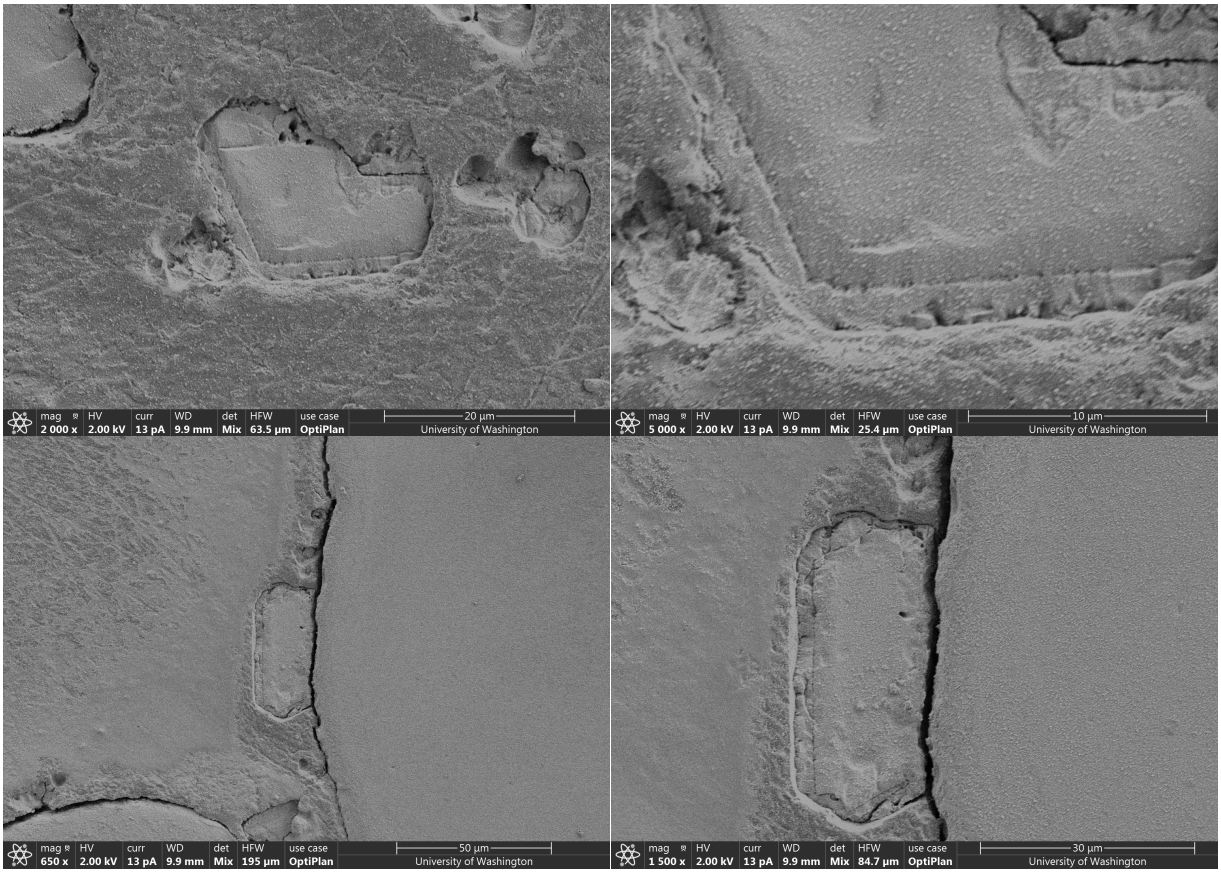

Fig. 3.9. SEM images of polished cross-sections from Experiment T5 (MICP - PolyMAF (0.01%) - 2nd MICP (50 mM $MgCl_2$)).

EDS scanning of treated soils from Experiment 5 was also performed to determine definitively where precipitation formed during the second cementation treatment resided. When magnesium was not added to other samples (e.g., Experiment T1), no detectable magnesium was observed, suggesting that this element could provide a reliable chemical signature for Experiment T5. As shown in **Figure 3.10**, when granular samples were scanned, concentrations of magnesium appeared to be greatest at select locations on the surface of calcium carbonate crystals but were not found to exist alone on clean silica surfaces without calcium carbonate being present. This

suggested that the mineral coating resulting from the second cementation treatment was likely magnesian calcite and not a pure magnesium carbonate mineral (i.e., magnesite). To better understand material layering during these treatments, material cross-sections were also examined using EDS. **Figure 3.11.** presents EDS scans of one material cross-section location from Experiment 5. As shown, high concentrations of both magnesium and chloride can be observed only on the outermost layer of the larger calcite crystals. Although magnesium was expected, indicating the coating was formed during the second cementation injection, the presence of chloride was unexpected and may have suggested some incorporation of this counter-ion within the polymer layer upon the introduction of the second cementation treatment. Interestingly, these high magnesium and chloride concentrations were not observed on the clean silica surfaces and instead appeared to only exist on the outermost layer of calcium carbonate crystals wherein the material layering was observed again suggesting that materials formed during the second cementation selectively coated existing larger crystals and not clean silica particle surfaces.

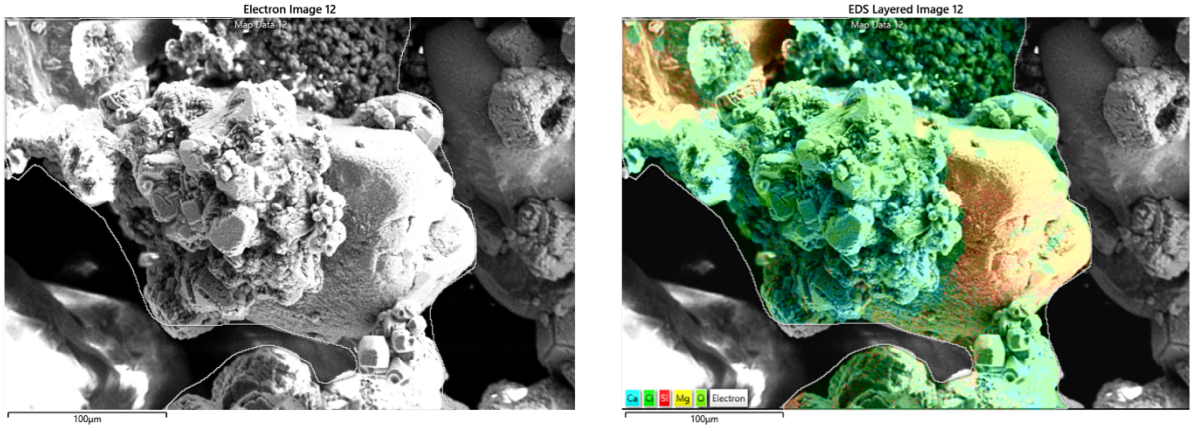

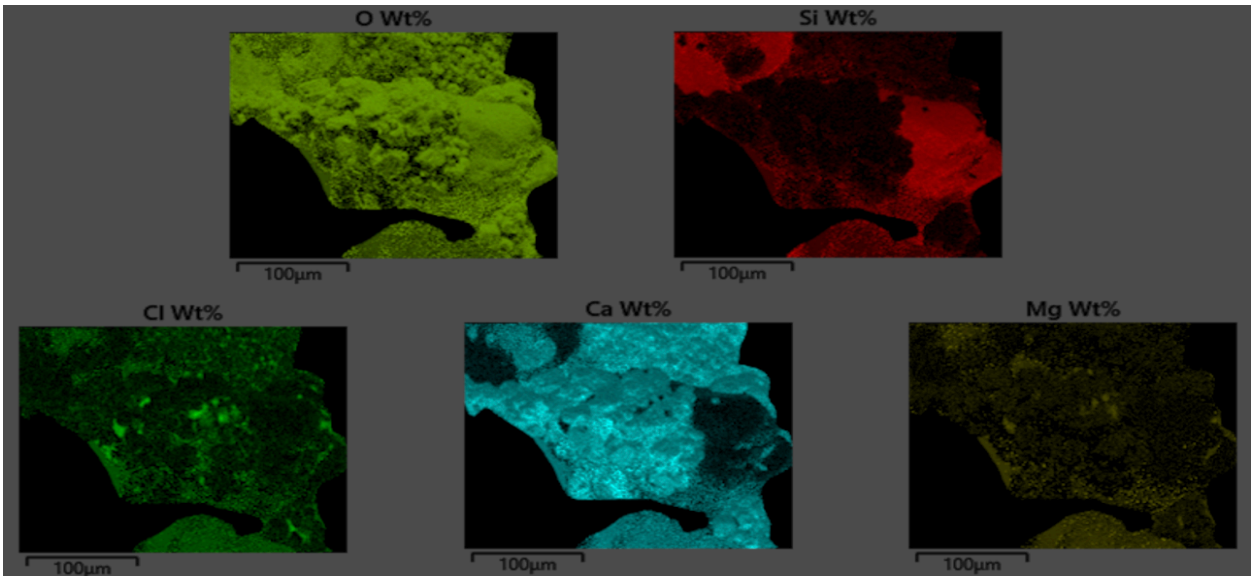

Fig. 3.10. SEM image (upper left) of a select region from Experiment T5 (MICP - PolyMAF (0.01%) - 2nd MICP (50 mM $MgCl_2$)) with an EDS layered image (upper right), and EDS elemental composition maps (bottom series of images).

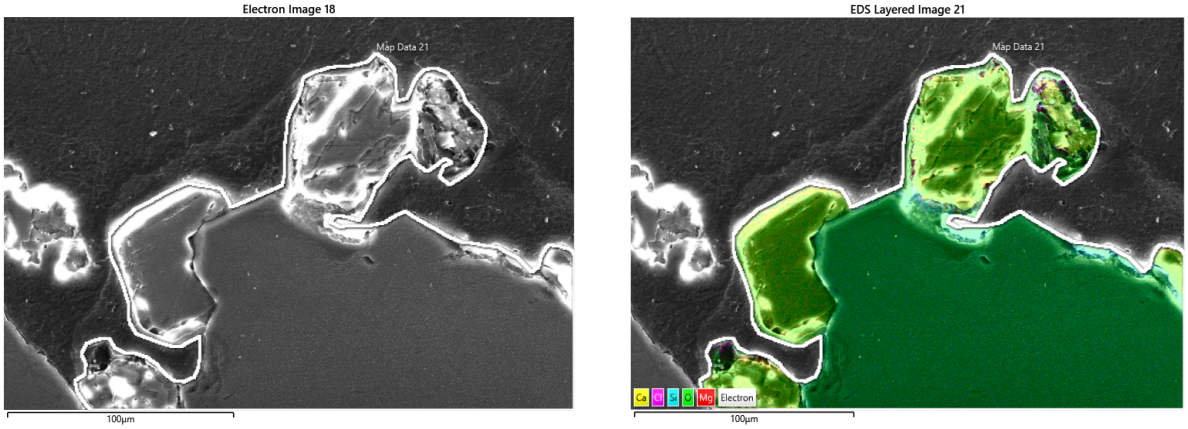

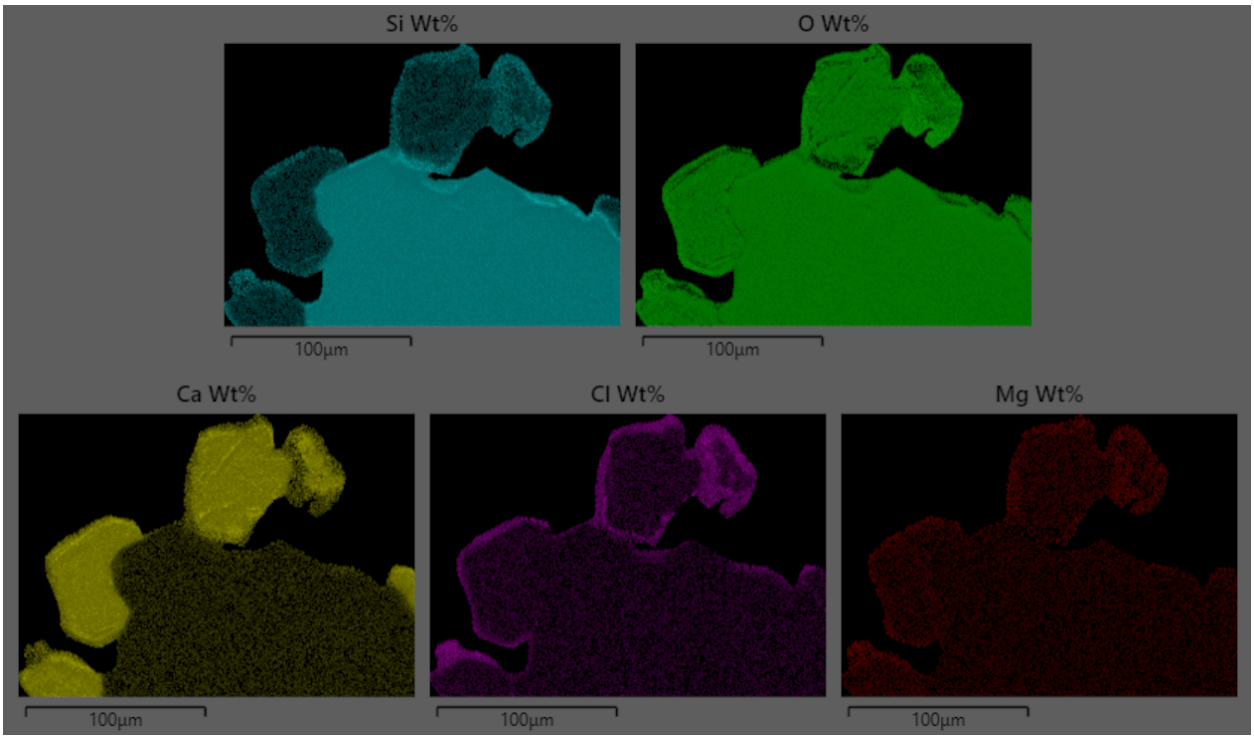

Fig. 3.11. SEM image (upper left) of a material cross-section from Experiment T5 (MICP - PolyMAF (0.01%) - 2nd MICP (50 mM $MgCl_2$)) with an EDS layered image (upper right), and EDS elemental composition maps (bottom series of images).

In Experiment T6, a similar $MgCl_2$ tracer was applied during the second cementation treatment but at a higher concentration of 250 mM. **Figure 3.12** presents images for Experiment T6 which received a biocementation treatment followed by a 0.01% sodium alginate PolyMAF treatment and a second biocementation treatment containing 250 mM magnesium chloride. As shown, similar crystal morphologies as Experiment T5 were observed in Experiment T6 with many smaller crystals precipitating during the second cementation treatment on the surface of the larger existing calcium carbonate crystals. This coating appeared thicker than that observed in Experiment T5 with crystal surfaces appearing to have a rougher and more jagged surface texture. Spherical voids were again also present at the surface of these materials indicating either

incomplete coatings, voids between crystals, or possibly the presence and collapse of gas voids. **Figure 3.13.** presents images of polished material cross-sections from Experiment T6, which were again intended to examine material internal structures. As shown, the second cementation coating appeared thicker and had more voids when compared to the Experiment T5 cross-section. The outer layer also appeared to be increasingly rough and caused some disturbances during the cross-sectioning process, with more material fracturing, uneven cuts in the epoxy, and delamination present at times. This also appeared to dull the slow saw blade during the cutting process. Unfortunately, these disturbances prevented more definitive changes in structure from being distinguished, however, voids were again clearly visible at what was suspected to be the material discontinuity resulting from the polymer film.

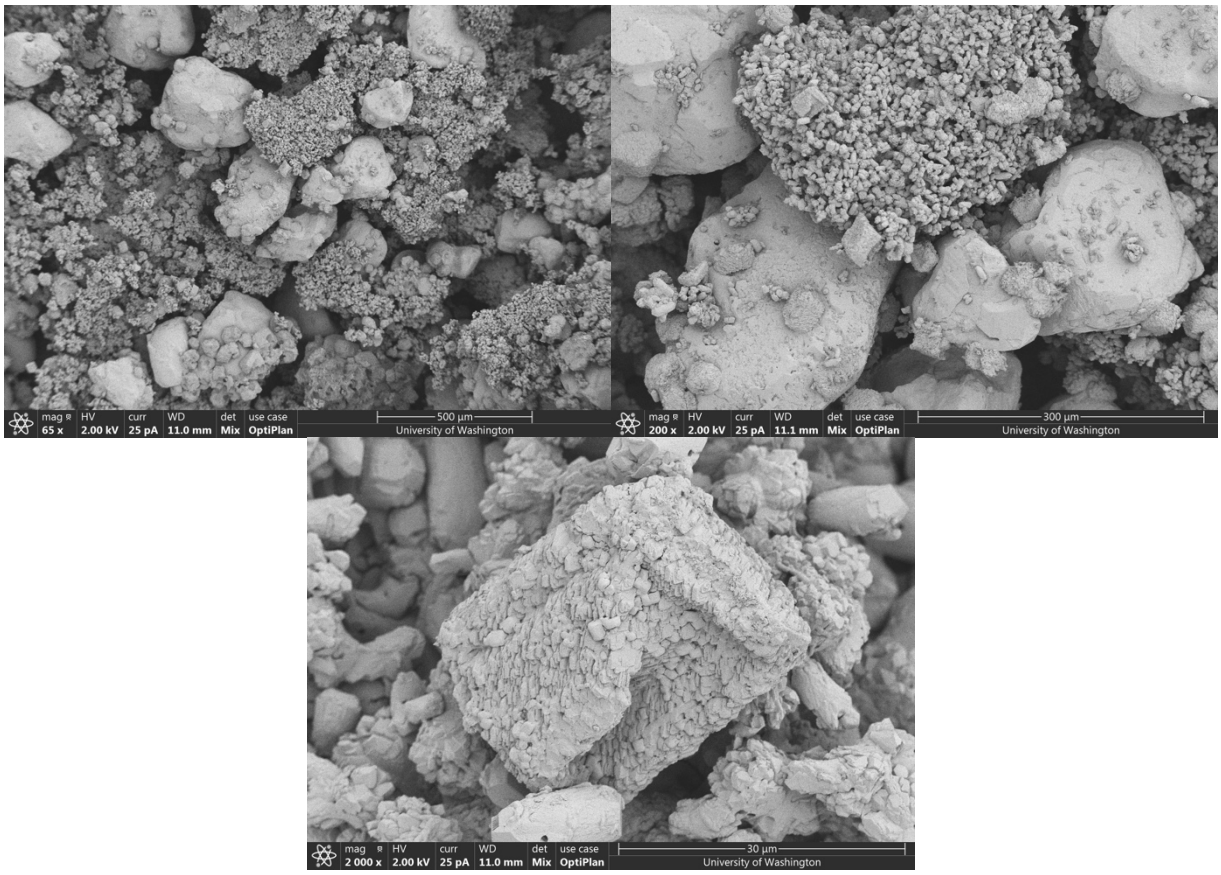

Fig. 3.12. SEM images of treated soil samples from Experiment T6 (MICP - PolyMAF (0.01%) - 2nd MICP (250 mM $MgCl_2$)) at various magnifications.

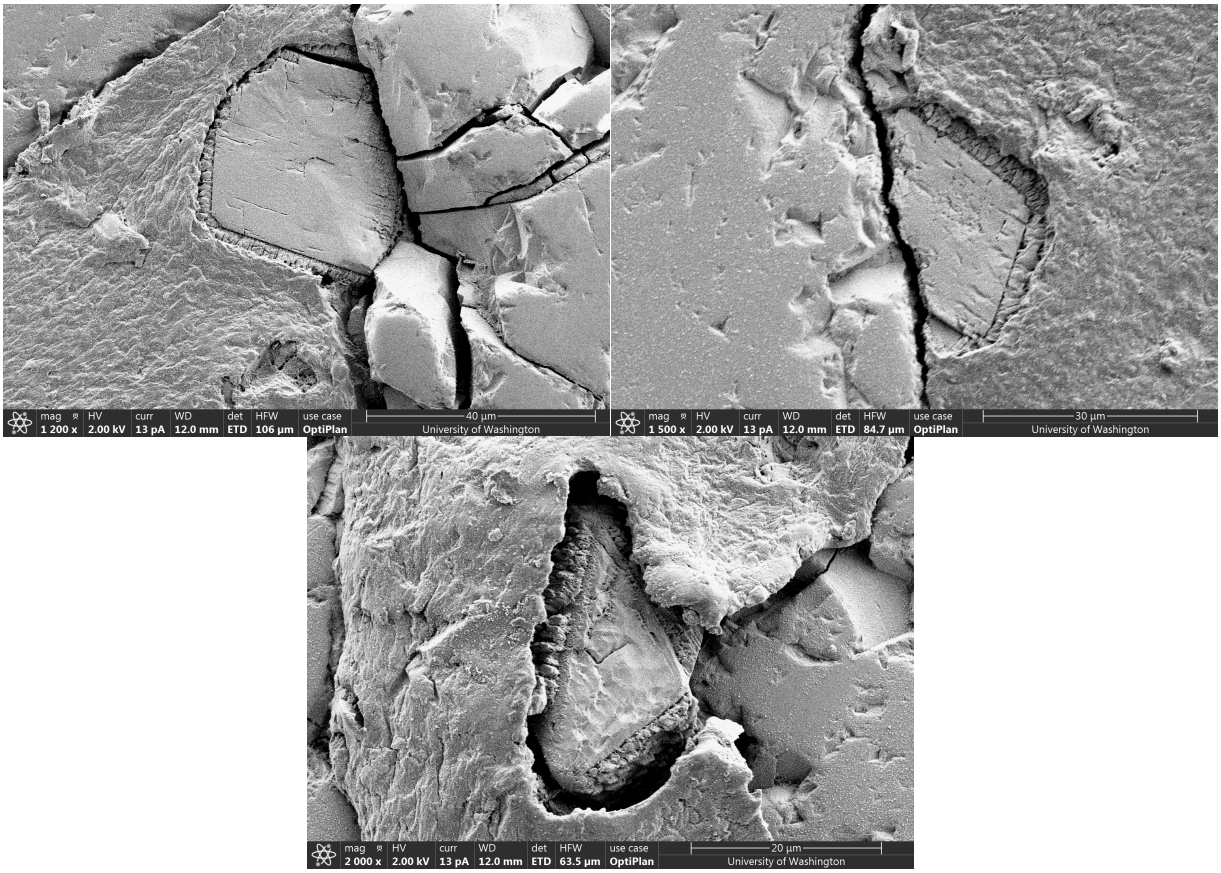

Fig. 3.13. SEM images of polished cross-sections from Experiment T6 (MICP - PolyMAF (0.01%) - 2nd MICP (250 mM $MgCl_2$)).

Magnesium incorporated during the 2nd cementation treatment in Experiment T6 was also again detected via EDS (**Fig. 3.14**). Again, higher concentrations of chloride and magnesium appeared to be coincident with the locations of calcium carbonate crystals and in some locations also now appeared to exist on clean silica surfaces unlike Experiment T5. The observed morphologies were extremely rough and poorly formed when compared to earlier experiments without magnesium possibly suggesting the presence of new mineral phases and/or amorphous minerals. Clusters of

small crystals also again as expected showed increasing concentrations of magnesium. **Figure 3.15.** presents images of polished material cross-sections from Experiment T6, which were again intended to examine material internal structures. As shown, high abundances of magnesium and chloride were again detected in the surrounding areas of the larger calcium carbonate crystals and appeared to be more abundant than in Experiment T5, likely due to the use of higher magnesium concentrations.

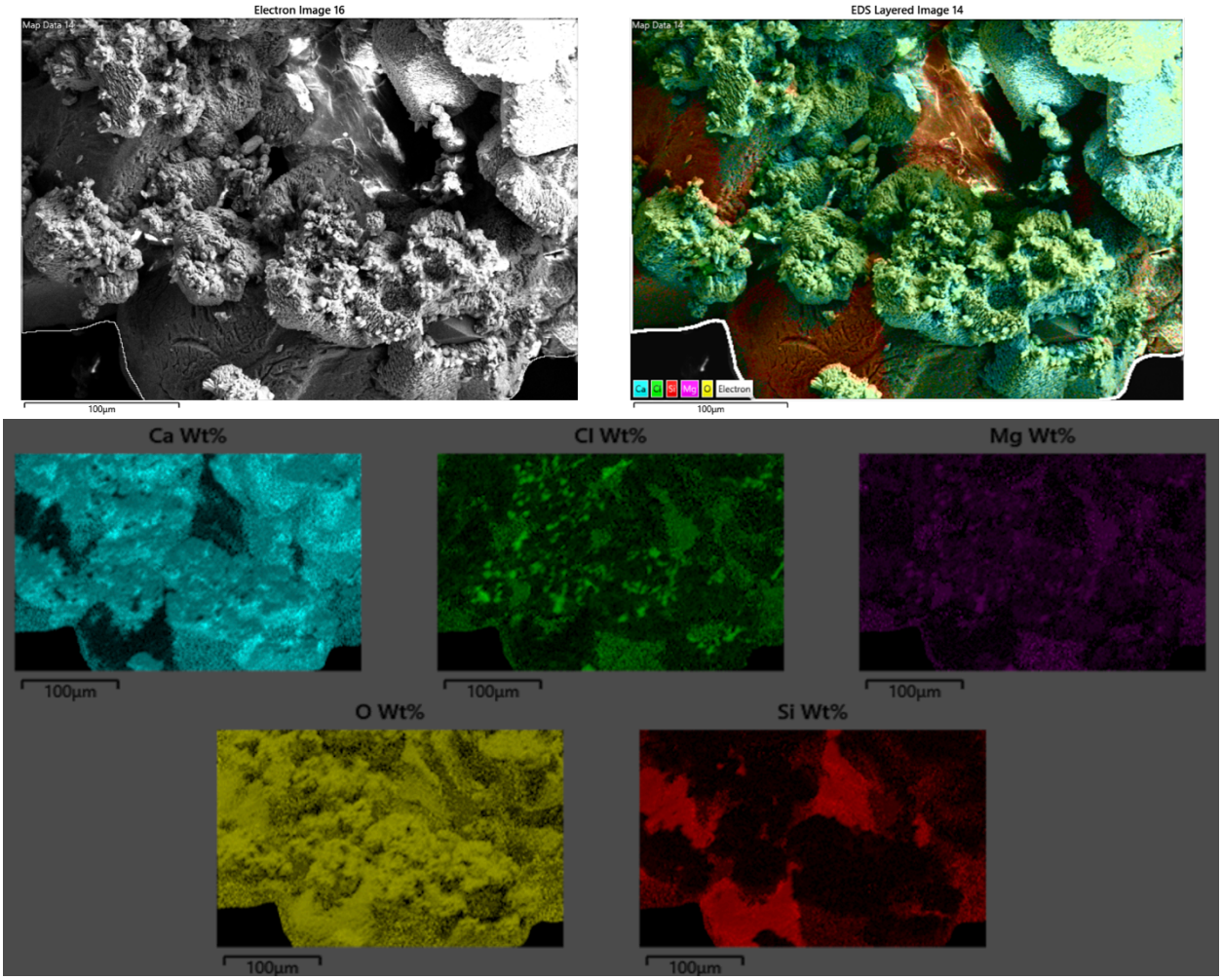

Fig. 3.14. SEM image (upper left) of a select region from Experiment T6 (MICP - PolyMAF (0.01%) - 2nd MICP (250 mM $MgCl_2$)) with an EDS layered image (upper right), and EDS elemental composition maps (bottom series of images).

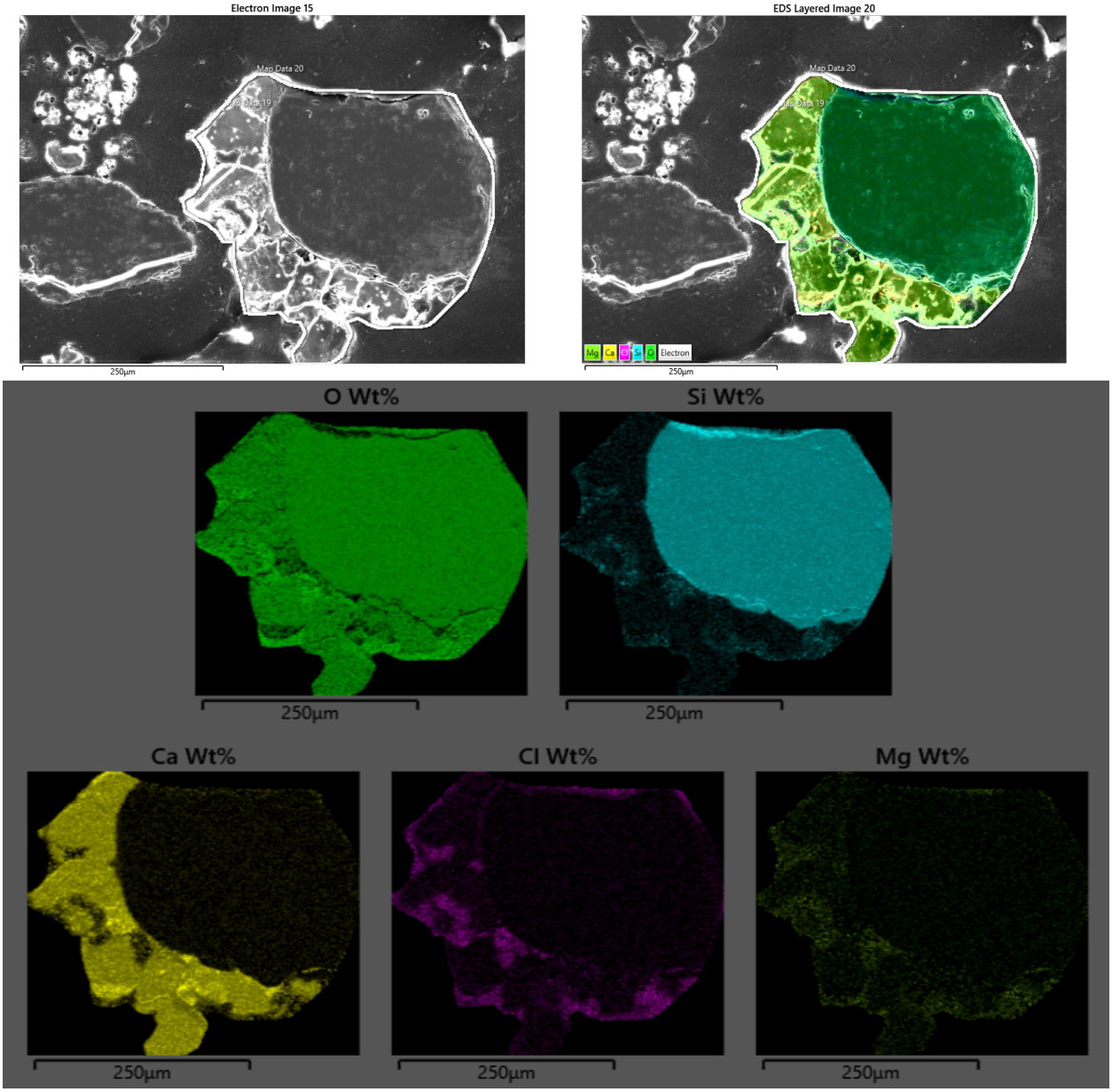

Fig 3.15. SEM image (upper left) of a material cross-section from Experiment T6 (MICP - PolyMAF (0.01%) - 2nd MICP (250 mM $MgCl_2$)) with an EDS layered image (upper right), and EDS elemental composition maps (bottom series of images).

Figure 3.16 presents images for Experiment T7 which received a biocementation treatment followed by a 0.01% sodium alginate PolyMAF treatment containing 500 mM sodium bromide

and a second biocementation treatment containing 250 mM magnesium chloride. The morphologies observed were similar to Experiment T7 suggesting that the sodium bromide polymer addition had minimal effects. Interestingly, however, some locations wherein smaller calcite crystals appeared to collapse on themselves leaving behind a spherical void were observed. When examining polished cross-section images (**Fig. 3.17**) internal strcutures appeared similar to other second cementation magnesium containing experiments. Small spherical voids could also be again observed at the polymer layer material discontinuty.

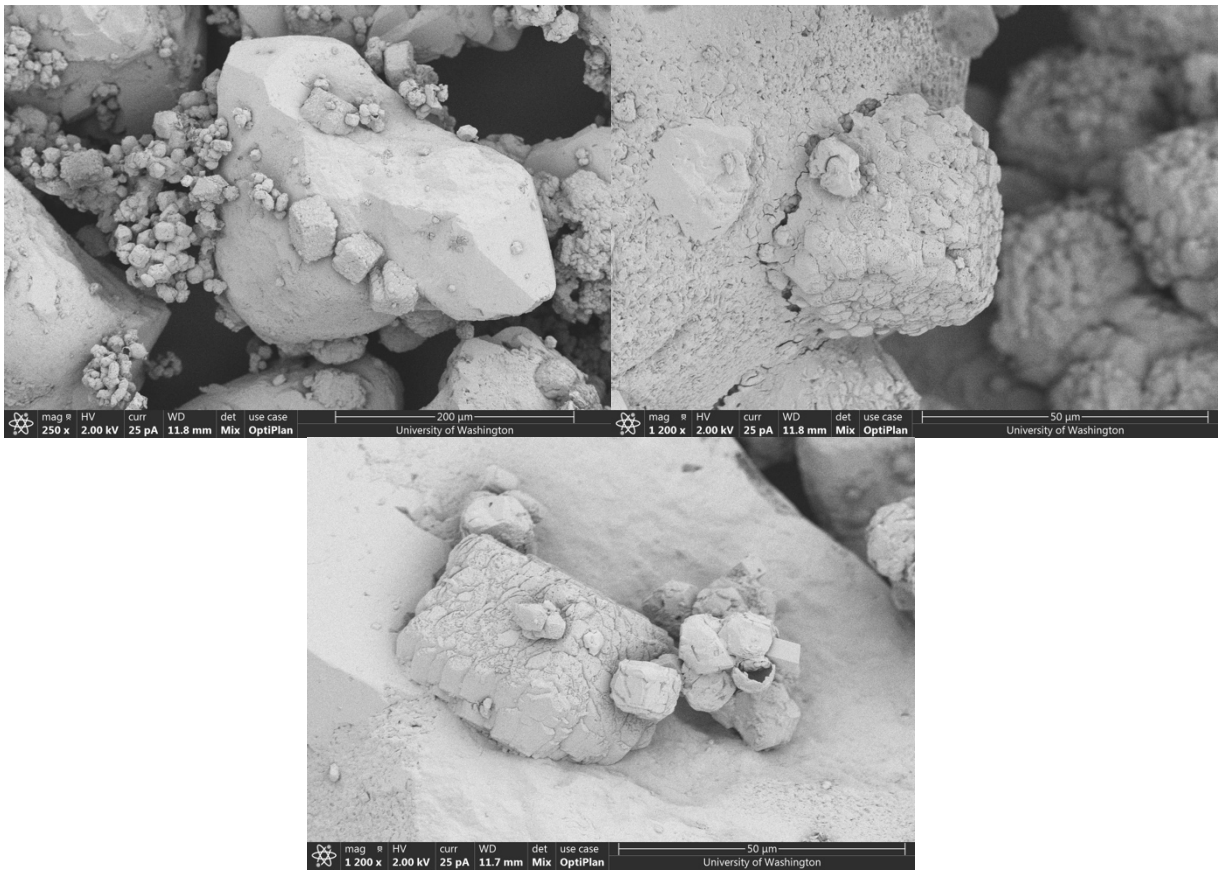

Fig. 3.16. SEM images of treated soil samples from Experiment T7 (MICP - PolyMAF (0.01%, 500 mM NaBr) - 2nd MICP (250 mM $MgCl_2$)) at various magntifications.

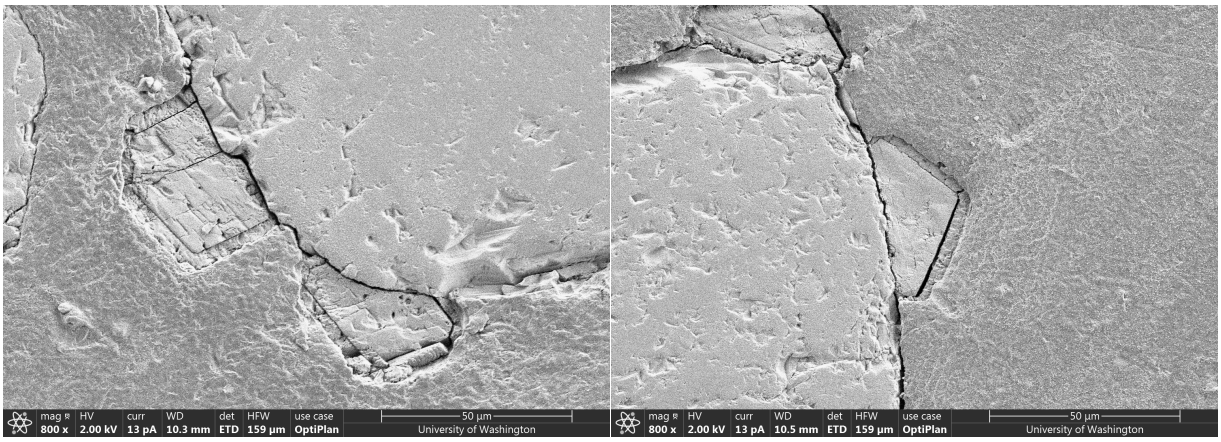

Fig. 3.17. SEM images of polished cross-sections from Experiment T7 (MICP - PolyMAF (0.01%, 500 mM NaBr) - 2nd MICP (250 mM $MgCl_2$)).

When examining this specimen with EDS, increases in magnesium and chloride were again detected in regions wherein smaller crystals were clustered (**Figure 3.18**) but with similar bromide concentrations observed across the entire sample. EDS scanning of polished cross-section samples was also completed as shown in **Figure 3.19**. Similar to previous $MgCl_2$-containing experiments, magnesium and chloride were detected at the surface of crystals and were even detected on silica particle surfaces likely due to the higher concentrations used (250 mM $MgCl_2$).

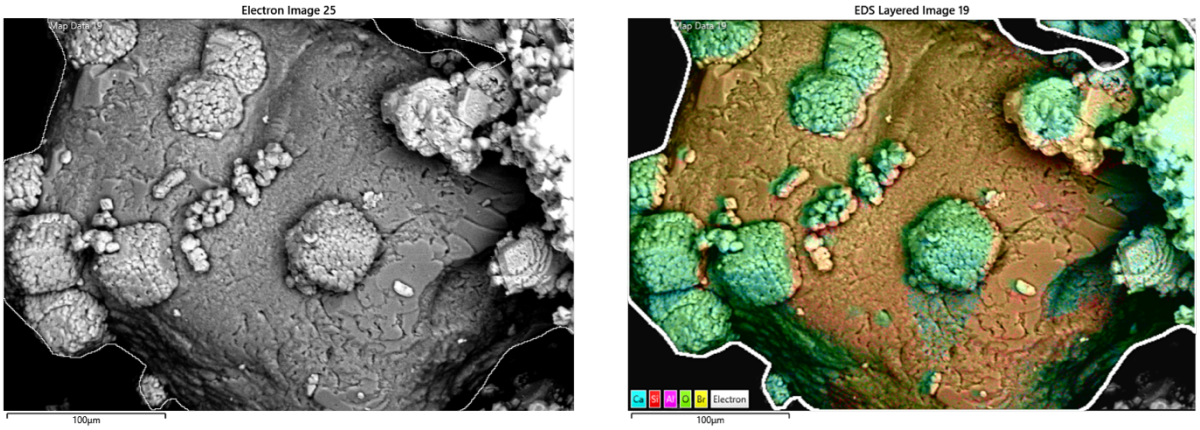

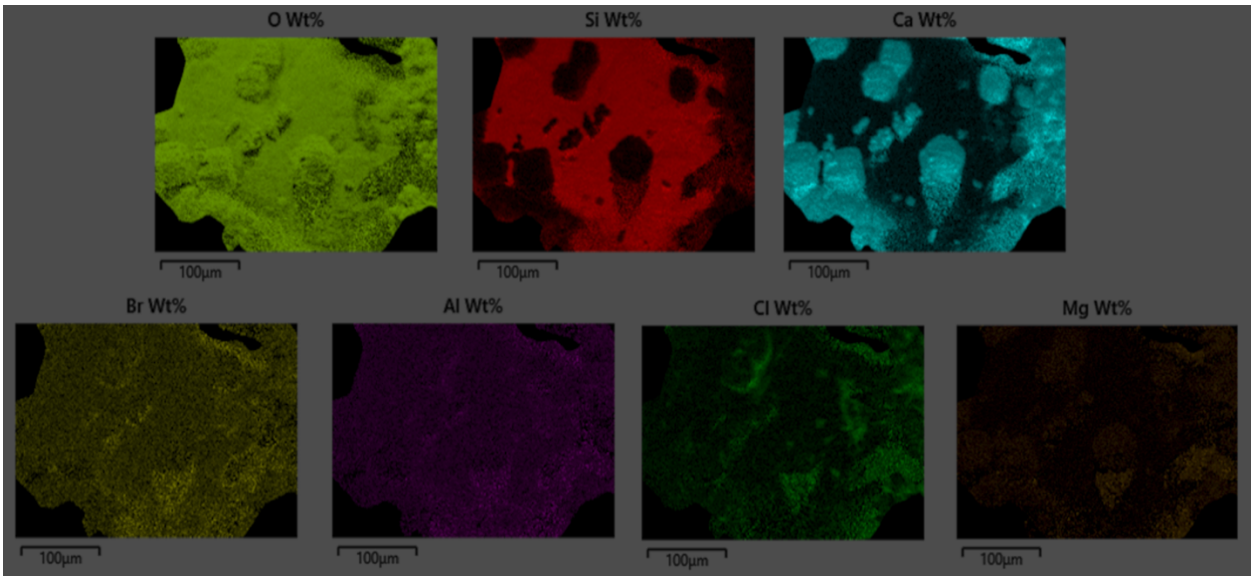

Fig. 3.18. SEM image (upper left) of a material cross-section from Experiment T7 (MICP - PolyMAF (0.01%, 500 mM NaBr) - 2nd MICP (250 mM $MgCl_2$)) with an EDS layered image (upper right), and EDS elemental composition maps (bottom series of images).

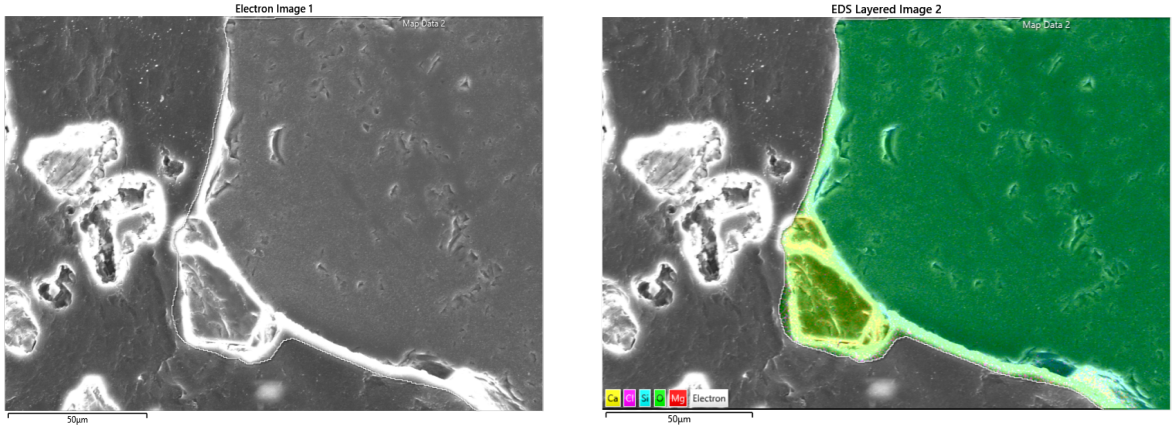

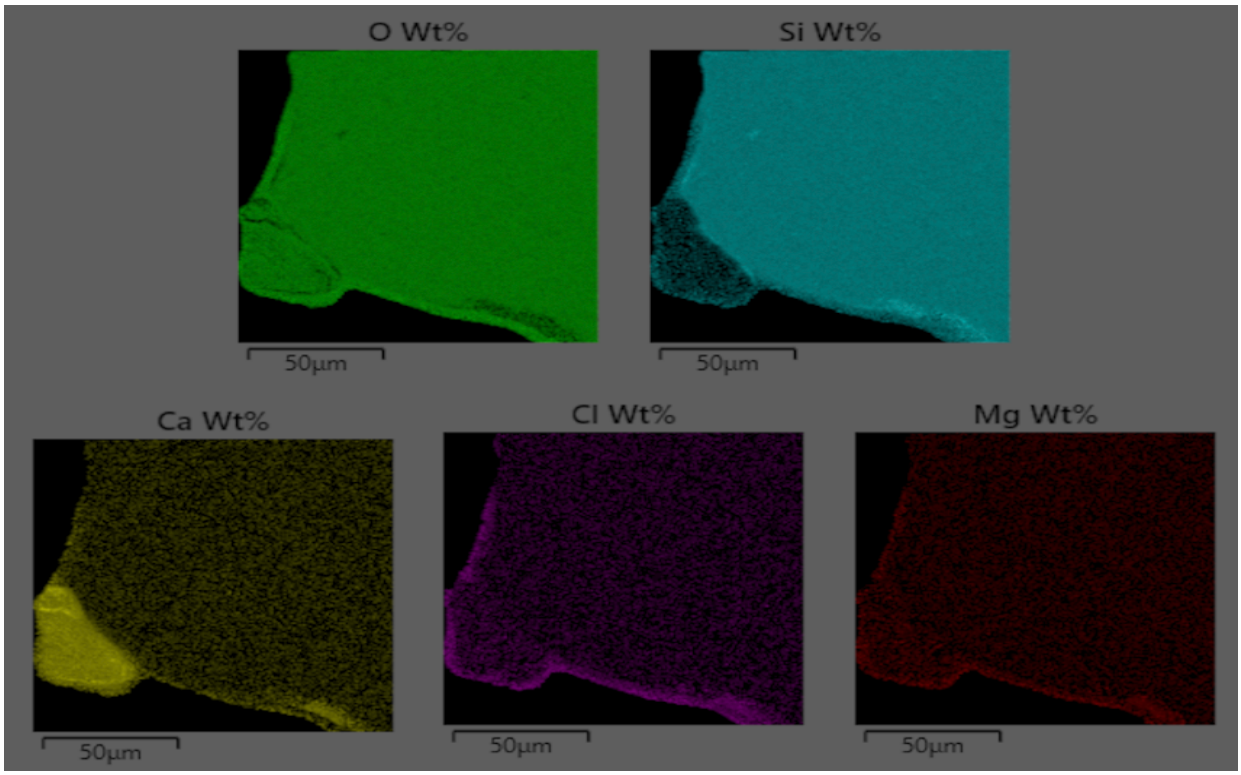

Fig 3.19. SEM image (upper left) of a material cross-section from Experiment T7 (MICP - PolyMAF (0.01%, 500 mM NaBr) - 2nd MICP (250 mM $MgCl_2$)) with an EDS layered image (upper right), and EDS elemental composition maps (bottom series of images).

Figure 3.20 presents images for Experiment T8 which received a biocementation treatment followed by a 0.01% sodium alginate PolyMAF treatment and a second biocementation treatment containing 500 mM potassium bromide. The morphology of the crystals appeared similar to Experiment T1, which did not have potassium bromide amendments, but perhaps appeared to have slightly more rounded edges on the smaller crystals. Unlike the magnesium amended experiments, however, the small crystals did not appear to coat surfaces preferentially and again appeared to exist more widespread within samples like Experiment T1. **Figure 3.21.** presents EDS scans of a subsection of the treated soil in Experiment T8. As shown, the locations where potassium was detected largely coincided with the locations of small precipitates, suggesting that it was a useful

addition towards enabling the tracking of precipitates formed during the second cementation treatment.

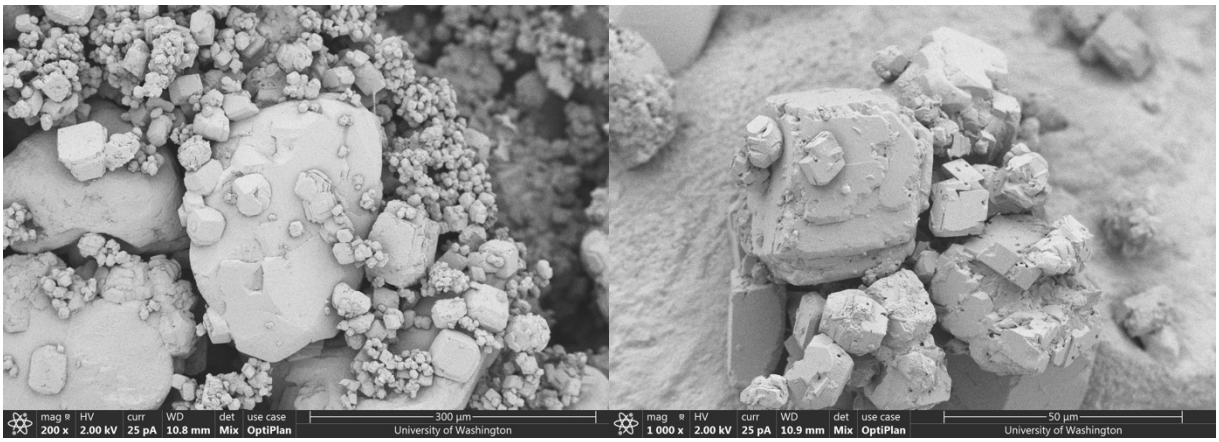

Fig. 3.20 SEM images of treated soil samples from Experiment T8 (MICP - PolyMAF (0.01%) - 2nd MICP (500 mM KBr)) at various magnifications.

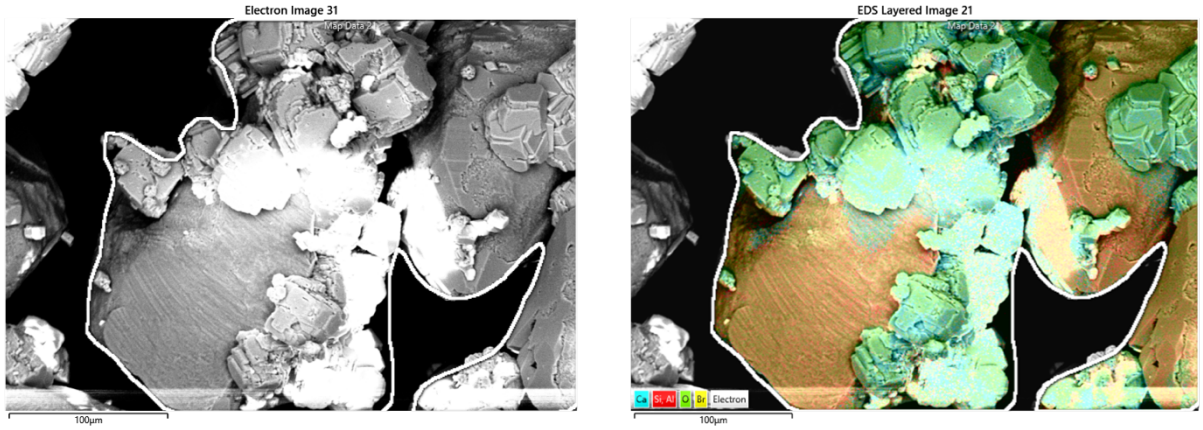

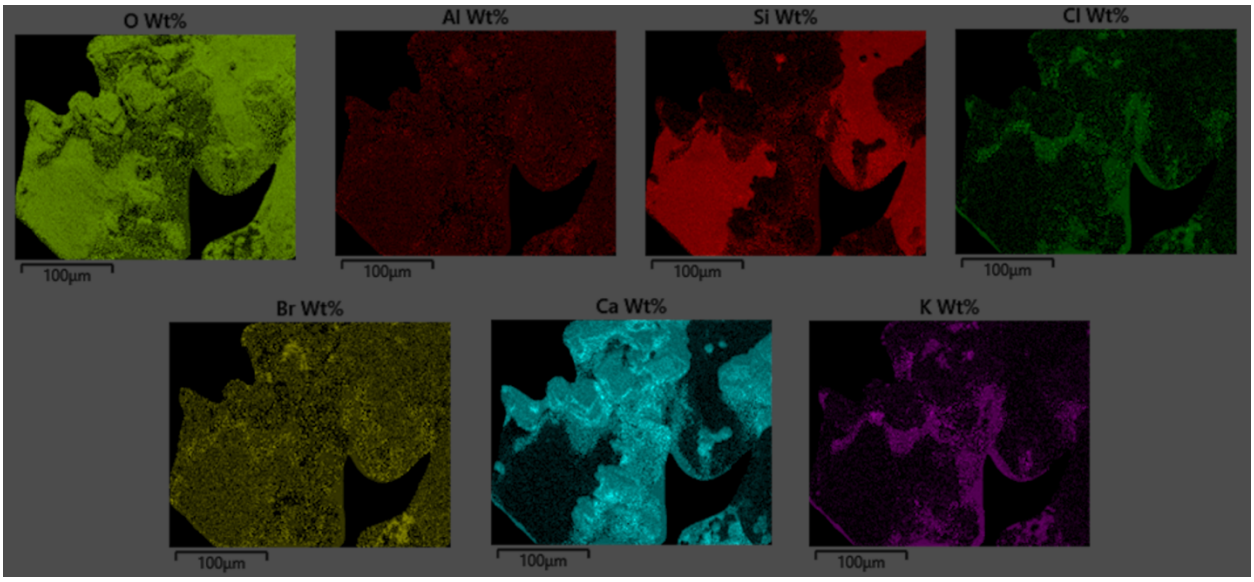

Fig. 3.21. SEM image (upper left) of a material cross-section from Experiment T8 (MICP - PolyMAF (0.01%) - 2nd MICP (500 mM KBr)) with an EDS layered image (upper right), and EDS elemental composition maps (bottom series of images).

As described earlier, three other experiments explored the effects of a calcium rinse treatment applied after the PolyMAF treatment intended to promote the formation of calcium alginate and increase gas bubble retention within the polymer layer. **Figure 3.22** presents SEM images of Experiment CR1 received a biocementation treatment followed by a 0.01% sodium alginate PolyMAF treatment, a calcium rinse, and a second biocementation treatment. As shown, it appeared that the addition of a calcium rinse promoted the formation of a polymer film over the existing calcium carbonate crystals. The polymer film coated both smaller and larger crystals and in some cases appeared to act as bonds between particles. Spherical voids that did not appear to be bacterial impressions were also found sporadically throughout the crystal surfaces possibly due to bubble formation and rupture. EDS scans of a section of Experiment CR1 was also performed as shown in **Figure 3.23.** The elemental composition appeared similar to Experiment T1 (MICP –

PolyMAF – 2nd MICP treatment) with perhaps slightly more calcium detected throughout the sample.

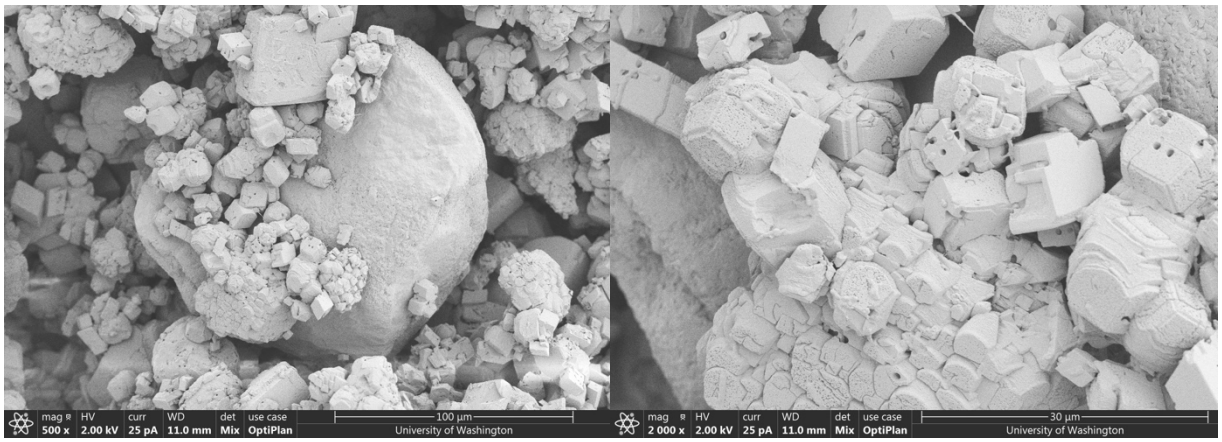

Fig. 3.22. SEM images of treated soil samples from CR1 (MICP - PolyMAF (0.01%) - Calcium Rinse - 2nd MICP) at various magnifications.

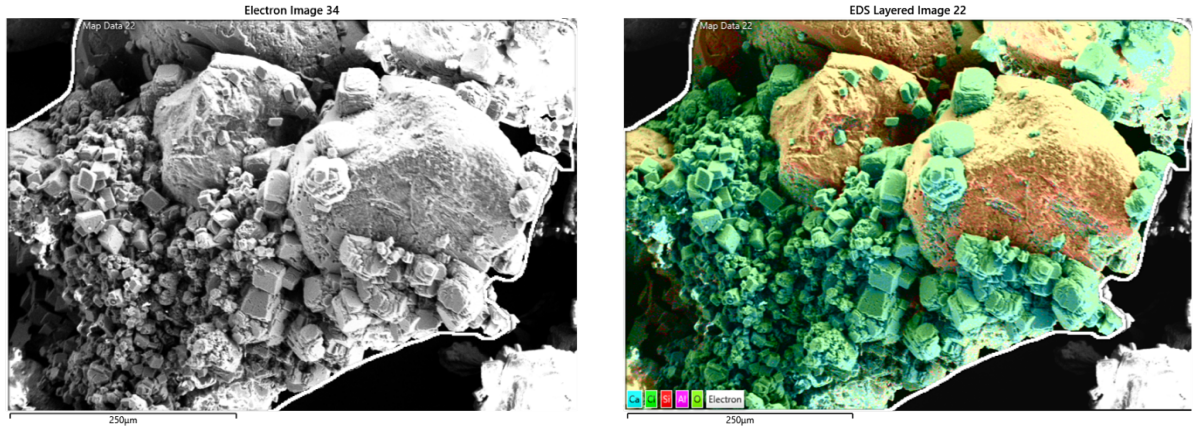

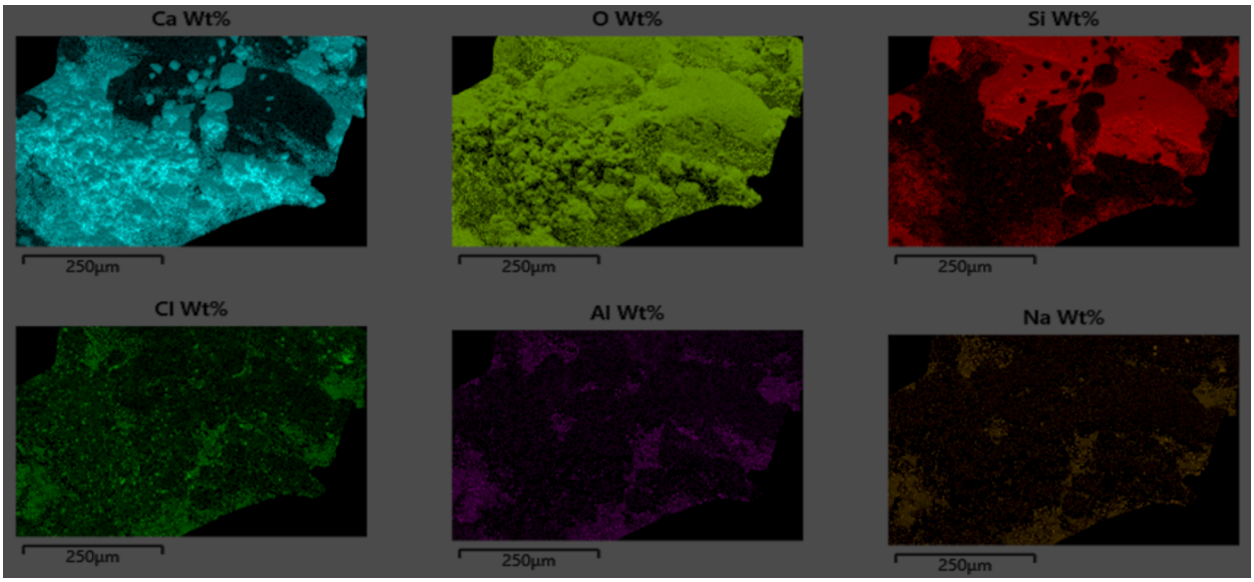

Fig. 3.23. SEM image (upper left) of a material section from Experiment CR1 (MICP - PolyMAF (0.01%) - Calcium Rinse - 2nd MICP) with an EDS layered image (upper right), and EDS elemental composition maps (bottom series of images).

Figure 3.24 presents SEM images of Experiment CR2 received a biocementation treatment followed by a 0.01% sodium alginate PolyMAF treatment with 500 mM sodium bromide, a calcium rinse, and a second biocementation treatment. Again the sodium bromide added to the PolyMAF treatment did not appear to result in any major changes in the morphology of the crystals. Similar to Experiment CR1, the calcium rinse appeared to possibly aid in bonding of smaller crystals with polymer. Spherical voids were also again present throughout the entire surface of calcite crystals. Bacterial impressions were also observed and appeared to be coated with the polymer film. Although an EDS scan of the sample was obtained as shown in **Figure 3.25**, results were largely consistent with other calcium rinse experiments and unfortunately abudances of sodum and bromide were not examined.

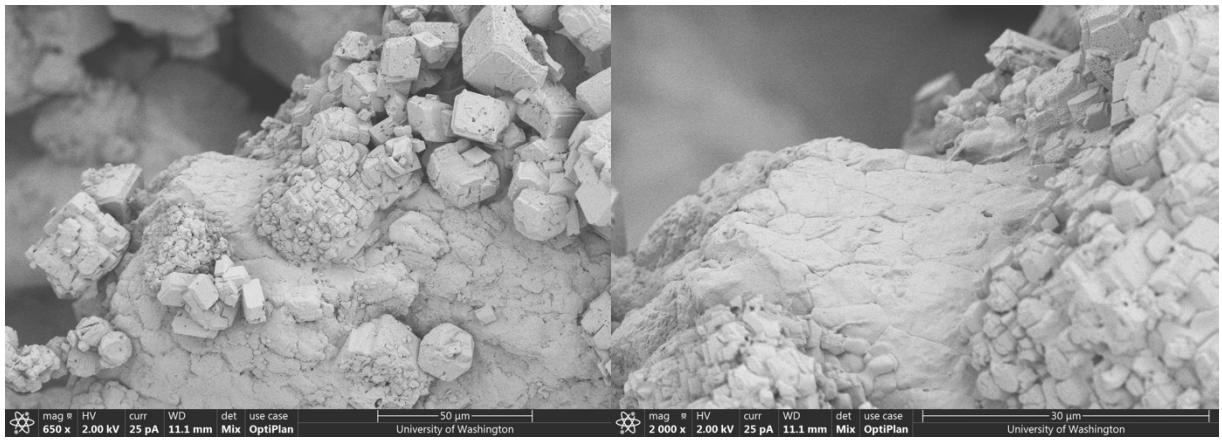

Fig. 3.24. SEM images of treated soil samples from Experiment CR2 (MICP - PolyMAF (0.01%, 500 mM NaBr) - Calcium Rinse - 2nd MICP) at various magnifications.

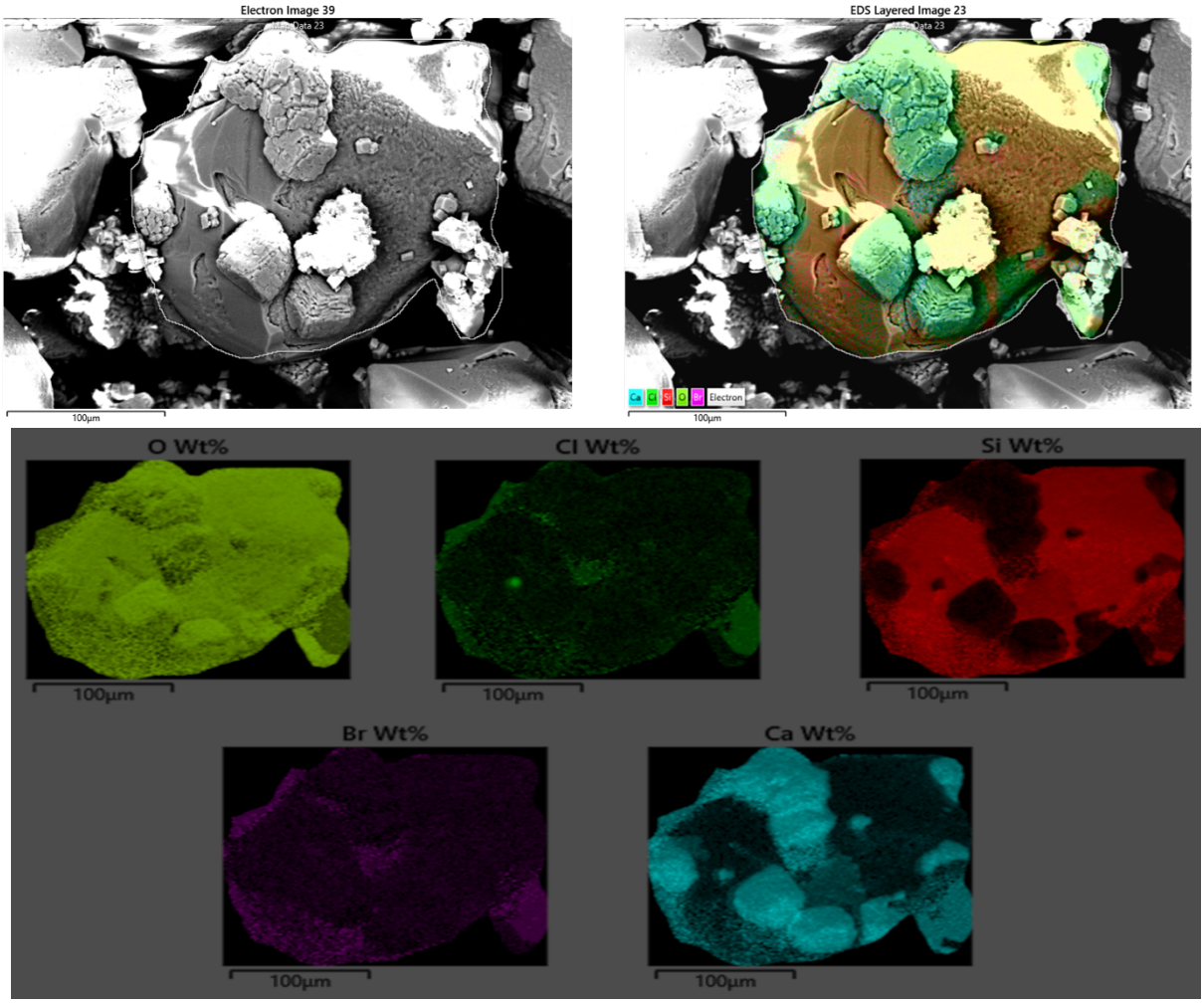

Fig. 3.25. SEM image (upper left) of a material section from Experiment CR2 (MICP - PolyMAF (0.01%, 500 mM NaBr) - Calcium Rinse - 2nd MICP) with an EDS layered image (upper right), and EDS elemental composition maps (bottom series of images).

Figure 3.26 presents SEM images of Experiment CR3 which received a biocementation treatment followed by a 0.01% sodium alginate PolyMAF treatment and a calcium rinse, but no second biocementation treatment. Examining the experiment prior to the second cementation treatment was intended to explore the effect of the calcium rinse prior to possible removal or dilution during subsequent cementation events. As shown, the polymer film was clearly visible and appeared to coat both soil particle and calcium carbonate crystals alike and, in some cases, completely incorporated crystals. Mineral dissolution induced by the PolyMAF treatment was also clearly visible with degraded mineral surfaces present through the sample.

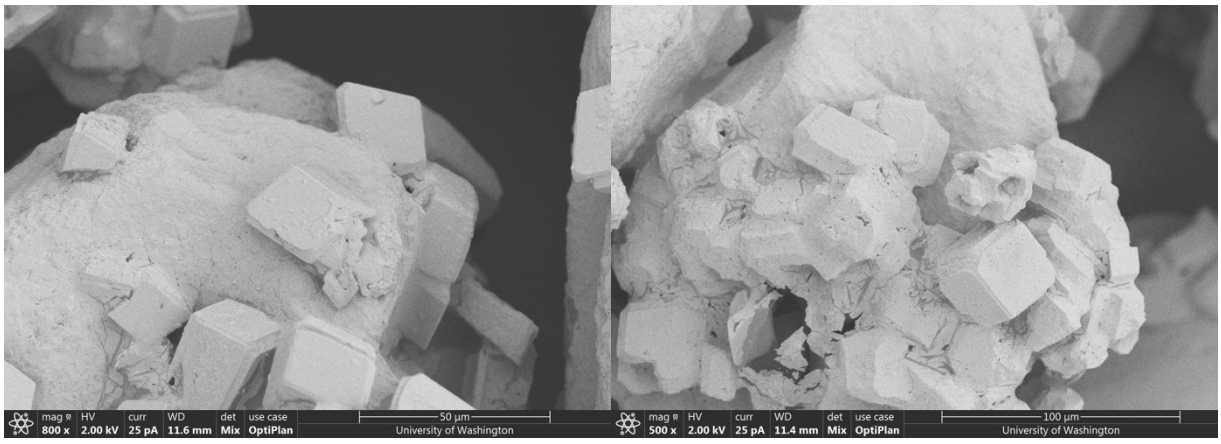

Fig. 3.26. SEM images of treated soil samples from Experiment CR3 (MICP - PolyMAF (0.01%) - Calcium Rinse) at various magnifications.

3.4 Conclusions & Remaining Knowledge Gaps

A series of experiments were performed to examine the ability of chemical additives to be supplied during the PolyMAF and seond cementation treatments to enable tracking of different material

formation events. In all cases, these additions had minimal effects on reaction rates observed during the first and second cementation events, but in some cases had large effects on resulting material structure. When chemical additives were supplied to the PolyMAF treatments, the additives were either not retained within the sample or were too widespread across the samples such that the location of the polymer film could not be definitively identified. However, improved detection of mineral phases were observed in experiments wherein chemical tracers were incorporated into the second MICP treatment solution. In these experiments, increased abundances of magnesium, potassium, and bromide (from $MgCl_2$ or KBr additions) were detected in regions where small clusters of crystals were precipitated indicating that these were formed during the second cementation treatment. In experiments containing magnesium chloride additions in the second cementation treatment, smaller calcite crystals appeared to form preferentially on the surface of larger calcium carboante crystals. This was different from other non-magneisum amended experiments wherein calcite crystals formed during the second cementation appeared to precipitate sporadically throughout samples on the surface of crystals, soils particles, and within soil void space. When coated with these magensioum-amended crystals, the surface of these larger crystals became signficantly rougher when compared to the smoother surfaces observed after the first cementation. When these materials were cross-sectioned, large voids could be observed between precipitate layers, likely suggesting the entrapment of gas bubbles within the polymer layer. EDS imaging of these polished sections also confirmed that the small crystals on the surface of these larger crystals were precipitated during the 2^{nd} MICP treatment, with increased magnesium and chloride both detected along the larger crystal surfaces. Since only a few experiments in this set contained $MgCl_2$, further investigations were expected to be needed to more fully understand the effect of magnesium on composite formation. Lastly, when calcium rinses

were employed in three select experiments, the formation of a more clearly visible polymer layer was observed suggesting that calcium rinses may promote the retention of generated gas bubbles and should be further investigated in subsequent experiments, particualrly those involving a magnesium amended second cementation treatment.

Chapter 4. In-depth Analysis of the Effects of Magnesium on the Second Cementation Treatment

4.1 Introduction

Following investigations completed in the earlier two chapters, methods were identified that were capable of generating and entrapping gas bubbles within polymer layers and could subsequently coat polymer surfaces with precipitates. This included the development of protocols to generate composites as well as the identification of optimal conditions including higher polymer concentrations during the PolyMAF treatment, the introduction of magnesium during the second cementation event, and the use of calcium rinses when transitioning specimens from the PolyMAF to the second cementation treatment. However, following the identification of successful gas entrapment methods, a more in-depth investigation of calcium rinses and magnesium amendments was needed to understand the conditions responsible for the large morphological changes that were observed. A set of fourteen batch experiments was designed to investigate the effects of magnesium chloride additions during the second cementation treatment as well as the effects of calcium rinses between PolyMAF and second cementation treatments. Specific objectives included to better understand (i) the effect of magnesium chloride concentrations, (ii) interactions between magnesium, polymer films, and MAF activity, and (iii) the potential of magnesium additions to permit precipitation events during the second cementation treatment in the absence of calcium chloride additions.

4.2 Materials and Methods

4.2.1 Experiment Overview

Chapter 4 batch experiments were treated using similar procedures as all previous chapters. Although each experiment differed slightly in treatment approach, the primary treatment phases

were as follows (with small differences described later): (i) a single cementation treatment intended to first biocement soils, (ii) a PolyMAF or Poly treatment including sodium alginate biopolymer with or without substrates required to enable mixed acid fermentation (i.e., MAF inoculant, glucose, yeast extract), and (iii) a second cementation treatment intended to coat the polymer film containing entrapped gases. Experiment Mg1 was identical to Experiment T5 from the previous chapter and received one cementation treatment, followed by a PolyMAF treatment, followed by a second cementation treatment with 50 mM $MgCl_2$. Experiment Mg2 was identical to Experiment T6 from the previous chapter and received one cementation treatment, followed by a PolyMAF treatment, followed by a second cementation treatment with the higher 250 mM $MgCl_2$. Experiment Mg3 served as a control for all experiments and received one cementation treatment, followed by a PolyMAF treatment, followed by a second cementation treatment with no $MgCl_2$ additions. Experiment Mg4 received one cementation treatment, followed by a Poly treatment, followed by a second cementation treatment with no $MgCl_2$ additions, to examine the effects of the polymer treatment without MAF. Experiment Mg5 further investigated the effects of adding a calcium rinse introduced in the previous set and received one cementation treatment, followed by a PolyMAF treatment with a calcium rinse, followed by a second cementation treatment with no $MgCl_2$ additions.

Several other experiments were designed to examine baseline conditions. For example, Experiment Mg6 examined the impact of $MgCl_2$ alone and received one cementation treatment followed by a second cementation treatment with 50 mM $MgCl_2$ (without a PolyMAF treatment). Experiment Mg7 received only one cementation treatment without added yeast extract. Experiment Mg8 received one cementation treatment followed by a PolyMAF treatment.

Experiment Mg9 received one cementation treatment followed by a PolyMAF treatment with a calcium rinse applied afterwards to examine possible improved gas entrapment. Experiments Mg10 and Mg11 both received one cementation treatment, followed by a PolyMAF treatment, followed by a second cementation treatment with either 50 mM or 250 mM $MgCl_2$, respectively, but no added calcium. This was intended to examine the possibility of magnesium carbonate mineral precipitation in the absence of calcium carbonate during the second cementation treatment. Experiment Mg12 received one cementation treatment, followed by a Poly treatment, followed by a second cementation treatment with 50 mM $MgCl_2$. Experiment Mg13 received one cementation treatment, followed by a PolyMAF treatment with a calcium rinse, followed by a second cementation treatment with 50 mM $MgCl_2$. Experiment Mg14 received one cementation treatment, followed by a Poly treatment with a calcium rinse, followed by a second cementation treatment with 50 mM $MgCl_2$. Experiment Mg15 received one cementation treatment followed by a second cementation treatment without $MgCl_2$ to examine the impact of repeated cementation events. Experiment Mg16 was similar to Experiment Mg15 and received one cementation treatment followed by a second cementation treatment without $MgCl_2$ but was not re-augmented prior to the second cementation in order to assess the potential impact of the re-augmentation. **Table 4.1 (in Appendix)** describes all sixteen experiments including test number, test name, and specific solution chemical compositions of the (i) first augmentation, cementation, and post-treatment rinse solutions, (ii) PolyMAF/Poly injections and post-treatment rinse solutions, and the (iii) second augmentation, cementation, and post-treatment rinse solutions.

4.2.2 Batch Experiment Set-up

All batch experiments contained solely Ottawa F-65 sand similar to Chapter 3. Each batch experiment contained 5.3 grams of soil, 44 mL of solution, and were conducted in Corning bottom glass petri dishes and were covered with aluminum foil to minimize temperature changes and mitigate evaporation effects and potential contamination.

4.2.3 Biogeochemical Sampling, Monitoring, and Imaging

All sampling, monitoring, and imaging methods were similar to those described in Chapter 3. Select experiments (Mg1, Mg2, Mg6, Mg12, Mg13, and Mg14) were also embedded in epoxy, sectioned, polished, and prepared for SEM imaging, however, due to issues with the equipment, some samples were substantially damaged during this preparation process.

4.2.4 Treatment Scheme and Overview

All samples were treated using similar protocols as used in earlier Chapter 3 experiments with small differences described. At the start of experiments, all soil specimens were augmented with *S. pasteurii* (ATCC 11859) (Yoon et al. 2001) a well-studied ureolytic bacteria used in many previous MICP studies (). *S. pasteurii* was grown in 500 mL volumes of standard ATCC 11859 growth media (15.74 g/L Tris Base, 20 g/L yeast extract, 10 g/L ammonium sulfate, pH adjusted to 9.0) using a process similar to that outlined in Burdalski (2020). After mixing, growth media was autoclaved using a liquid cycle for 24 minutes at 121^{o}C to sterilize prior to inoculation. After autoclaving, media volumes were inoculated with a -80^{o}C *S. pasteurii* glycerol stock culture, covered with sterile foil, and placed on an orbital shaker for approximately 36 hours at 180 rpm.

OD_{600} values were monitored in time and reached a value near 3.00E+09 cells/mL after 36 hours, after which cells were harvested for experiments.

During harvesting, 50 mL of growth media was transferred to a sterile 50 mL conical tube and centrifuged at 4200 rpm for 10 minutes. Following centrifugation, supernatant solutions were removed, and cells at the bottom of the conical tube were retained. Sterile isotonic saline solution (9 g/L sodium chloride in DI water) was then added to the conical tube, shaken to free cells from the bottom of the tube, and centrifuged at 4200 rpm for 10 minutes to rinse. After rinsing, the supernatant was again decanted, and an additional 10 mL of saline solution was added to the tube. The conical tube was then shaken to achieve homogenization of the cell pellet throughout the solution. Cell pellets were refrigerated until use (between one and two days after pelleting to ensure high cellular activity). Specified volumes of cell pellets were mixed with 5 mL of sterile saline solution and the 5.3 grams of the soil mixture in a 50 mL conical tube and placed in the refrigerator to reside overnight. Added volumes were determined from the growth media cell density in order to achieve a cell density of 7×10^7 cells/mL within experiments once fully mixed with cementation solutions. The augmented soil and cell pellet mixture was poured into glass dishes prior to the start of experiments.

All experiments had a total volume after adding the cementation solution of 44 mL. All cementation solutions were prepared using urea , calcium chloride dihydrate , and did not contain yeast extract. Cementation treatments were allowed to react within samples over 72 hours to ensure reaction completion. Following the cementation treatment period, solutions were decanted and samples were rinsed with 70% ethanol to remove treatment byproducts. For Experiments Mg1

through Mg9, PolyMAF or Poly treatments were applied 24 hours after the ethanol rinse. PolyMAF treatments were applied to Experiments Mg1 through Mg9 (except Experiment Mg4) and contained 0.01% sodium alginate polymer, 10 g/L glucose, 1 g/L yeast extract, and 1 mL per 300 mL of a mixed acid fermentation inoculation solution intended to enable mixed acid fermentation activity. All PolyMAF treatments contained sodium alginate prepared from a 0.50% stock solution. This stock solution was diluted to the specific concentrations required for each experiment. Experiment Mg4 received a Poly treatment with solely 0.01% sodium alginate polymer. After 72 hours, the remaining Experiments Mg10 through Mg14 also received PolyMAF treatments. After applying to batch experiments, PolyMAF treatments were allowed to reside within experiments for 72 hours without sampling disturbances to limit oxygen intrusion. After the residence period, solutions were carefully decanted. Experiments Mg5, Mg9, Mg13, and Mg14 then received a calcium rinse after PolyMAF treatments. Experiments Mg8 and Mg9 were then taken offline and prepared for post-processing. Select experiments were then re-augmented in preparation for the second cementation treatment by scraping the treated soil after the PolyMAF treatment into a conical tube containing cells and isotonic saline solution and allowing this to sit overnight (~12 hours). The applied cell density for the second augmentation identical to the first augmentation of 7×10^7 cells/mL when diluted with the cementation solution. After re-augmentation, select specimens received a second cementation treatment containing varying magnesium chloride additions that was allowed to reside within samples for 72 hours. Following the 72 hour residence period, samples were rinsed with 35% ethanol and then oven-dried. Additional experimental differences are further described in **Table 4.1 (in Appendix).**

4.3 Results and Discussion

4.3.1 Biogeochemical Behavior

Urea concentrations were monitored in all experiments during the initial cementation treatment up to 72 hours. **Figure 4.1** presents measured urea concentrations versus elapsed time for all experiments during the first and second cementation treatments. All experiments exhibited similar reaction rates during the first cementation treatment, with near 200 mM urea being hydrolyzed within the first six hours following treatments. After 24 hours, urea concentrations in all experiments were near zero suggesting that urea hydrolysis was largely complete. Urea concentrations were also monitored during the second cementation treatment for all experiments receiving a second cementation treatment. Ureolytic rates during the second cementation exhibited slightly greater variability between experiments. This was especially noticeable between experiments containing calcium chloride in the second cementation treatment and those that had no calcium but either 50 mM or 250 mM $MgCl_2$. These experiments (Experiments Mg10 and Mg11) had slightly higher urea concentrations remaining at the conclusion of the treatment period perhaps due to higher pH conditions present at the end of these experiments due to a lack of carbonate consumption and/or interferences with the assay by added magnesium. Experiment Mg16 which received an augmentation only prior to the first cementation treatment had a slower reaction rate during the second cementation treatment, suggesting that reductions in ureolytic activity could be expected without reaugmentation likely due to cell death and the lack of added growth factors (e.g., yeast extract). Nonetheless, the activity was enough to successfully reduce urea concentrations to near zero by 24 hours similar to all other experiments.

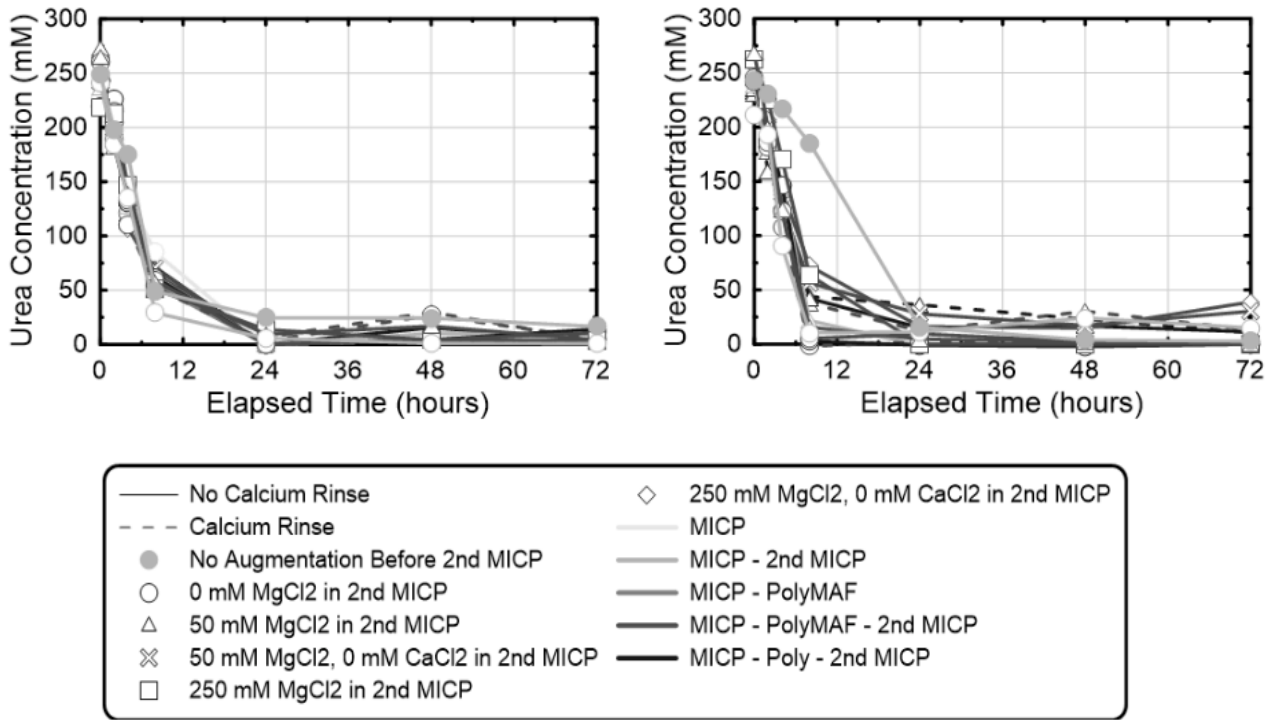

Fig 4.1 Urea concentrations versus time during first (upper left) and second (upper right) cementation treatments.

4.3.2 Morphological Effects

Several experiments were repeated from previous chapters in order to isolate the effects of the first cementation treatment, the presence of sodium alginate polymer, the effect of MAF, the influence of calcium rinses, the effect of re-augmentation, the presence of a second cementation treatment, and the critical role that magnesium may have during the second cementation treatment. **Figure 4.2** presents SEM images of Experiment Mg7 which received only one biocementation treatment. As shown, cubic morphologies typical of calcite can again be observed with the presence of sharp crystal edges. In many locations, bacterial impressions can also be observed on the surface of these crystals. These crystals were generally between 25 and 100 micron in diameter and existed on both clean silica sand surfaces as well as between adjacent soil particles.

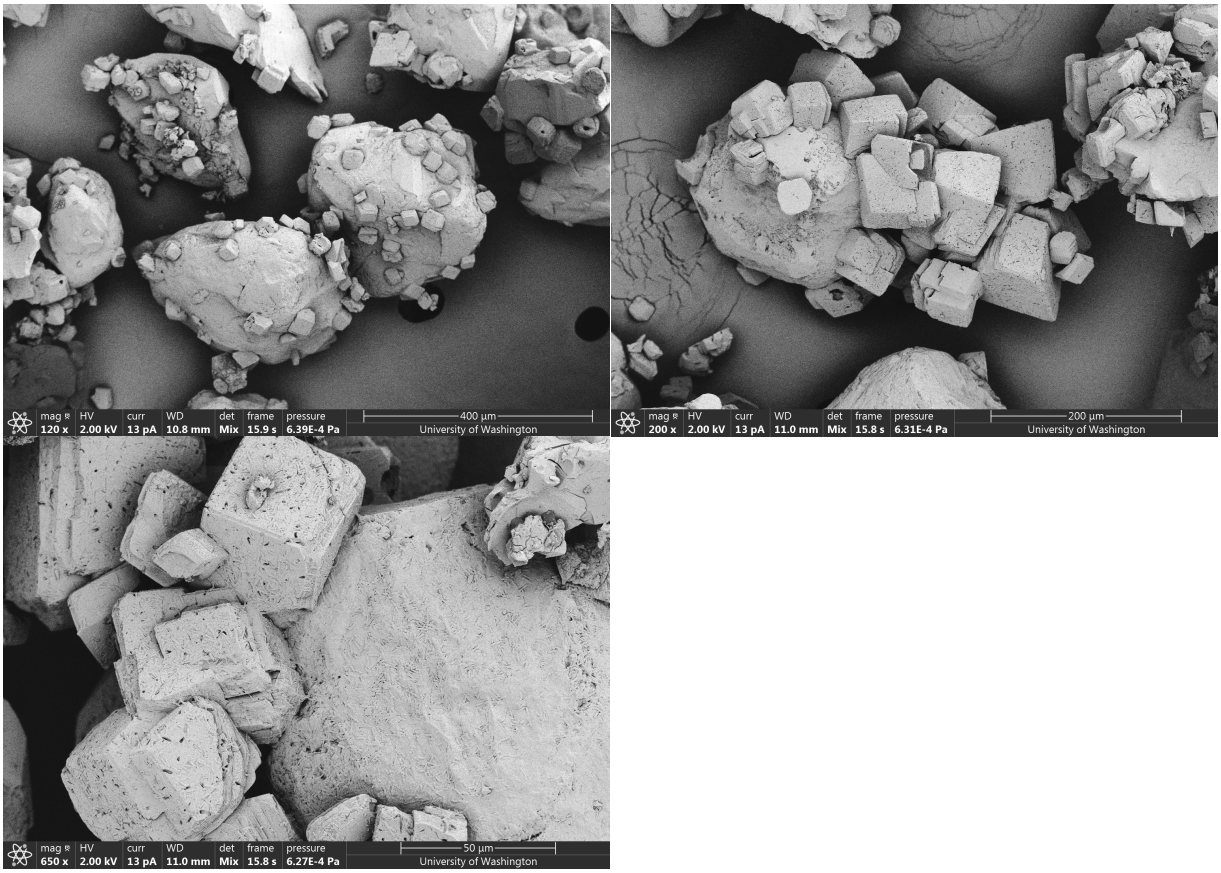

Fig 4.2. SEM images of treated soil samples from Experiment Mg7 (MICP) at various magnifications.

Figure 4.3 presents SEM images of Experiment Mg8 which received one biocementation treatment followed by one PolyMAF treatment. As expected, again precipitated crystals had cubic morphologies typical of calcite, but with noticeable surficial damage likely resulting from MAF induced mineral dissolution. In some locations, the presence of a polymer film could also be observed which appeared to coat existing crystals and soil particles. Both of these observations were consistent with other similar experiments described in previous chapters.

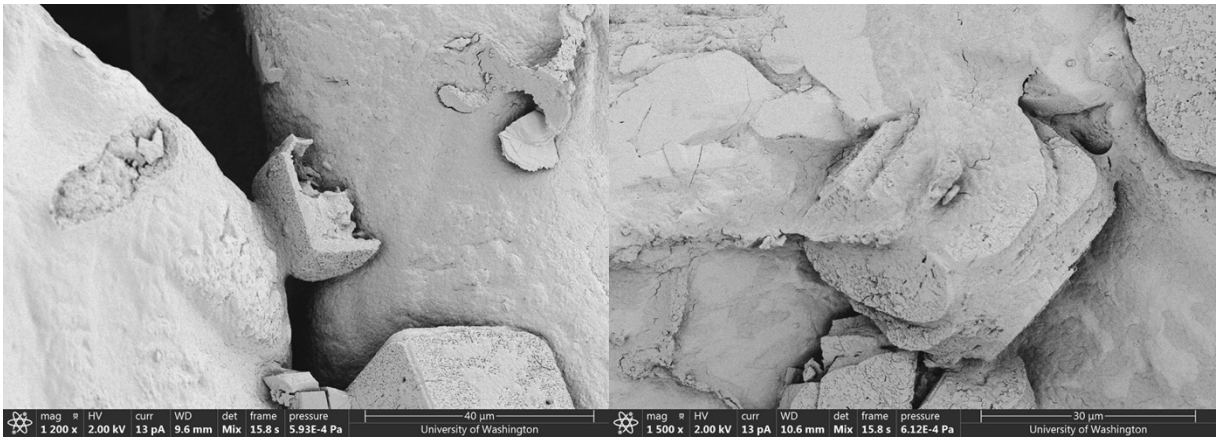

Fig. 4.3. SEM images of treated soil samples from Experiment Mg8 (MICP - PolyMAF (0.01%)) at various magnifications.

Figure 4.4 presents SEM images of Experiment Mg3, which received one biocementation treatment followed by one PolyMAF treatment and a second cementation treatment. Again, large calcite crystals were observed likely resulting from the first cementation event with surficial damage of crystals likely resulting from MAF. In some cases (**Figure 4.4 top right image**), select crystal surfaces appeared to be collapsed with spherical-shaped voids possibly due to gas bubble formation. Unlike Experiment Mg8, which did not receive a second cementation treatment, the sample from Experiment Mg3 appeared to have clusters of smaller calcium carbonate crystals distributed throughout the sample. These smaller crystals appeared to be more clearly defined suggesting that they were again likely formed during the second cementation event and did not experience dissolution. Larger crystal surfaces also appeared to be more weathered with the previous bacterial impressions observed in Experiment Mg7 being less visible in this sample likely due to MAF-induced damage.

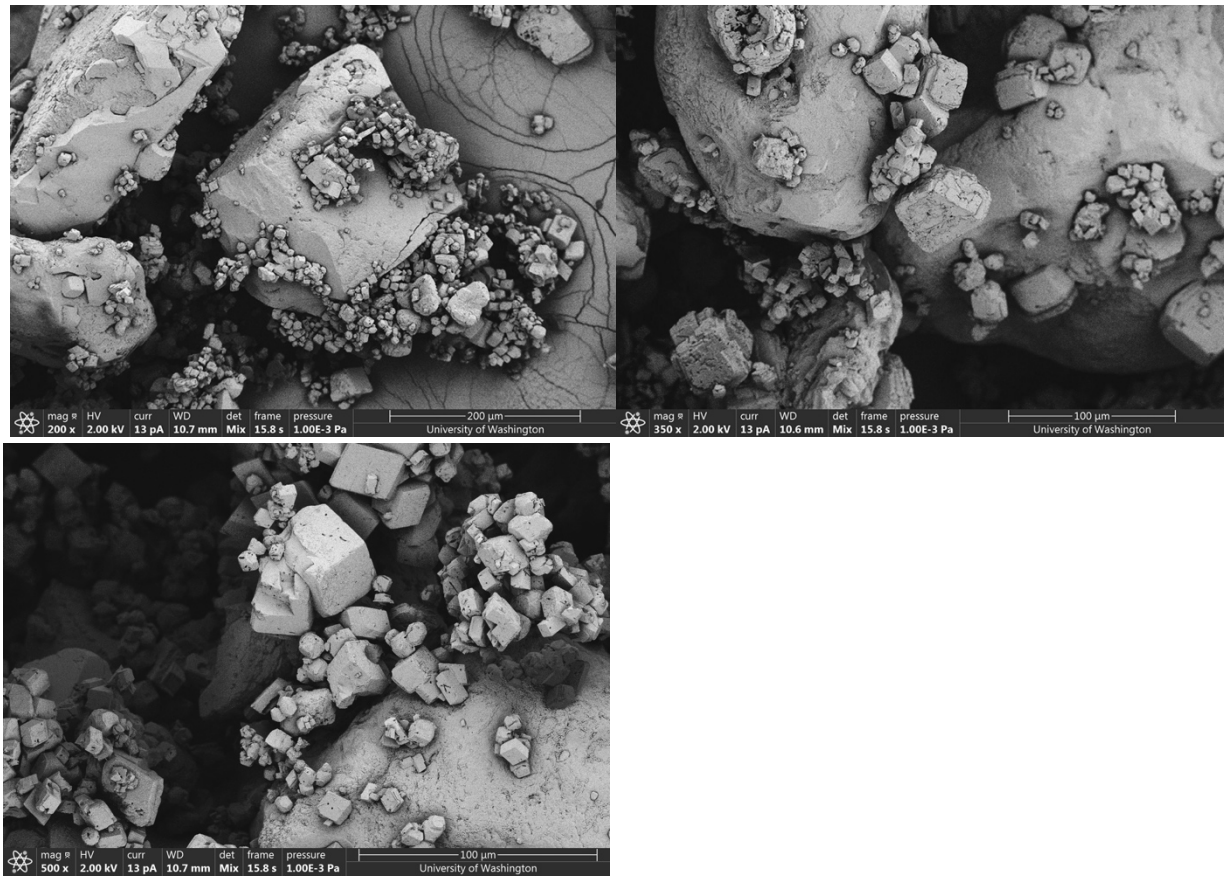

Fig. 4.4. SEM images of treated soil samples from Experiment Mg3 (MICP - PolyMAF (0.01%) - 2nd MICP) at various magnifications.

In order to isolate the effect of MAF activity a similar experiment was performed with the polymer injection but without MAF. **Figure 4.5** presents SEM images of Experiment Mg4, which received one biocementation treatment followed by one Poly treatment (without MAF) and a second cementation treatment. It was expected that this sample would have the same polymer film but would not have the crystal surface damage expected following MAF. As shown, the collapsed crystal forms found in the earlier experiments with MAF were not observed when only the polymer was applied. Some polymer coatings could be still observed in Experiment Mg4, however, and appeared to exist on both silica sand surfaces and calcium carbonate crystals alike.

Fig. 4.5. SEM images of treated soil samples from Experiment Mg4 (MICP - Poly (0.01%) - 2nd MICP) at various magnifications.

As shown in Chapter 3, the addition of magnesium appeared to increase the association of crystals formed during the second cementation treatment with existing calcium carbonate crystal surfaces. However, it was unclear if this effect was solely related to magnesium additions or if other interactions with the polymer, mixed acid fermentation, and calcium rinses were critical toward enabling this behavior. Experiments Mg6, Mg15, and Mg16 were therefore performed to further investigate these remaining knowledge gaps and in particular the role of MAF activity and the presence of a polymer. **Figure 4.6** presents SEM images of Experiment Mg15 which received one cementation treatment followed by a second cementation treatment without the presence of the polymer or MAF activity. **Figure 4.6** also presents SEM images of Experiment Mg16 which was identical to Experiment Mg15 but was not re-augmented prior to the second cementation event. As shown, large calcium carbonate crystals could be observed in both samples with the presence of small crystals also observed. When comparing crystal distributions between experiments, it appeared that the presence of the second augmentation in Experiment Mg15 may have promoted

greater nucleation of smaller crystals during the second cementation event. In contrast, smaller crystals in Experiment Mg16 were less frequently observed with larger crystals from the first cementation appearing to instead increase in size. This suggested that the second augmentation may have been the primary cause of the smaller crystals formed during the second cementation event and that this was not significantly influenced by the presence of polymer or MAF activity. However, it should be mentioned that Experiment Mg16 also had a notably slower reaction rate than Experiment Mg15 due to the lack of a second augmentation which could have also contributed to differences in crystal nucleation during the second cementation event.

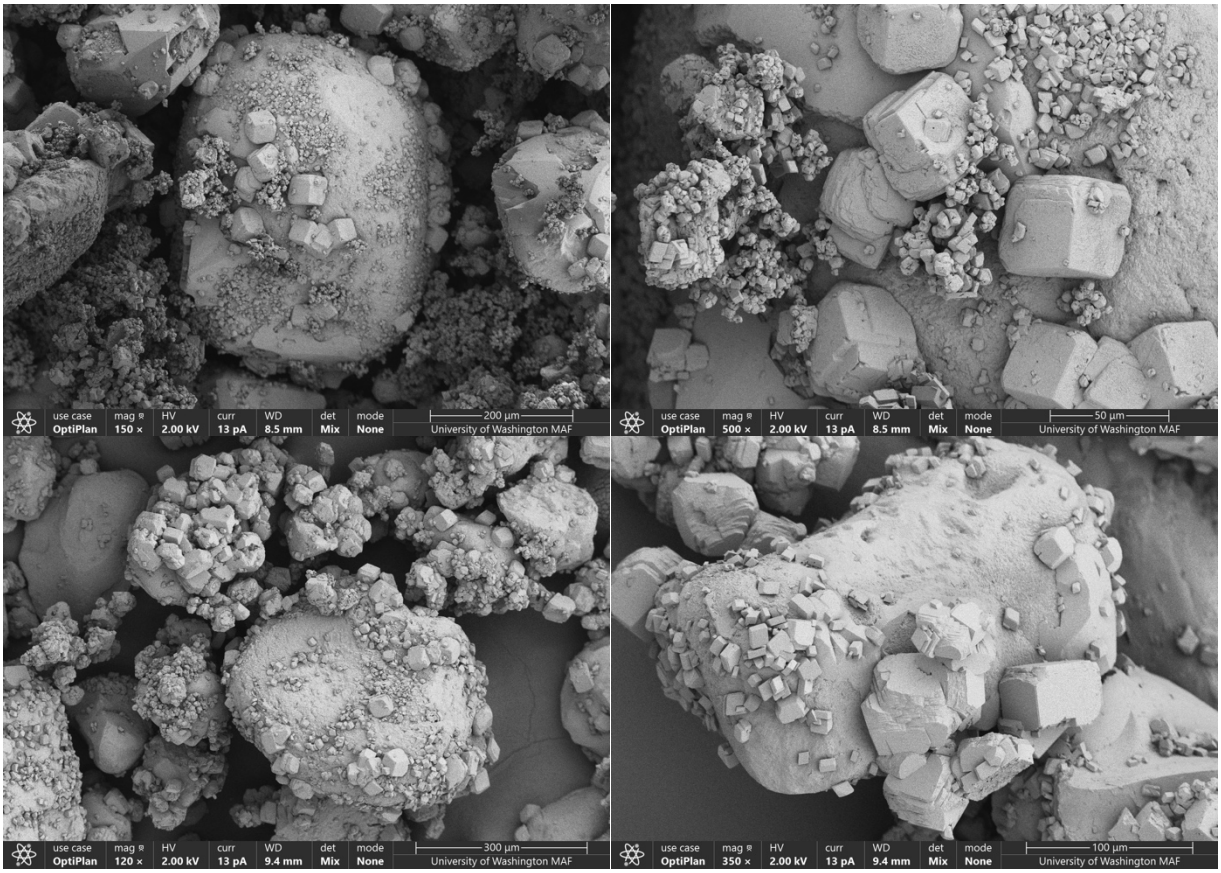

Fig. 4.6. SEM images of treated soil samples from Experiment Mg15 (top left and right, MICP - 2nd MICP) and Experiment Mg16 (bottom left and right, MICP - 2nd MICP (No Augmentation Before 2nd MICP)) at various magnifications.

Figure 4.7 presents SEM images of Experiment Mg6 which received one cementation treatment followed by a second cementation treatment with 50 mM $MgCl_2$, but without the presence of the polymer or MAF activity. This experiment was therefore identical to Experiment Mg15 but had added magnesium during the second cementation event. As shown, in Experiment Mg6 the same coating of larger crystals observed in experiments with polymer and MAF, still persist even when these factors are absent. A rougher mineral coating can be seen covering large calcite crystal surfaces at multiple locations and again appeared to preferentially form on these larger crystals as opposed to free silica sand surfaces. These crystals were dramatically different than those observed in Experiment Mg15 and Experiment Mg16, again suggesting that magnesium was the primary factor that responsible for the aggregation of minerals formed during the second cementation event on existing larger calcite crystals. These same samples were cross-sectioned as shown in **Figure 4.8** wherein the stark discontinuity between large crystals and smaller crystal mineral coatings found in earlier samples were not easily observed in this sample. This suggested again that this discontinuity between layers was likely an artifact resulting from the presence of a polymer film and possibly gas inclusions.

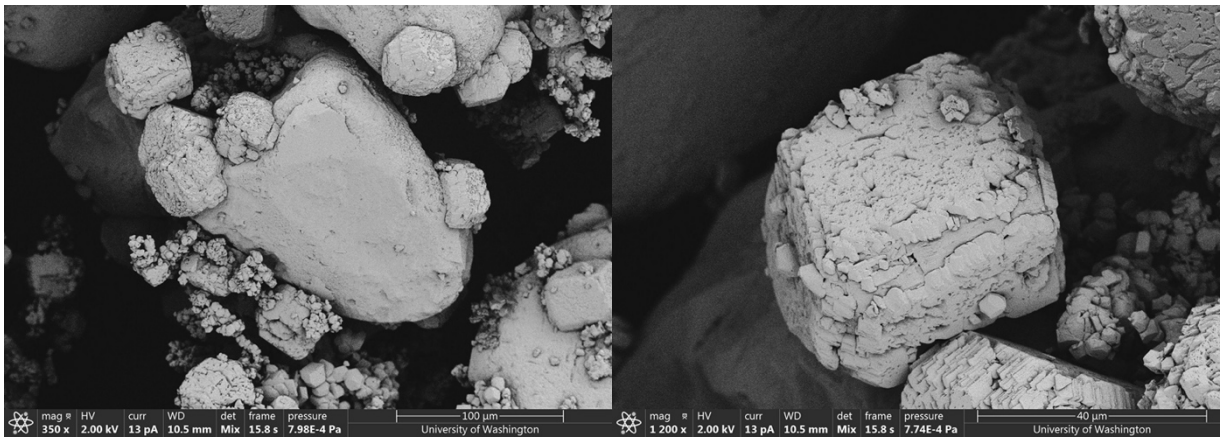

Fig. 4.7. SEM images of treated soil samples from Experiment Mg6 (MICP – 2nd MICP w/ 50 mM of $MgCl_2$) at various magnifications.

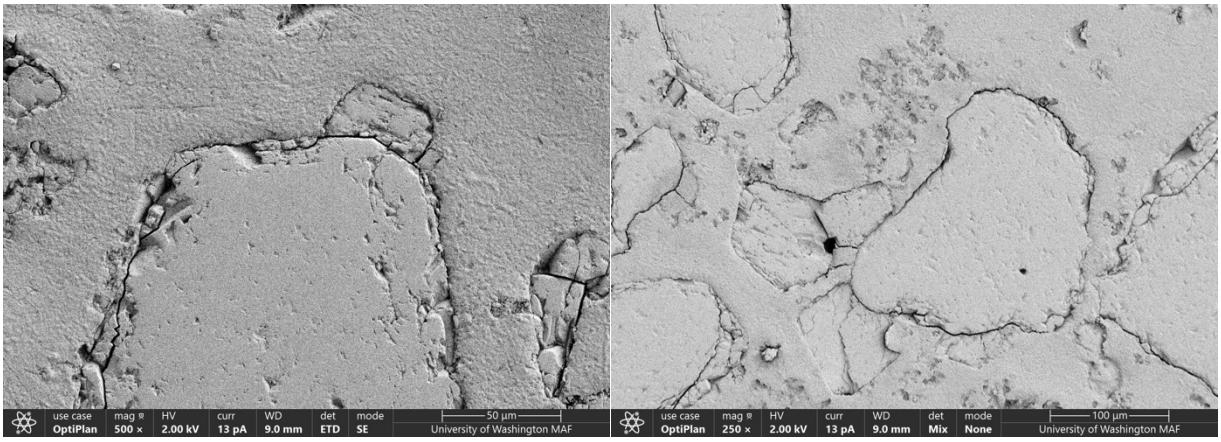

Fig. 4.8. SEM images of polished material cross-sections from Experiment Mg6 (MICP – 2nd MICP (50 mM of $MgCl_2$)).

Figure 4.9 presents SEM images of both Experiment Mg1 and Mg2. Experiment Mg1 was treated identically to Experiment T5 from Chapter 3 and received one cementation treatment, followed by a PolyMAF treatment, and a second cementation treatment with 50 mM $MgCl_2$. Experiment Mg2 was treated identically to Experiment T6 from Chapter 3 and received one cementation treatment, followed by a PolyMAF treatment, and a second cementation treatment with a higher 250 mM

$MgCl_2$. As shown in Experiment Mg1, similar observations to Experiment T5 were observed with a rougher precipitate layer appearing to form preferentially around the larger existing calcite crystals. Despite the presence of the PolyMAF intermediate treatment, the morphology of the materials from Experiment Mg1 appeared to be similar to Experiment Mg6 which did not have MAF activity nor the presence of a polymer treatment. Similar features could also be observed in Experiment Mg2, however, due to the higher magnesium concentrations the mineral coatings in this sample again appeared to be rougher than Experiment Mg1. Collapsed crystals likely caused by the PolyMAF treatment were also occasionally observed in this sample, as shown. These same samples were cross-sectioned as shown in **Figure 4.10**. After sectioning, both of these samples showed some evidence of a precipitate coating. In some locations, the mineral coating observed in Experiment Mg1 also appeared to be delineated from the larger calcite crystals by a clear discontinuity, which may have contained the polymer film with gas inclusions.

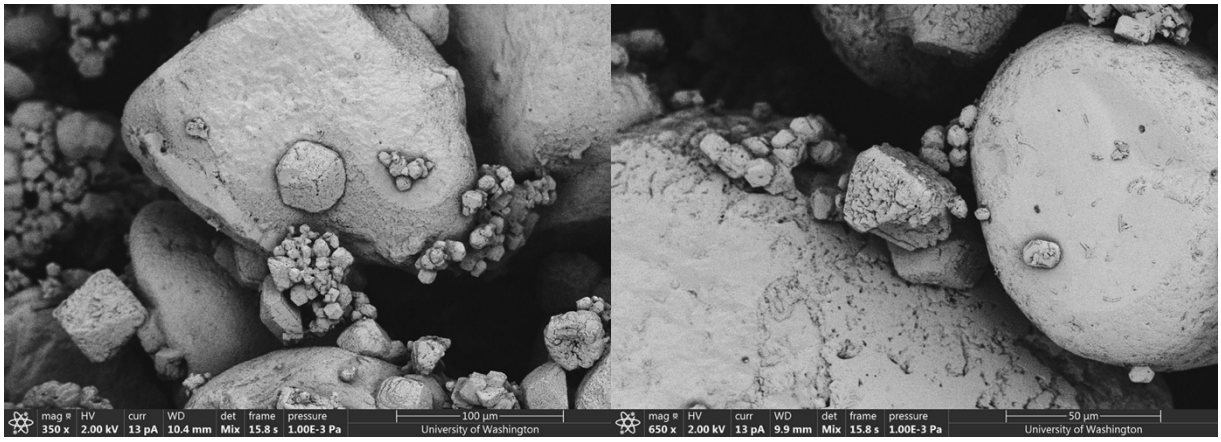

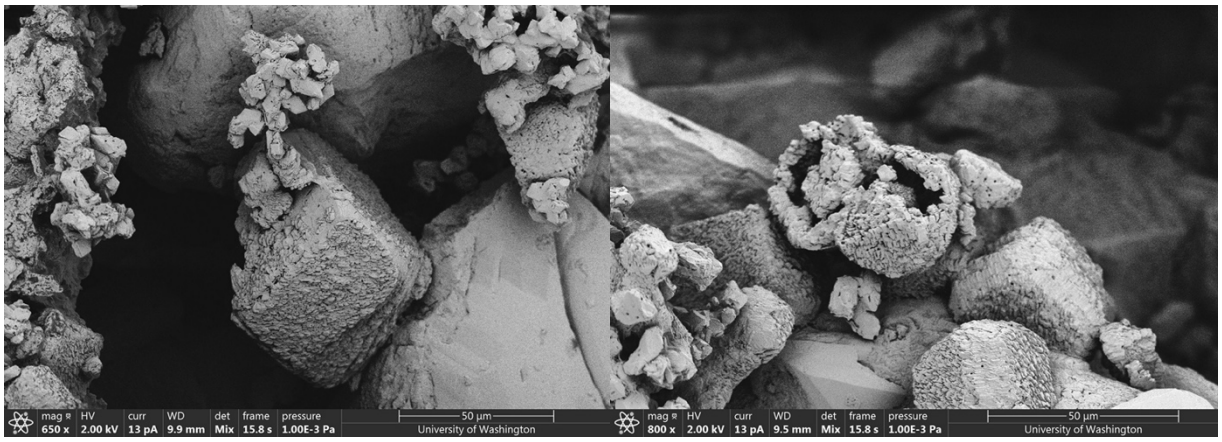

Fig. 4.9. SEM images of treated soil samples from Experiment Mg1 (top, MICP - PolyMAF (0.01%) - 2nd MICP (50 mM $MgCl_2$)) and Experiment Mg2 (bottom, MICP - PolyMAF (0.01%) - 2nd MICP (250 mM $MgCl_2$)) at various magnifications.

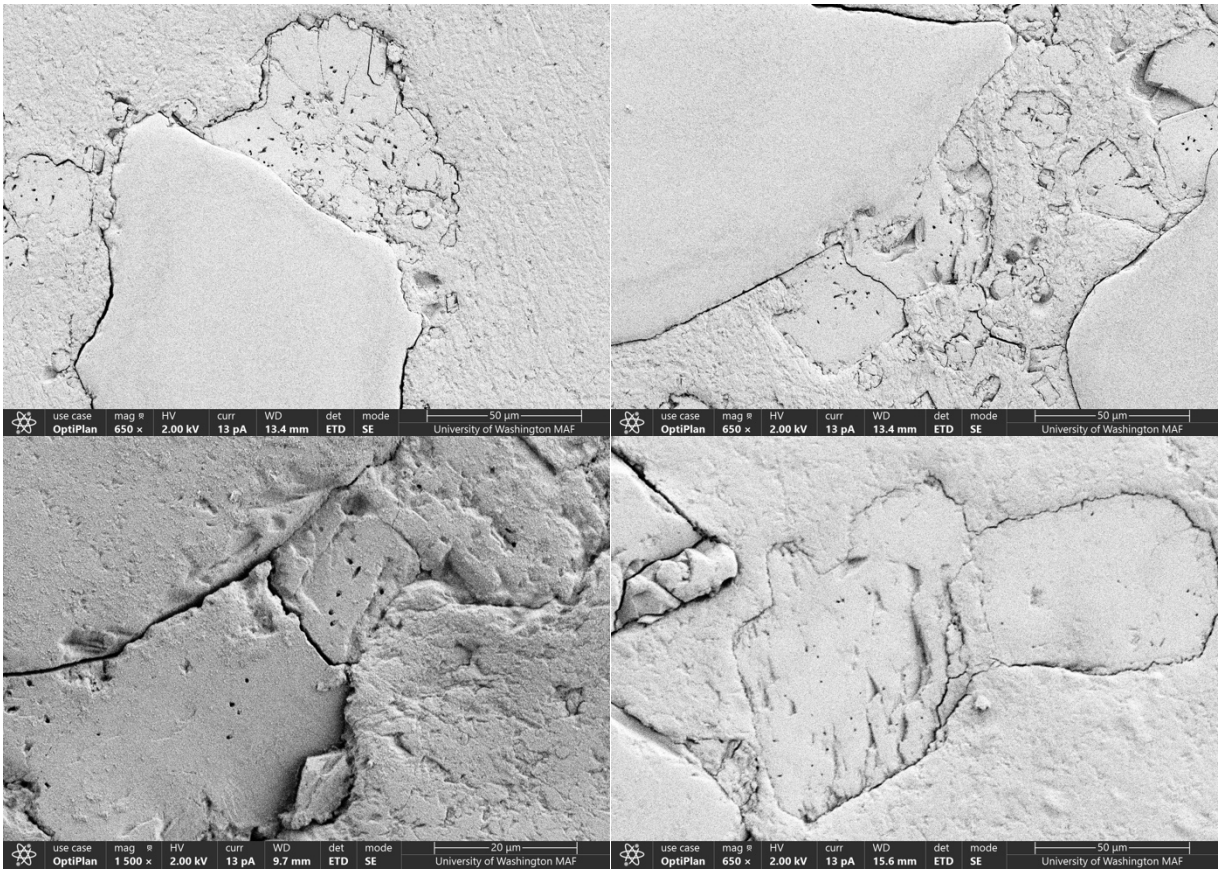

Fig. 4.10. SEM images of polished material cross-sections from Experiment Mg1 (top left and right, MICP - PolyMAF (0.01%) - 2nd MICP (50 mM $MgCl_2$)) and Experiment Mg2 (bottom left and right, MICP - PolyMAF (0.01%) - 2nd MICP (250 mM $MgCl_2$)).

As shown in earlier experiments, the presence of the rough mineral coating on the exterior of larger calcite crystals appeared to be definitively related to the presence of magnesium in the second cementation treatment and minimally influenced by the presence of the polymer film and MAF activity. However, it was unclear what this mineral coating may have been composed of and what role magnesium may have played in its formation. In particular it was suspected that this mineral phase could be either a pure magnesium carbonate mineral (e.g., magnesite) or may have simply been magnesian calcite wherein some amount of magnesium can replace calcium within the calcite mineral. In order to further study this aspect, Experiments Mg10 and Mg11 were preformed wherein all experiments received one cementation treatment, followed by a PolyMAF treatment, and a second cementation treatment with either 50 mM $MgCl_2$ or 250 mM MgCl, but no added calcium. Thus, during the second cementation treatment, it was expected that only magnesium carbonate minerals could be formed due to the absence of soluble calcium. In both experiments, urea degradation was achieved during the second cementation treatment, however, notably the materials appeared to be weakly cemented within the glass dishes and an ammonia odor was observed suggesting that high pH conditions were achieved post-reaction. Both observations suggested that minimal carbonate consumption occurred and that likely minimal magnesium carbonate could be expected to have precipitated in both experiments. **Figure 4.11** presents SEM images of both Experiment Mg10 and Mg11. As shown, Experiment Mg10 had morphologies similar to samples only receiving a single cementation treatment followed by a PolyMAF treatment, but without a second cementation event. Large crystal surfaces appeared to be damaged

from MAF, but the presence of smaller crystals was sparingly observed suggesting that minimal precipitation was formed during the second cementation treatment. When examining the morphology of Experiment Mg 11, large differences were observed with an abundance of fibrous minerals throughout the specimen. Although definitive characterizations are needed, these fibrous minerals appeared to be similar to morphologies observed by Unluer & Al-Tabbaa (2013) for nesquehonite, a metastable magnesium carbonate. Although unexpected, such minerals again were not similar to the mineral coatings observed when both calcium and magnesium were present during the second cementation, indicating that the coating effect could not be replicated with magnesium additions alone. Further, this observation suggested that the mineral coatings formed in other experiments may have been magnesian calcite as opposed to a strictly magnesium carbonate mineral.

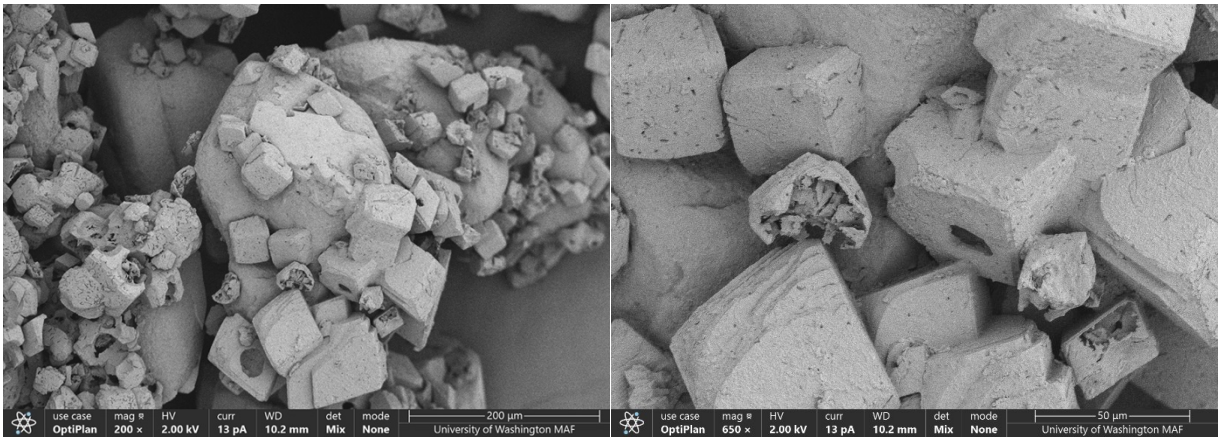

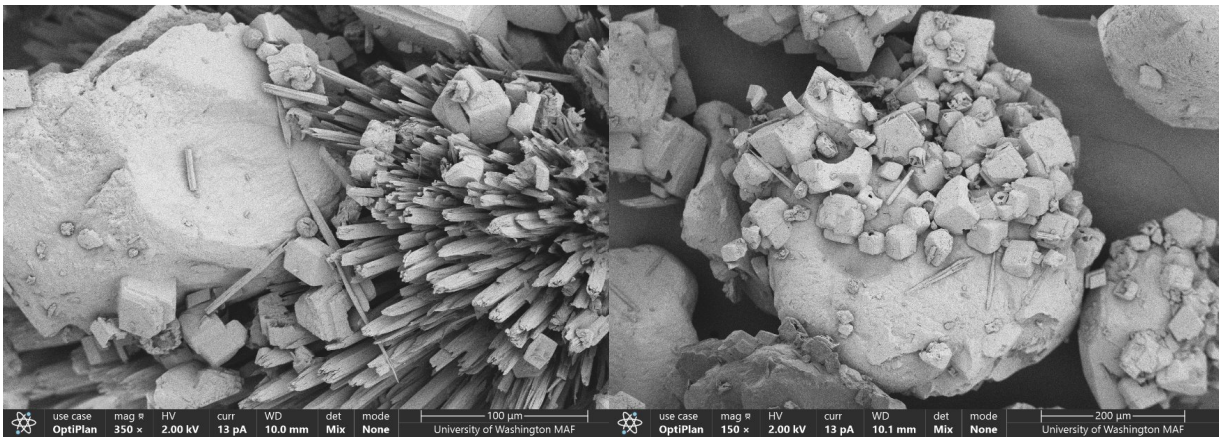

Fig. 4.11. SEM images of treated soil samples from Experiment Mg10 (top, MICP - PolyMAF (0.01%) - 2nd MICP (50 mM $MgCl_2$, 0 mM $CaCl_2$)) and Experiment Mg11 (bottom, MICP - PolyMAF (0.01%) - 2nd MICP (250 mM $MgCl_2$, 0 mM $CaCl_2$)) at various magnifications.

Figure 4.12 presents SEM images of Experiment Mg12 which received one cementation treatment, followed by a Poly treatment (without MAF), and a second cementation treatment with 50 mM $MgCl_2$. This was intended to assess the role of MAF activity in this process by comparing with Experiment Mg1, which did have MAF. As shown, due to a lack of MAF, precipitated minerals appeared to be more clearly formed without existing deterioration of mineral surfaces nor collapsed surfaces. Again, due to the presence of magnesium in the second cementation treatment, a clear mineral coating over larger crystals was again observed. These samples were then sectioned and imaged as shown in **Figure 4.13**. As shown, clear mineral disocontinies were again not observed possibly due to the lack of gas inclusions. This was noteworthy given that both the magnesium calcite exterior crystal coatings and the polymer film were both present in this sample, suggesting that both were not primarily responsible for the discontinuty observed in other specimens with MAF activity and presumably gas inclusions.

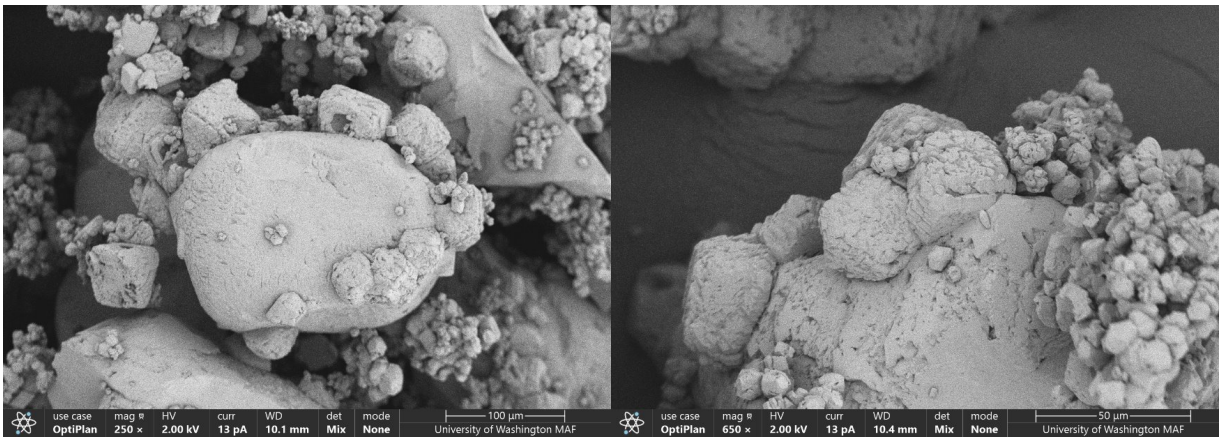

Fig. 4.12. SEM images of treated soil samples from Experiment Mg12 (MICP - Poly (0.01%) - 2nd MICP (50 mM $MgCl_2$)) at various magnifications.

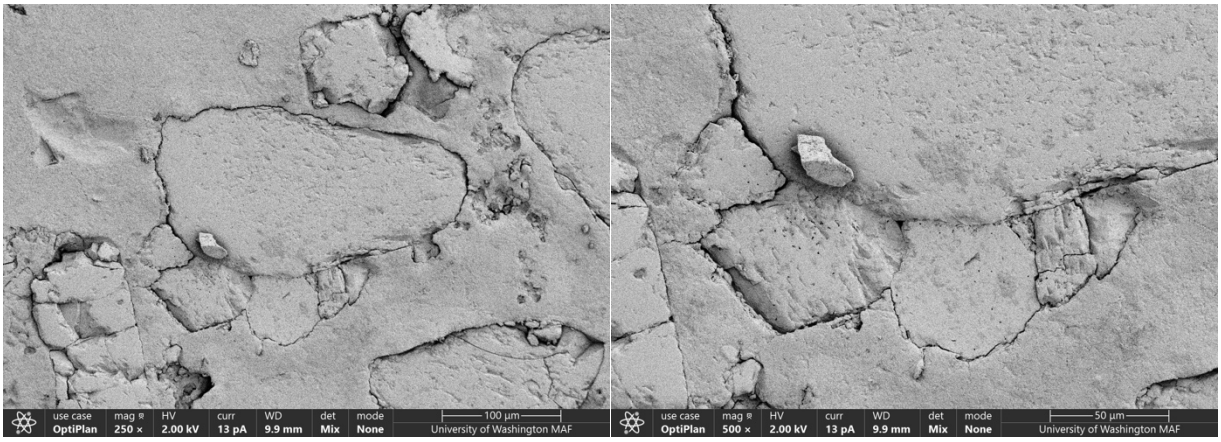

Fig. 4.13. SEM images of polished material cross-sections from Experiment Mg12 (MICP - Poly (0.01%) - 2nd MICP (50 mM $MgCl_2$)).

Figure 4.14 presents SEM images of Experiment Mg9 which received one cementation treatment, followed by a PolyMAF treatment and a calcium rinse, but no second cementation treatment. This was similar to other previous experiments; however, this sample lacked the introduction of other chemical tracers which may have influenced previous observations. As shown, a clear polymer coating can be observed in Experiment Mg9 over silica sand surfaces and calcium carbonate

crystals. Rough mineral surfaces following MAF deterioration also appeared to be less pronounced in this sample possibly due to the coating of these surface imperfections with calcium alginate, which was likely increasingly formed during the calcium rinse process. This outcome suggested that calcium rinses may be preferred and afford the best opportunity for retaining gas inclusions prior to the second cementation event.

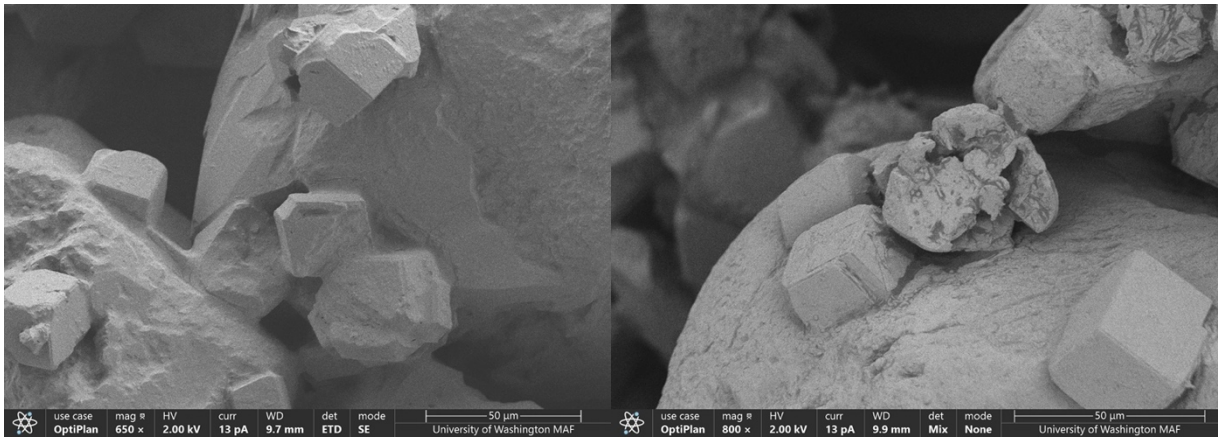

Fig. 4.14. SEM images of treated soil samples from Experiment Mg9 (bottom, MICP - PolyMAF (0.01%) - Calcium Rinse) at various magnifications.

Figure 4.15 presents SEM images of Experiment Mg5 which received one cementation treatment, followed by a PolyMAF treatment and a calcium rinse, and a second cementation treatment (without added magnesium). As shown, some large calcite crystals could be observed with an abundance of smaller calcite crystals that were precipitated on both silica sand surfaces and on the surface of existing larger calcite crystals. Less damage to crystal surfaces was observed than expected likely due to the calcium rinse which may have again coated these surface features resulting from MAF. Overall morphologies observed in Experiment Mg5 were similar to Experiment Mg3, which had the same treatments but no calcium rinse, with the exception of

somewhat smoother soil and crystal surfaces that were likely coated with a thicker layer of calcium alginate.

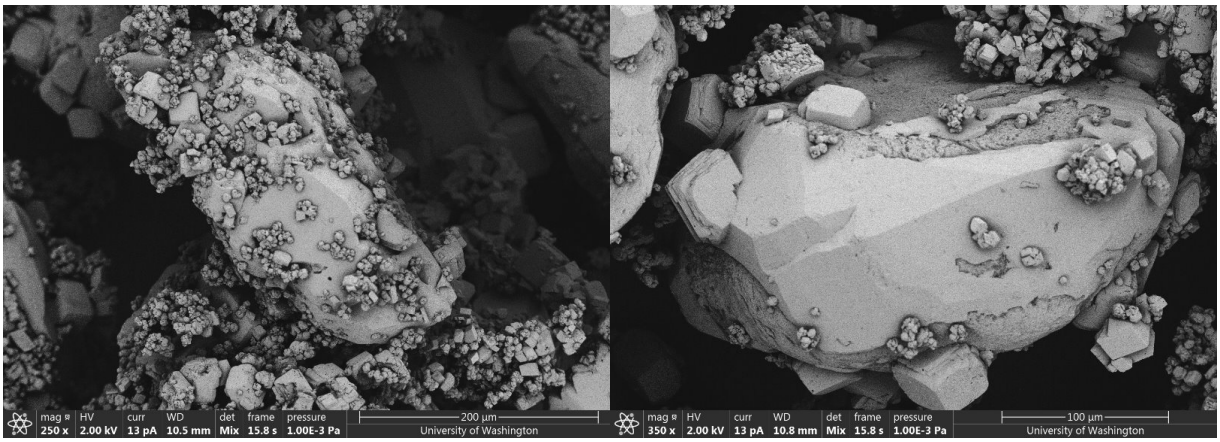

Fig. 4.15. SEM images of treated soil samples from Experiment Mg5 (MICP - PolyMAF (0.01%) - Calcium Rinse - 2nd MICP) at various magnifications.

Figure 4.16 presents SEM images of Experiment Mg13 which received one cementation treatment, followed by a PolyMAF treatment and a calcium rinse, and a second cementation treatment with 50 mM $MgCl_2$. This treatment combination represented what was expected to provide the best opportunity for gas entrapment and incorporation within biocementation. As shown, again significant coating of larger calcite crystals with smaller crystals was observed, consistent with other experiments containing magnesium in the second cementation treatment. When compared to Experiment Mg5, which received similar treatments but without $MgCl_2$ in the second cementation treatment, mineral surfaces again appeared to be rougher again indicating the influence of magnesium additions on the exterior mineral coating. These exterior coatings were observed on nearly all larger crystal surfaces that were imaged. At one location, the exterior layer appeared to have been delaminated possibly due to the removal of a surrounding soil particle. This

allowed for better visualization of the interface between the larger calcite crystal and the surrounding smaller crystal exterior coating. As shown, the inner calcite crystal appeared to be smoother and did not contain voids. The exterior coating in contrast appeared to be composed of smaller crystals containing small voids at times. At the interface between the interior crystal and the exterior coating, small spherical voids were observed that were likely indicative of entrapped gas inclusions. In other locations, calcite crystals were again observed that appeared to collapse over a spherical void, which may have again resulted from a trapped and collapsed gas bubble. These observations were similar to those for Experiment Mg3, however, the calcium rinse employed in Experiment Mg13 may have afforded the ability to better bond crystal structures with surrounding soil particle surfaces due the presence of greater calcium alginate. Images were also obtained after sectioning this sample as shown in **Figure 4.17**. In these sections the bonds between precipitates and adjacent soil particles appeared to be less well defined, again possibly due to the presence of calcium alginate. The presence of calcium alginate may have also made the sectioning process more difficult due to the movement of embedded materials along these weaker interfaces, thereby rending small features more difficult to definitively identify.

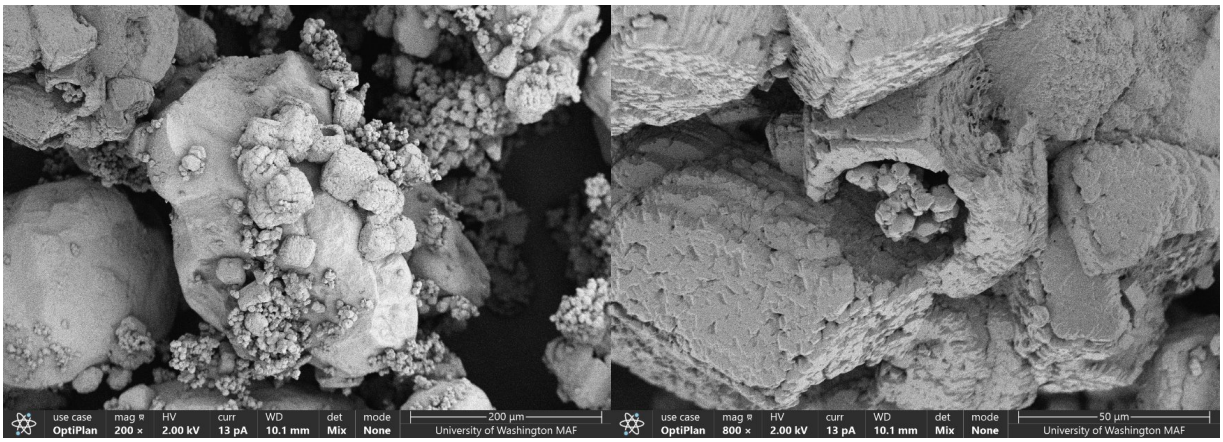

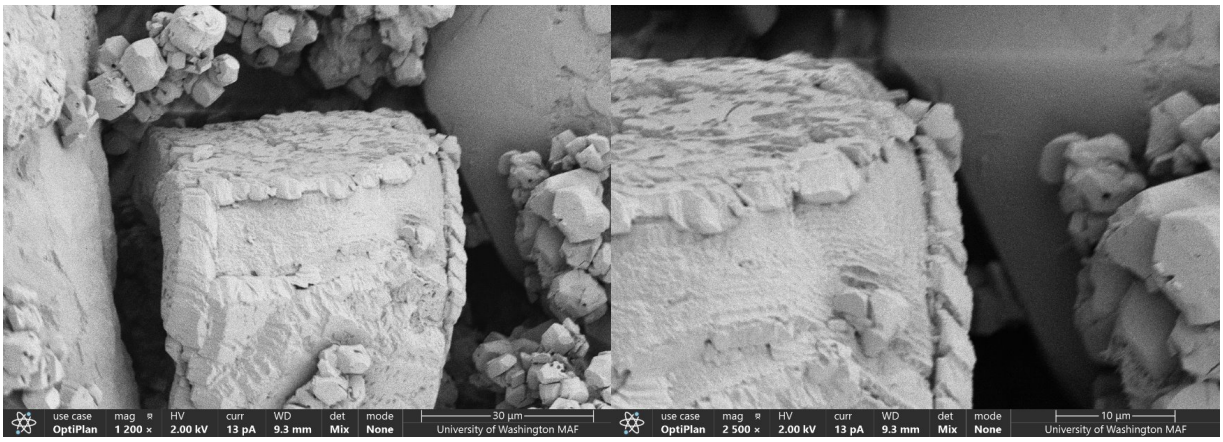

Fig. 4.16. SEM images of treated soil samples from Experiment Mg13 (MICP - PolyMAF (0.01%) - Calcium Rinse - 2nd MICP (50 mM $MgCl_2$)) at various magnifications.

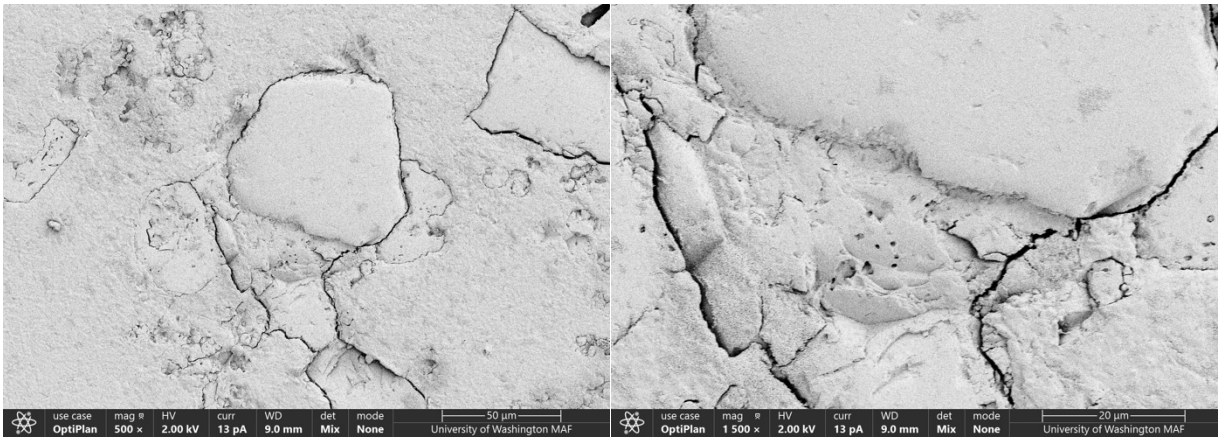

Fig. 4.17. SEM images of polished material cross-sections from Experiment Mg13 (MICP - PolyMAF (0.01%) - Calcium Rinse - 2nd MICP (50 mM $MgCl_2$)).

Figure 4.18 presents SEM images of Experiment Mg14 which received one cementation treatment, followed by a Poly treatment (no MAF) and a calcium rinse, and a second cementation treatment with 50 mM $MgCl_2$. As shown, similar morphologies were observed to all other experiments containing magnesium in the second cementation treatment. When compared to Experiment Mg13, which was identical but had MAF activity, interestingly the collapsed calcite

crystals observed in Experiment Mg13 were not present in Experiment Mg14. This again suggested that these collapse features were likely the result of damage to the brittle mineral exteriors surrounding gas inclusions during the sample preparation process. These gas inclusions, however, could only be generated when MAF activity was present, thus making this activity critical to the gas inclusion process.

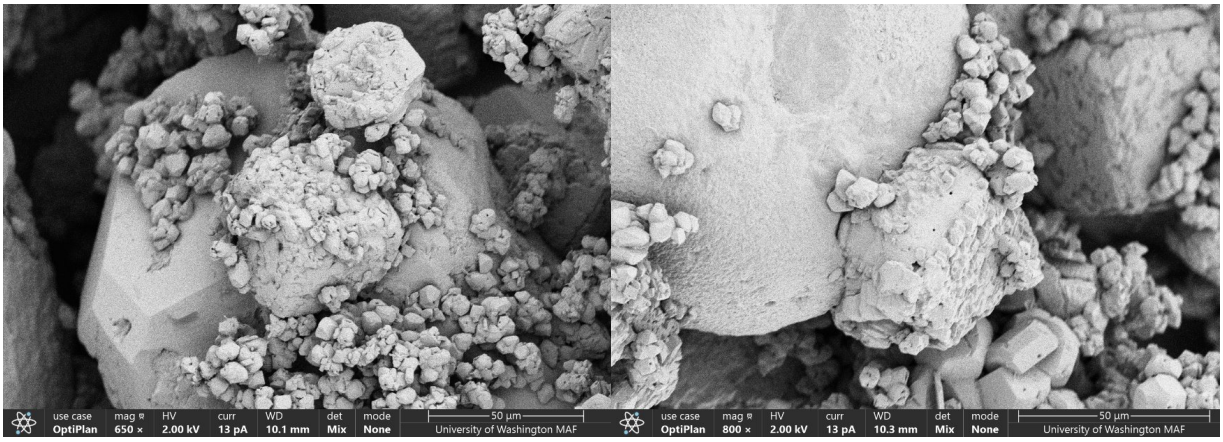

Fig. 4.18. SEM images of treated soil samples from Experiment Mg14 (MICP - Poly (0.01%) - Calcium Rinse - 2nd MICP (50 mM $MgCl_2$)) at various magnifications.

4.4 Conclusions and Remaining Knowledge Gaps

A series of experiments were performed to further examine the behavior of magnesium amended samples identified earlier in Chapter 3 to enable improved mineral surface coatings and improved gas entrapment. These experiments were designed to further isolate effects resulting from (i) the first cementation treatment, (ii) the presence of sodium alginate polymer, (iii) the present of MAF activity, (iv) the influence of calcium rinses, (v) effects resulting from reaugmentation, (vi) effects resulting from the second cementation treatment, and (vii) the critical role that magnesium may play during the second cementation treatment towards enabling the preferential coating of existing

calcium carbonate mineral surfaces. In these experiments, magnesium additions during the second cementation treatment were found to be primarily responibsle for the coating of existing calcium carbonate crystals observed in earlier experiments. Such effects were observed irrespective of the presence of polymers or MAF activity and enabled coating of polymer films with entrapped gasses. However, this mineral coating was only achieved when both calcium and magnesoium were applied in the second cementation treatment and could not be replicated through the additon of magnesium alone (without calcium) during the second cementation treatment. Collectively, this suggested that the mineral coatings produced may be magesian calcite, however, the particular mechanism responsible for the preferenial precipitaiton of this mineral on existing calcium carboante mineral surfaces remains poorly understood.

When examining the impact of calcium rinses applied immediately after the polymer treatments and before the second cementation events, calcium rinses appeared to result in a more robust calcium alginate polymer coating on existing crystals and soil particle surfaces when compared to similar experiments without this rinse injection. When combined with magneisum amended second cementation treatments, calcium rinses also appeared to result in greater gas inclusions within the polymer film between the magnesian calcite exterior layer generated during the second cementation treatment and the interior calcite crystals generated during the first cementation treatment. In samples receiving PolyMAF treatments, calcium rinses, and a second cementation treatment collapsed minerals were also observed near spherical voids suggesting that these exterior minerals may have been coating larger gas inclusions that were distrubed during the sample preparation process. Although these results suggest that gas inclusions can be reliably incorporated within biocemented composites using the treatment techniques demonstrated in this chapter,

further work remains needed to quanitfy the volume of these inclusions, establish the distribtuion of these inclusions, and characterize their impact on resulting engineering responses.

Chapter 5: Conclusions & Future Work

In this study, the ability of gas inclusions to be incorporated within biocemented composites was investigated through a series of batch experiments. These gas inclusions may afford the ability to improve the undrained shearing behavior of biocemented sands through the release of gas bubbles following the deterioration of cemented bonds during extreme loading events. These gas bubbles may afford improvements in engineering behaviors through increases in pore fluid compressibility and reductions in excess pore pressure generation. From the experiments performed in this research the following primary conclusions can be made:

- Carbon dioxide gasses can be generated using mixed acid fermentation (MAF) activity in the presence of biocementation. These gasses result from both the chemical degradation of calcium carbonate crystals and as fermentation byproducts. Produced gas bubbles can be retained using viscous biopolymers such as sodium alginate.
- When biocementation is dissolved during PolyMAF treatments, released calcium can enable the formation of a calcium alginate gel that may improve gas entrapment within the polymer. The application of a calcium rinse after PolyMAF treatments and before the second cementation treatment appears to enhance the formation calcium alginate.
- When a second cementation treatment is applied after a re-augmentation event, smaller calcium carbonate crystals appeared to be widely distributed throughout samples. In other samples without a re-augmentation, the second cementation treatment appears to predominantly grow existing larger crystals rather than nucleating new smaller crystals.
- When magnesium chloride is provided in the second cementation treatment, smaller nucleated crystals can be preferentially precipitated on existing calcite crystals. This occurs

irrespective of the presence of sodium alginate or previous MAF activity suggesting that magnesium is primarily responsible for this outcome.

- In our experiments, gas inclusions were shown to be successfully entrapped within a polymer film existing between larger calcite crystals precipitated during the first cementation event and the exterior magnesian calcite coating precipitated during the second cementation treatment when magnesium was present. Gas entrapment appeared to be further improved by combining calcium rinses with magnesium amended second cementation treatments.
- While these results are promising, further work is needed to quantitatively characterize generated gas inclusions found within these biocemented composites and investigate their implications for undrained soil shearing behaviors.

Despite these significant advancements in the development of biocemented composites with gas inclusions, several important knowledge gaps still remain. These include: (i) the need for quantitative assessment metrics for the presence of gas inclusions beyond visual images which can require interpretation, (ii) the need for non-destructive assessment methods which can be used to detect gas inclusions without inducing mechanical disturbances that can compromise these characterizations, and (iii) the need for an improve understanding of how gas inclusions can alter macro-scale soil shearing behaviors relevant to a variety of different geotechnical applications including the mitigation of earthquake-induced soil liquefaction. Further work is also needed to understand the potential of biocemented composites beyond gas inclusions including the potential of polymer films, inclusions, and fibers to alter material ductility, fracture toughness, and other small- and large-strain behaviors.

Appendix

Table 2.1. Summary of Chapter 2 Batch Experiments.

Test Information		*Initial MICP*			*MAF*					*Rinse*	*2nd MICP*			
Experiment Number	***Treatment Procedure***	***CaCl2 (mM)***	***Urea (mM)***	***YE (g/L)***	***Polymer Conc. (%)***	***Glucose***	***Yeast Extract (g/L)***	***MAF Inoc.***	***Tracer Used & Conc.***	***Type of Rinse and Conc.***	***CaCl2 (mM)***	***Urea (mM)***	***YE (g/L)***	***Tracer Used***
1	MICP - PolyMAF (0.0005%) - 2nd MICP	250	250	0.2	0.0005%	10	1	1 mL per 300 mL	-----	-----	250	250	0.2	-----
2	MICP	250	250	0.2	-----	-----	-----	-----	-----	-----	-----	-----	-----	-----
3	MICP - PolyMAF (0.0005%)	250	250	0.2	0.0005%	10	1	1 mL per 300 mL	-----	-----	-----	-----	-----	-----
4	MICP - PolyMAF (0.0005%) - 2nd MICP	250	250	0.2	0.0005%	10	1	1 mL per 300 mL	-----	-----	250	250	0.2	-----
5	MICP - Poly (0.0005%) - 2nd MICP	250	250	0.2	0.0005%	0	0	-----	-----	-----	250	250	0.2	-----
6	MICP - PolyMAF (0.001%) - 2nd MICP	250	250	0.2	0.001%	10	1	1 mL per 300 mL	-----	-----	250	250	0.2	-----
7	MICP - PolyMAF (0.005%) - 2nd MICP	250	250	0.2	0.005%	10	1	1 mL per 300 mL	-----	-----	250	250	0.2	-----
8	MICP - PolyMAF (0.01%) - 2nd MICP	250	250	0.2	0.01%	10	1	1 mL per 300 mL	-----	-----	250	250	0.2	-----

Table 3.1. Summary of Chapter 3 Batch Experiments.

Treatment Information		*Initial MICP*			*MAF*					*Rinse*	*2nd MICP*			
Experiment Number	*Treatment Procedure*	*CaCl2 (mM)*	*Urea (mM)*	*YE (g/L)*	*Polymer Conc. (%)*	*Glucose*	*Yeast Extract (g/L)*	*MAF Inoc.*	*Tracer Used & Conc.*	*Type of Rinse and Conc.*	*CaCl2 (mM)*	*Urea (mM)*	*YE (g/L)*	*Tracer Used*
T1	MICP - PolyMAF (0.01%) - 2nd MICP	250	250	0	0.01%	10	1	1 mL per 300 mL	-----	-----	250	250	0	-----
T2	MICP - PolyMAF (0.01%, 500 mM KBr) - 2nd MICP	250	250	0	0.01%	10	1	1 mL per 300 mL	KBr - 500 mM	-----	250	250	0	-----
T3	MICP - PolyMAF (0.01%, 50 mM MgCl2) - 2nd MICP	250	250	0	0.01%	10	1	1 mL per 300 mL	MgCl2 - 50 mM	-----	250	250	0	-----
T4	MICP - PolyMAF (0.01%, 500 mM NaBr) - 2nd MICP	250	250	0	0.01%	10	1	1 mL per 300 mL	NaBr - 500 mM	-----	250	250	0	-----
T5	MICP - PolyMAF (0.01%) - 2nd MICP (50 mM MgCl2)	250	250	0	0.01%	10	1	1 mL per 300 mL	-----	-----	250	250	0	MgCl2 - 50 mM
T6	MICP - PolyMAF (0.01%) - 2nd MICP (250 mM MgCl2)	250	250	0	0.01%	10	1	1 mL per 300 mL	-----	-----	250	250	0	MgCl2 - 250 mM
T7	MICP - PolyMAF (0.01%, 500 mM NaBr) - 2nd MICP (250 mM MgCl2)	250	250	0	0.01%	10	1	1 mL per 300 mL	NaBr - 500 mM	-----	250	250	0	MgCl2 - 50 mM
T8	MICP - PolyMAF (0.01%) - 2nd MICP (500 mM KBr)	250	250	0	0.01%	10	1	1 mL per 300 mL	-----	-----	250	250	0	KBr - 500 mM
CR1	MICP - PolyMAF (0.01%) - Calcium Rinse - 2nd MICP	250	250	0	0.01%	10	1	1 mL per 300 mL	-----	Ca+2 - 250 mM	250	250	0	-----

CR2	MICP - PolyMAF (0.01%, 500 mM NaBr) - 2nd MICP	250	250	0	0.01%	10	1	1 mL per 300 mL	NaBr - 500 mM	Ca+2 - 250 mM	250	250	0	-----
CR3	MICP - PolyMAF (0.01%) - Calcium Rinse	250	250	0	0.01%	10	1	1 mL per 300 mL	-----	Ca+2 - 250 mM	OFFLINE			

Table 4.1. Summary of Chapter 4 Batch Experiments.

Test Information		*Initial MICP*			*MAF*					*Rinse*	*2nd MICP*			
Experiment Number	***Treatment Procedure***	***CaCl2 (mM)***	***Urea (mM)***	***YE (g/L)***	***Polymer Conc. (%)***	***Glucose***	***Yeast Extract (g/L)***	***MAF Inoc.***	***Tracer Used & Conc.***	***Type of Rinse and Conc.***	***CaCl2 (mM)***	***Urea (mM)***	***YE (g/L)***	***Tracer Used***
1	MICP - PolyMAF (0.01%) - 2nd MICP (50 mM MgCl2)	250	250	0	0.01%	10	1	1 mL per 300 mL	-	-	250	250	0	MgCl2 - 50 mM
2	MICP - PolyMAF (0.01%) - 2nd MICP (250 mM MgCl2)	250	250	0	0.01%	10	1	1 mL per 300 mL	-	-	250	250	0	MgCl2 - 250 mM
3	MICP - PolyMAF (0.01%) - 2nd MICP	250	250	0	0.01%	10	1	1 mL per 300 mL	-	-	250	250	0	-
4	MICP - Poly (0.01%) - 2nd MICP	250	250	0	0.01%	0	0	0	-	-	250	250	0	-
5	MICP - PolyMAF (0.01%) - Calcium Rinse - 2nd MICP	250	250	0	0.01%	10	1	1 mL per 300 mL	-	Ca+2 - 250 mM	250	250	0	-
6	MICP - 2nd MICP (50 mM MgCl2)	250	250	0	-	-	-	-	-	-	250	250	0	MgCl2 - 50 mM
7	MICP	250	250	0	-	-	-	-	-	-	-	-	-	-
8	MICP - PolyMAF (0.01%)	250	250	0	0.01%	10	1	1 mL per 300 mL	-	-	-	-	-	-

9	MICP - PolyMAF (0.01%) - Calcium Rinse	250	250	0	0.01%	10	1	1 mL per 300 mL	-	Ca+2 - 250 mM	-	-	-	-
10	MICP - PolyMAF (0.01%) - 2nd MICP (50 mM MgCl2, 0 mM CaCl2)	250	250	0	0.01%	10	1	1 mL per 300 mL	-	-	0	250	0	MgCl2 - 50 mM
11	MICP - PolyMAF (0.01%) - 2nd MICP (250 mM MgCl2, 0 mM CaCl2)	250	250	0	0.01%	10	1	1 mL per 300 mL	-	-	0	250	0	MgCl2 - 250 mM
12	MICP - Poly (0.01%) - 2nd MICP (50 mM MgCl2)	250	250	0	0.01%	0	0	0	-	-	250	250	0	MgCl2 - 50 mM
13	MICP - PolyMAF (0.01%) - Calcium Rinse - 2nd MICP (50 mM MgCl2)	250	250	0	0.01%	10	1	1 mL per 300 mL	-	Ca+2 - 250 mM	250	250	0	MgCl2 - 50 mM
14	MICP - Poly (0.01%) - Calcium Rinse - 2nd MICP (50 mM MgCl2)	250	250	0	0.01%	0	0	0	-	Ca+2 - 250 mM	250	250	0	MgCl2 - 50 mM
15	MICP - 2nd MICP	250	250	0	-	-	-	-	-	-	250	250	0	-
16	MICP - 2nd MICP (No Augmentation Before 2nd MICP)	250	250	0	-	-	-	-	-	-	250	250	0	-

References

Baek, S.-H., Kwon, T.-H., & DeJong, J. T. (2024). Reductions in Hydraulic Conductivity of Sands Caused by Microbially Induced Calcium Carbonate Precipitation. *Journal of Geotechnical and Geoenvironmental Engineering*, *150*(2), 04023134. https://doi.org/10.1061/JGGEFK.GTENG-11570

Berner, R. A. (1975). The role of magnesium in the crystal growth of calcite and aragonite from sea water. *Geochimica et Cosmochimica Acta*, *39*(4), 489–504. https://doi.org/10.1016/0016-7037(75)90102-7

Burdalski R.J. 2020. Investigating the effect of biological and chemical factors on the reaction kinetics and mineralogy of ureolytic bio- cementation (Master of Science in Civil & Environmental Engineering). University of Washington, Seattle, Washington.

Burdalski, R. J., Ribeiro, B. G. O., Gomez, M. G., & Gorman-Lewis, D. (2022). Mineralogy, morphology, and reaction kinetics of ureolytic bio-cementation in the presence of seawater ions and varying soil materials. *Scientific Reports*, *12*(1), 17100. https://doi.org/10.1038/s41598-022-21268-3

Byle, M. J., Johnsen, L., Bruce, D. A., El Mohtar, C. S., Gazzarrini, P., & Richards, T. D. (Eds.). (2017). *Grouting 2017. Grouting, drilling, and verification: Selected papers from sessions of Grouting 2017, July 9-12, 2017, Honolulu, Hawaii*. American Society of Civil Engineers.

Ching, S. H., Bansal, N., & Bhandari, B. (2017). Alginate gel particles–A review of production techniques and physical properties. *Critical Reviews in Food Science and Nutrition*, *57*(6), 1133–1152. https://doi.org/10.1080/10408398.2014.965773

DeJong, J. T., Fritzges, M. B., & Nüsslein, K. (2006). Microbially Induced Cementation to Control Sand Response to Undrained Shear. *Journal of Geotechnical and Geoenvironmental Engineering*, *132*(11), 1381–1392. https://doi.org/10.1061/(ASCE)1090-0241(2006)132:11(1381)

Der Star, W. R. L. V., Taher, E., Harkes, M. P., Blauw, M., Loosdrecht, M. C. M. V., & Paassen, L. A. V. (2009). Use of Waste Streams and Microbes for in situ Transformation of Sand Into Sandstone. *Ground Improvement Technologies and Case Histories*, 177–182. https://doi.org/10.3850/GI126

Eseller-Bayat, E. E. (2009). *Seismic response and prevention of liquefaction failure of sands partially saturated through introduction of gas bubbles* [Northeastern University]. https://doi.org/10.17760/d20000133

Gomez, M. G., Anderson, C. M., Graddy, C. M. R., DeJong, J. T., Nelson, D. C., & Ginn, T. R. (2017). Large-Scale Comparison of Bioaugmentation and Biostimulation Approaches for Biocementation of Sands. *Journal of Geotechnical and Geoenvironmental Engineering*, *143*(5), 04016124. https://doi.org/10.1061/(ASCE)GT.1943-5606.0001640

Gomez, M. G., & DeJong, J. T. (2017). Engineering Properties of Bio-Cementation Improved Sandy Soils. *Grouting 2017*, 23–33. https://doi.org/10.1061/9780784480793.003

Gomez, M. G., DeJong, J. T., Anderson, C. M., Nelson, D. C., & Graddy, C. M. (2016). Large-Scale Bio-Cementation Improvement of Sands. *Geotechnical and Structural Engineering Congress 2016*, 941–949. https://doi.org/10.1061/9780784479742.079

Gomez, M. G., Martinez, B. C., DeJong, J. T., Hunt, C. E., deVlaming, L. A., Major, D. W., & Dworatzek, S. M. (2015). Field-scale bio-cementation tests to improve sands. *Proceedings of the Institution of Civil Engineers - Ground Improvement*, *168*(3), 206–216. https://doi.org/10.1680/grim.13.00052

Hall, C. A., Hernandez, G., Darby, K. M., Van Paassen, L., Jr., E. K., DeJong, J., & Wilson, D. (2018). Centrifuge Model Testing of Liquefaction Mitigation via Denitrification-Induced Desaturation. *Geotechnical Earthquake Engineering and Soil Dynamics V*, 117–126. https://doi.org/10.1061/9780784481455.011

He, J., Chu, J., Wu, S., & Peng, J. (2016). Mitigation of soil liquefaction using microbially induced desaturation. *Journal of Zhejiang University-SCIENCE A*, *17*(7), 577–588. https://doi.org/10.1631/jzus.A1600241

Knorst, M. T., Neubert, R., & Wohlrab, W. (1997). Analytical methods for measuring urea in pharmaceutical formulations. *Journal of Pharmaceutical and Biomedical Analysis*, *15*(11), 1627–1632. https://doi.org/10.1016/S0731-7085(96)01978-4

Lee, M., & Gomez, M. G. (2023). Liquefaction triggering and post-triggering behavior of biocemented loose sand. *Canadian Geotechnical Journal*, cgj-2023-0132. https://doi.org/10.1139/cgj-2023-0132

Lee, M., Gomez, M. G., El Kortbawi, M., & Ziotopoulou, K. (2022). Effect of Light Biocementation on the Liquefaction Triggering and Post-Triggering Behavior of Loose Sands. *Journal of Geotechnical and Geoenvironmental Engineering*, *148*(1), 04021170. https://doi.org/10.1061/(ASCE)GT.1943-5606.0002707

Montoya, B. M., & DeJong, J. T. (2015). Stress-Strain Behavior of Sands Cemented by Microbially Induced Calcite Precipitation. *Journal of Geotechnical and Geoenvironmental Engineering*, *141*(6), 04015019. https://doi.org/10.1061/(ASCE)GT.1943-5606.0001302

Montoya, B. M., DeJong, J. T., Boulanger, R. W., Wilson, D. W., Gerhard, R., Ganchenko, A., & Chou, J.-C. (2012). Liquefaction Mitigation Using Microbial Induced Calcite Precipitation. *GeoCongress 2012*, 1918–1927. https://doi.org/10.1061/9780784412121.197

Morse, J. W., Arvidson, R. S., & Lüttge, A. (2007). Calcium Carbonate Formation and Dissolution. *Chemical Reviews*, *107*(2), 342–381. https://doi.org/10.1021/cr050358j

Mortensen, B. M., & DeJong, J. T. (2011). Strength and Stiffness of MICP Treated Sand Subjected to Various Stress Paths. *Geo-Frontiers 2011*, 4012–4020. https://doi.org/10.1061/41165(397)410

O'Donnell, S. T., Kavazanjian, E., & Rittmann, B. E. (2017). MIDP: Liquefaction Mitigation via Microbial Denitrification as a Two-Stage Process. II: MICP. *Journal of Geotechnical and Geoenvironmental Engineering*, *143*(12), 04017095. https://doi.org/10.1061/(ASCE)GT.1943-5606.0001806

Okumura, M., Kitano, Y., & Idogaki, M. (1986). Behavior of bromide ions during the formation of calcium carbonate. *Marine Chemistry*, *19*(2), 109–120. https://doi.org/10.1016/0304-4203(86)90043-5

Park, W. K., Ko, S.-J., Lee, S. W., Cho, K.-H., Ahn, J.-W., & Han, C. (2008). Effects of magnesium chloride and organic additives on the synthesis of aragonite precipitated calcium carbonate. *Journal of Crystal Growth*, *310*(10), 2593–2601. https://doi.org/10.1016/j.jcrysgro.2008.01.023

Raju. (n.d.). *Ground improvement-applications and quality control (needs more info)*.

Ribeiro, B. G. O., Lee, M., & Gomez, M. G. (2024). An Examination of the Effect of Chemically Induced Damage on the Monotonic and Cyclic Shearing Behavior of Biocemented Sands.

Geotechnical Testing Journal, *47*(2), GTJ20230302. https://doi.org/10.1520/GTJ20230302

San Pablo, A. C. M., Lee, M., Graddy, C. M. R., Kolbus, C. M., Khan, M., Zamani, A., Martin, N., Acuff, C., DeJong, J. T., Gomez, M. G., & Nelson, D. C. (2020). Meter-Scale Biocementation Experiments to Advance Process Control and Reduce Impacts: Examining Spatial Control, Ammonium By-Product Removal, and Chemical Reductions. *Journal of Geotechnical and Geoenvironmental Engineering*, *146*(11), 04020125. https://doi.org/10.1061/(ASCE)GT.1943-5606.0002377

Stallings Young, E. G., Mahabadi, N., Zapata, C. E., & Van Paassen, L. A. (2021). Correction to: Microbial-Induced Desaturation in Stratified Soil Conditions. *International Journal of Geosynthetics and Ground Engineering*, *7*(2), 47. https://doi.org/10.1007/s40891-021-00293-8

Stocks-Fischer, S., Galinat, J. K., & Bang, S. S. (1999). Microbiological precipitation of CaCO3. *Soil Biology and Biochemistry*, *31*(11), 1563–1571. https://doi.org/10.1016/S0038-0717(99)00082-6

Sun, J., & Bhushan, B. (2012). Hierarchical structure and mechanical properties of nacre: A review. *RSC Advances*, *2*(20), 7617. https://doi.org/10.1039/c2ra20218b

Takemura, J., Okamura, M., Igarashi, R., Masuda, M., & Izawa, J. (2009). Centrifuge model tests on soil desaturation as a liquefaction countermeasure. *Proc. 17 ICSMGE, Alexandria*.

Unluer, C., & Al-Tabbaa, A. (2014). Characterization of light and heavy hydrated magnesium carbonates using thermal analysis. *Journal of Thermal Analysis and Calorimetry*, *115*(1), 595–607. https://doi.org/10.1007/s10973-013-3300-3

Van Paassen L.A. (2009). *Biogrout: Ground improvement by microbially induced carbonate precipitation. (PhD Dissertation). Delft University of Technology, Delft, Netherlands*.

Yoon, J. H., Lee, K. C., Weiss, N., Kho, Y. H., Kang, K. H., & Park, Y. H. (2001). Sporosarcina aquimarina sp. Nov., a bacterium isolated from seawater in Korea, and transfer of Bacillus globisporus (Larkin and Stokes 1967), Bacillus psychrophilus (Nakamura 1984) and Bacillus pasteurii (Chester 1898) to the genus Sporosarcina as Sporosarcina globispora comb. Nov., Sporosarcina psychrophila comb. Nov. And Sporosarcina pasteurii comb. Nov., and emended description of th. *International Journal of Systematic and Evolutionary Microbiology*, *51*(3), 1079–1086. https://doi.org/10.1099/00207713-51-3-1079

Zhang, Y., & Dawe, R. A. (2000). Influence of Mg2+ on the kinetics of calcite precipitation and calcite crystal morphology. *Chemical Geology*, *163*(1–4), 129–138. https://doi.org/10.1016/S0009-2541(99)00097-2